University of Udine

Ph.D. program
Environmental and Energy Engineering Science

XXVIII Cycle

Innovative engine configurations and waste heat recovery solutions employed on large cruise ship to meet new environmental regulations

Dr. Ing. Silvia Daniotti

Commitee	
Prof. Ing. Piero Pinamonti	SUPERVISOR
Prof. Ing. Mauro Reini	CO-SUPERVISOR
Dott. Ing. Alessandro Armellini	CO-SUPERVISOR
Dott. Ing. Giovanni Caprino	REVIEWER
Prof. Ing. Michele Pinelli	REVIEWER
Prof. Ing. Maurizio De Lucia	REFEREE
Prof. Ing. Pietro Giannattasio	REFEREE
Prof. Ernesto Salzano	REFEREE
Prof. Alfredo Soldati	COORDINATOR

Academic Year 2015-2016

Author's e-mail:
silvia.daniotti@gmail.com

Author's address:
Dipartimento di Ingegneria Elettrica, Gestionale e Meccanica
Università degli Studi di Udine
Via delle Scienze, 106
33100 Udine - Italy

Web:
http://www.diegm.uniud.it

La vita ha 4 sensi: amare, soffrire, lottare e vincere. Chi ama soffre, chi soffre lotta, chi lotta vince. Ama molto, soffri poco, lotta tanto, vinci sempre.
(Oriana Fallaci)

Abstract

Due to recent regulations imposed by IMO (Int. Maritime Org.), pollution emissions produced by large ships are now under strict control, and a widening part of the seas (called SECA) is now accessible only by ships with a limited SOx and NOx output.
To meet the new regulations, ships propelled by HFO burning Internal Combustion Engines (ICEs) can be equipped with abatement devices such as scrubbers and SCR systems. Although the employment of those devices seems to be the route ship-owners will prefer, other methods can be considered such as the use of MGO, a more expensive fuel but with lower sulphur content. The use of MGO allows considering a further and more drastic modification of the power system, namely the use of Gas Turbines (GTs) in place of ICEs. Gas Turbines, despite of being less efficient, are much lighter, more compact, and can easier reach low NOx emissions than ICEs. Even if these aspects are theoretically well known, there are still difficulties in finding studies reporting quantitative analysis (weight, dimensions, fuel consumption) that compare GTs and ICEs power systems employed on board. The present thesis aims at providing these data by analyzing different solutions applied to a real case. Unlike other studies, the work is focused on a cruise ship rather than on a cargo ship, because cruise ship's operation profile is more variable during the trip. Finally, solutions to minimize the gap of fuel consumption between GTs and ICEs is also discussed.

Acknowledgments

First of all I would like to thank Fincantieri S.p.A. for having allowed me to access the data necessary for my research.

A very special thanks to my supervisor, Prof. Ing. Piero Pinamonti for having given me his complete support and for having put up with me in my bad moments. I am also grateful to Prof. Ing. Mauro Reini for his astute suggestions.

I really appreciate the help, which Dott. Ing. Alessandro Armellini gave me: he was a reference point during all my ph.d. course always sustaining me both as mentor and as friend.

I would like to acknowledge Prof. Ing. Michele Pinelli and Ing. Giovanni Caprino for offering to be my thesis' reviewers.

Un caloroso, sentito nonché doveroso grazie va a mamy e papy per essermi stati sempre da sostegno in questi anni con la loro iper-pazienza, sensibilità, comprensione, rispetto, amore incondizionato, simpatia e…"Rumpstoff".

I would like to thank Rudi, Pic, Ruben, Rudolf….my love.. ."I'm looking for a reason to stay, I'm all wound up and tired enough today, I'm looking for a reason not to go, when the morning comes I'll be on my way…..". You are definitely my reason!!!!Thank you for everything.

Ringrazio i colleghi/professori che con me hanno lavorato in questi anni: Luca, Dario, Claudio, Alberto, Melchiorre. In particolar modo, ringrazio Matteo e Luca…"Sex machine"!

Contents

PART II - Model application

Nomenclature

COP	Coefficient Of Performance	
$COP_{abs.}$	Absorption chiller's Coefficient of Performance	
$c_{p,g}$	thermal capacity	[kJ/(kg*K)]
C_{tA}	Autumn thermal load	[MW]
C_{tW}	Winter thermal load	[MW]
C_{urea}	urea solution concentration	[weight-%]
DBP	Diesel Brake Power	[MW]
dSFOC	Delta Specific Fuel Oil Consumption	
DWT	Dead Weight Tonnage	[ton]
EEDI	Energy Efficiency Design Index	[gCO_2/ton/miles]
$E_{el.}$	global electric load	[kJ]
$El._{chilling}$	Electric loads for chilling porpoises	[kW]
EF_h	h-th pollutants Emission factor	[$g_{h\text{-}th,pollutants}/kg_{fuel}$]
EF_{ICE_NOx}	ICE's NO_x emission factor	[g_{NOx}/kg_{fuel}]
EF_{ICE_SOx}	ICE's NO_x emission factor	[g_{SOx}/kg_{fuel}]
E_{fuel}	Single cruise's phase fuel energy	[kJ]
$E_{fuel,GTs}$	Single cruise's phase fuel energy for gas turbines	[kJ]
$E_{fuel,OFBs}$	Single cruise's phase fuel energy for Oil Fired Boilers	[kJ]
$E_{fuel,Type\ A}$	Single cruise's phase fuel energy for Type A gas turbines	[kJ]
$E_{fuel,Type\ B}$	Single cruise's phase fuel energy for Type B gas turbines	[kJ]
$E_{fuel,Type\ ICEs}$	Single cruise's phase fuel energy for internal combustion engines	[kJ]
$E_{fuel.global}$ (=FE)	Global cruise's fuel energy	[kJ]
$E_{TH,ACC.\text{-}EGBs}$	Accommodation thermal loads recovered in Exhaust gas boilers	[kJ]
$E_{TH,Acc.\text{-}OFBs}$	Accommodation thermal loads supplied by Oil Fired Boilers	[kJ]

$E_{TH,FW.-Cogen}$	Fresh water production's thermal load covered by cogeneration	[kJ]
$E_{TH,FW.-OFBs}$	Fresh water production's thermal load covered by Oil Fired Boilers	[kJ]
$E_{TH.ACC}$	Accommodation thermal loads	[kJ]
$E_{TH.FW}$	Fresh water production thermal loads	[kJ]
$E_{TH.WHR}$	Thermal loads covered by waste heat recovery	[kJ]
Fuel	Fuel burned	[ton]
$Fuel_{ICE}$	Fuel burned in Internal Combustion engines	[ton]
$Fuel_{OFB}$	Fuel burned in Oil Fired Boilers	[ton]
$Fuel_{GTs}$	Fuel burned in gas turbines	[ton]
H_i	Lower heating values	[kJ/kg]
$H_{i(ISO)}$	Lower heating values @ ISO conditions	[kJ/kg]
LHV	Lower Heating Values	[LHV]
m_g	Exhaust gas mass flow	[kg/s]
MCR	Maximum Continuous Rating	
$m_{g,Type\ A}$	Exhaust gas mass flow Typa A gas turbine	[kg/s]
$m_{g,Type\ B}$	Exhaust gas mass flow Typa B gas turbine	[kg/s]
MM_{NO2}	NO_2 molecular mass	[g/mol]
NP	Internal Combustion Engines' Nominal Power	[kW]
OFB_{TL}	Thermal Loads covered by Oil Fired Boilers	[kW]
$P_{TH.,chilling}$	Thermal loads for chilling porpoises	[kW]
$P_{HT\_FW.ICE}$	Thermal power for fresh water production from Internal Combustion engines' high temperature circuit	[kW]
P_{TH,FW_GT}	Thermal power for fresh water production for gas turbines	[kW]
ρ_{urea}	Urea density	[g/l]
PE_h	h-th pollutants emissions	[ton]
$P_{TH,ECO,GT}$	Thermal power exchanged in Gas turbine's Exhaust gas boilers economizer	[kW]
$P_{TH,ECO,ICE}$	Thermal power exchanged in Internal Combustion Engines Exhaust gas boilers economizer	[kW]
$P_{TH,EVA,GT}$	Thermal power exchanged in Gas turbine's Exhaust gas boilers evaporator	[kW]
$P_{TH,EVA,ICE}$	Thermal power exchanged in Internal Combustion Engines Exhaust gas boilers evaporator	[kW]
P_{TH,WHR_GT}	Thermal power recovered in Exhaust gas boilers in gas turbines	[kW]
P_{TH,WHR_ICE}	Thermal power recovered in Exhaust gas boilers in internal combustion engines	[kW]
SFOC	Specific Fuel Oil Consumption	[g/kWh]

$SFOC_{AE}$	Specific Fuel Oil Consumption for auxiliaries engine	[g/kWh]
$SFOC_{ISO}$	Specific Fuel Oil Consumption @ ISO conditions	[g/kWh]
$SFOC_{is}$	Specific Fuel Oil Consumption in service	[g/kWh]
$SFOC_{ME}$	Specific Fuel Oil Consumption for main engine	[g/kWh]
T	Weighted average exhaust gas temperature	[°C]
TL	Thermal Loads	[kW]
$t._{air.W}$	Winter air temperature	[°C]
T_g	Exhaust gas temperature	[°C]
$t._{in}$	Internal ship's temperature	[°C]
$t._{sea.A}$	Autumn sea temperature	[°C]
$T_{g,OUT,EGB}$	Exhaust Gas Boilers' outlet exhaust gas temperature	[°C]
T_c	Chimney's exhaust gas temperature	[°C]
$TOT_{Type\ A}$	Type A GT's Turbine Outlet Temperature	[°C]
$TOT_{Type\ B}$	Type B GT's Turbine Outlet Temperature	[°C]
UA_{eco}	Economizer global heat transfer coefficient	[W/K]
UA_{eva}	Evaporator global heat transfer coefficient	[W/K]
V_{ECO}	Economizer volume	[m^3]
V_{EVA}	Evaporator volume	[m^3]
Vref	Design loading condition reference speed	[knot]
$\dot{V}_{urea}$	Urea volume rate	[l/h]
W_{ECO}	Economizer weight	[ton]
W_{EVA}	Evaporator weight	[ton]
x	independent operation optimization variables	
w	Independent design optimization variables	
z	independent synthesis optimization variables	
η_{OFB}	Oil Fired Boilers efficiency	
η_{SCR}	Selective Catalytic Reactor efficiency	
$\eta_{scrubber}$	Scrubber efficiency	
η_{ship}	Cruise phase ship's energy efficiency	
$\eta_{ship,global}$	Global ship's energy efficiency	

Acronyms

1.x	Hybrid engines' configurations based on the employment of 3 gas turbines and 1 internal combustion engine as prime movers
2.x	Hybrid engines' configurations based on the employment of 2 gas turbines and 2 internal combustion engines as prime movers
3.x	Hybrid engines' configurations based on the employment of 1 gas turbine and 3 internal combustion engines as prime movers
1.x Trigen.	Hybrid engines' configurations based on the employment of 3 gas turbines and 1 internal combustion engine as prime movers and the use of absorption chillers for chilling porpoises
3.x Pow.	Hybrid engines' configurations based on the employment of 1 gas turbine and 3 internal combustion engines as prime movers with Power management
A	autumn
ACC.	Accommodation
DC	Direct Current
DeSOx	SO_x abatement devices
E.R.	Engine Room
EAs	Evolutionary Algorithms
ECA	Environmental Controlled Area
EGBs	Exhaust Gas Boilers
FW	Fresh Water
GHG	Green House Gas
GT	Gas Turbine
GTs class	"One-kind" (namely GTs) engines' configurations
HFO	Heavy Fuel Oil
HYBRID class	Hybrid engines' configurations consisting of the general employment of both ICEs and GTs
ICE	Internal Combustion Engine
ICE_eco	Internal Combustion Engine in "ecofriendly" mode with SCR and scrubber installed on board
ICEs class	"One-kind" (namely ICEs) engines' configurations
IEA	International Energy Agency
IFO	Intermediate Fuel Oil

IGV	Inlet Guide Vanes
IMO	International Maritime Organization
IPS	Integrated Power System
LNG	Liquefied Natural Gas
LPT	Low pressure turbine
MARPOL	Maritime Pollution
MDO	Marine Diesel Oil
MGO	Marine Gas Oil
MINLP	Mixed Integer Non Linear Programming
MSF	MultiStage Flash evaporator
Npep	Non Propulsion Electric Power
OFBs	Oil Fired Burners
Pprop	Propulsion Power
Ptot	Total electric power
PM	Particulate matter
PMs	Prime Movers
RO	Reverse Osmosis
S	Summer
SCR	Selective Catalytic Reactor
SECA	SOx Environmental Controlled Area
SEEMP	Ship Energy Efficiency Management Plan
TH	Tanks Heating
Trigen.	"One-kind" (namely GTs) engines' configurations with the absorption chillers' adoption for chilling porpoises
W	Winter
WHR	Waste Heat Recovery

List of Figures

List of Tables

Chapter 1

INTRODUCTION

1.1 Maritime sector environmental impact

Reporting what the International Energy Agency (IEA) assessed in its final report, Greenhouse gas (GHG) emissions from the transport sector have more than doubled since 1970, and have increased at a faster rate than any other energy end-use sector [1]. Within which, the shipping industry is the most energy efficient and its efficiency is still increasing [2], still more and more research is revealing the severity of ship's emissions. Ship's emissions include not only those leading to global warming but also those responsible for other environmental problems, such as NO_x and SO_x.

Maritime transport sector consists of a heterogeneous group of vessels, but for the sake of simplicity, it could be divided into two major classes depending on their main purpose: "goods transport" (cargos, bulk carriers, merchants fleet) and "passenger transport" (ferries, cruise ships). Each one of these classes is important in its sector: the first class accounts for 90% of the overall worldwide transportation [3] and the second has doubled its market in the last decade [4].

The Mediterranean is the world's second largest cruise shipping market: it represented 21.7% of the annual cruise capacity for 2013 while the anticipated value for 2014 is 18.9% [4], [5]. In 2013 a total of 166 cruise ships were active in Mediterranean waters, with a capacity of 220,352 beds and an average of 1327 beds per ship [4], [5].

It is clear that vessel's engines have to burn fossil fuels to conduct their activities, causing both GHGs and non-GHGs emissions. The former are responsible for the climate change, the latter for acid rain, the agricultural yields decrease, water contamination, modification of soil biology, deforestation and for damaging monuments.

GHGs includes six gases and they are carbon dioxide (CO_2), methane (CH_4), nitrous oxide (N_2O), hydrofluorocarbons (HFCs), perfluorooctane sulphonate (PFCs), and sulphur hexafluoride (SF_6). The first, whose emission level has doubled in the last two decades, is the most significant for the shipping industry representing 3% of global CO_2 emissions. Figure 1-1 reports the global CO_2 emissions from shipping observed in the period from 2000 and 2007.

From Figure 1-1, it can be noted that in 8 years, global CO_2 emissions have seen an

increase equal to 31%, reaching, in the 2007, the total amount of 1050 Mt.

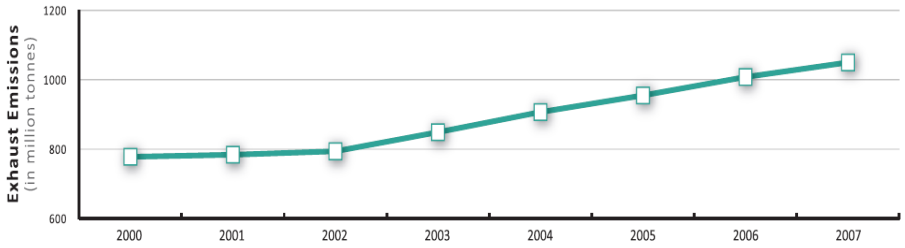

Figure 1-1 GHGs emissions from shipping maritime sector [2]

Other GHGs represent 21 Mt of CO_2 equivalent, and emissions of PCFs and SF6 can be considered negligible [3].

Sulphur oxides (SO_x), nitrogen oxides (NO_x) and particulate matter (PM) are the non-GHGs emissions that have to be considered the most. According to the IMO [3] in 2007 the shipping industry emitted globally 15 million tonnes of SO_x and 25 million tonnes of NO_x, meaning 50% and 39% more than their 1997 levels respectively. Likewise, PM emissions increased by 50% in ten years [3].

Global NO_x and SO_x emissions from all shipping represent about 15% and 13% of global NOx and SO_x from anthropogenic sources reported in the latest IPCC Assessment Report (AR5); international shipping NO_x and SO_x represent approximately 13% and 12% of global NO_x and SO_x totals respectively [6].

The global trend of NOx, SOx, PM, CO and NMVOC emissions caused by the shipping sector is depicted in Figure 1-2.

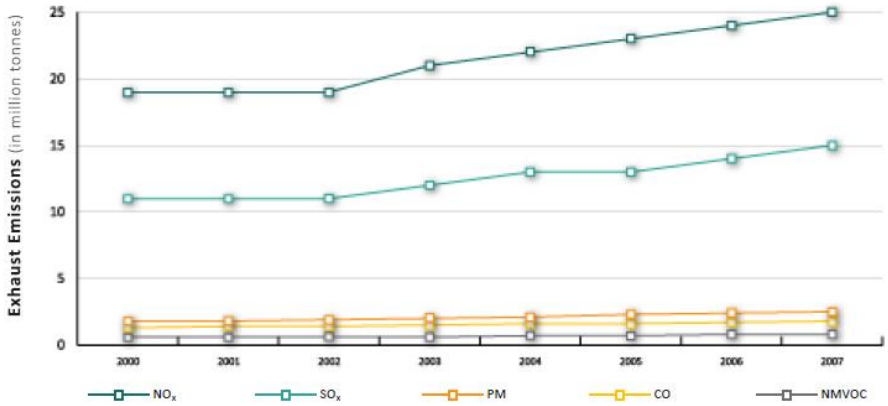

Figure 1-2 Non GHGs emissions from maritime sector [2]

Analyzing Figure 1-2, it can be inferred that both NOx and SOx emissions are increased of 32% and 36% respectively. On the other hand, it has been not registered any strong increase in the other pollutants' emissions in 8 years.

It is also well worth reminding that engines employed on board are always switched on, even if they are at berth (in particular for those vehicles that require a non–propulsive

load, e.g. cruise ships). Knowing that, to study the environmental impact of the shipping industry, ship's activity can be divided into three different moments: 1) International Waters; 2) National Waters and Harbor maneuvering; 3) Berth. To underline the importance of this classification, a 2003 paper [7] suggests that 70% of the total ship's emissions occur within 400 km from land.

1.2 IMO Regulations

Emissions trading, financial incentives/taxes, emission reporting/monitoring obligations and energy efficiency/emissions standards are regulators and policy makers most used mechanisms in order to reduce the environmental impact connected to the shipping industry. The most noteworthy regulator in the shipping industry is the International Maritime Organization: a specific branch of the United Nations, whose aim is to develop and maintain a regulatory framework for shipping.

Shipping's GHG emissions are currently not regulated by the United Nations Framework Convention on Climate Change (commonly known as the Kyoto Protocol). This is due to the particular nature of the maritime transport sector: indeed there can't be a lone country responsible for emission of an oceangoing ship. Nevertheless, the international shipping community believed that the only way to reduce emissions from the shipping industry was to have IMO directing the measures [8].
In January 2013 IMO introduced two new policy mechanisms aiming a cutting down in GHG emissions: the "Energy Efficiency Design Index" (EEDI) and the "Ship Energy Efficiency Management Plan" (SEEMP). The first one is determined by Eq. (1-1):

$$EEDI = \frac{P_{ME} \times C_{FME} \times SFOC_{ME} + P_{AE} \times C_{FAE} \times 9m_{AE} - f_{eff} \times P_{AEeff} \times C_{FAE} \times SFOC_{AE}}{Capacity \times V_{ref}} \quad (1\text{-}1)$$

where

- $EEDI$ is given in gCO_2/ton/miles
- C_F is a conversion factor between burnt fuel amount (in g) and CO_2 emissions (also in g) and is based on fuel carbon content taking values 3.15 g CO_2/g fuel for the case of light Diesel fuel, 3.206 g CO_2/g fuel for the case of heavy Diesel fuel and 2.750 g CO_2/g fuel for the case of Liquefied Natural Gas (LNG);
- ME and AE refer to the main and auxiliary engine(s), respectively;
- $Capacity$ is taken the ship deadweight (DWT) for the cargo ships and the ship gross tonnage for the Ro-Pax ferries;
- P_{ME} is defined as the 75% of the rated installed power of the main engine after having deducted any installed shaft generator power;
- P_{AE} is the required auxiliary engine power to supply normal maximum sea load including necessary power for propulsion/machinery systems but excluding any other power e.g. ballast pumps, thrusters, cargo gear, etc., in the condition where the ship engaged in voyage at the speed V_{ref} under the design loading condition;

- P_{AEeff} is the auxiliary power reduction due to innovative electrical energy efficient technology (e.g. waste heat recovery) measured at P_{ME};
- f_{eff} is the availability factor of each innovative energy efficiency technology;
- $SFOC_{ME}$ and $SFOC_{AE}$ are the brake Specific Fuel Oil Consumption (SFOC) (in [g/kWh]) of the main and auxiliaries engines at the 75% and 50% engine loads, respectively.

Both "energy efficiency/emissions standards" mechanisms are the first mandatory GHG regulations for the shipping industry. These mechanisms are applied to all ships of 400 tons gross tonnage. While the EEDI sets the minimum energy efficiency standard for new ships, the SEEMP enables ship owners to measure the fuel efficiency of existing ships and to monitor the effects of any changes in operation [9]. Based on the EEDI, the CO_2 reduction level (grams of CO_2 per ton/mile) for the first phase (2015-2019) is set at 10% and will be tightened every five years. The baseline is the average efficiency for ships built between 2000 and 2010 [9].

Non-GHG emissions are also regulated by the IMO. The most prominent convention the International Convention for the Prevention of Pollution from Ships (Maritime Pollution, MARPOL), was adopted in 1973 and targets several aspects of air pollution. "Annex VI," which was added to the convention in 1997, addresses exhaust gas emissions such as SO_x, NO_x, and particulates [10]. Regulations apply to both newly built and existing ships. Given that NO_x and SO_x emissions caused by ships have been increasing in the last year, as stated above, IMO is setting lower threshold values. Particular attention has been given to sea areas (called SECA) considered to be in need of a more immediate intervention. There are currently four active Emissions Control Areas (ECAs) in the world:

- Baltic Sea area: only for SO_x;
- North Sea area: only for SO_x;
- North American area: for SO_x, NO_x and PM;
- United States Caribbean Sea area: for SO_x, NO_x and PM (came into force in January 2013 and will be in effect from January 2014).

Some new ECAs in the Mediterranean region, Singapore and Japan may enter into force in the coming years.

The map shown in Figure 1-3 shows the current and upcoming ECAs.

SO_x and NO_x emissions are separately treated: each one having its own sets of regulations and threshold values to observe. A timeline has also being scheduled, to describe further and future emissions limits ships will have to attend to.

MARPOL addresses to NO_x pollutants with three tiers: each tier consisting in a description of limits imposed on ships in relation to ICEs engine's RPM, as reported in Table 1-1.

Nowadays only ships travelling in the SECA areas have to observe emission limits of tier III, but starting from January 1st 2016 every ship will have to.

Figure 1-3 Actual ECA areas and future ones [11]

Table 1-1 IMO NO_x limits as a function of ICEs' speed (g/kWh) [11]

MARPOL Tier	RPM<130	130<RPM<2000	RPM>2000
Tier II	14.4	$44 \times RPM^{-0.2}$	7.7
Tier III	3.4	$9 \times RPM^{-0.2}$	2

For example for a medium speed Internal Combustion Engine (ICE) the threshold limit values imposed by Tier II and Tier III, are described by the following equation (corresponding to those reported in Table 1-1's second column) respectively [11]:

$$NO_x = 44 \times RPM^{-0.2} \quad \text{[g/kWh]} \quad (1\text{-}2)$$

$$NO_x = 9 \times RPM^{-0.2} \quad \text{[g/kWh]} \quad (1\text{-}3)$$

Regarding SO_x emissions, MARPOL currently sets limits on the fuel's sulphur content differentiating from SECA and not-SECA areas. Ships travelling in the SECA seas have to use fuel with less than 1% sulphur content. Outside the SECA the limit imposed is set at 3.5%. A year from now limits will be lowered to 0.1% in SECA areas and starting from 2020 also non-SECA areas will be subjected to a drastic reduction of the sulphur threshold value of the fuel employed at 0.5% [11], see Table 1-2.

Table 1-2 IMO fuel Sulphur content limits [11]

%S content	Area	Year
3.5	Not-SECA	now
1	SECA	now
0.5	Not-SECA	2020
0.1	SECA	2015

Actual threshold limit values and the upcoming ones are reported in the graphs in Figure 1-4 (a) and (b) for SO_x and NO_x emissions respectively.

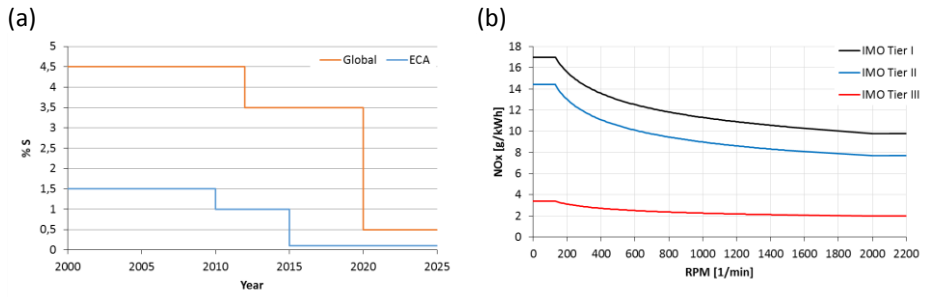

Figure 1-4 Threshold limits value: (a) SOx, (b) NOx [11].

Since fuel's quality have a strong influence on the ship's emissions, an overview on available fuel's variety has to be done.

1.3 Ship Fuel

A brief description of different fuels, used for maritime purpose, is depicted below. They are Heavy Fuel Oil (HFO), Marine Gas Oil (MGO), Marine Diesel Oil (MDO). The main difference is ascribable to the fact that the first one is the residual oil produced by the oil refinery process and the others are distillates obtained through the same process. The different level of oil refining involves dissimilarities concerning viscosity, density, flash point, and pour point. Another fuel, named Intermediate Fuel Oil (IFO) is also considered, whose peculiarity lies on the fact that it is a residual oil mixed with distillates.

At the end, a remark of Liquefied Natural Gas (LNG) has been given.

Among maritime fuels, HFO has extreme "performances": it is the cheapest and the most polluting: indeed the highest level of Sulphur is contained in the heaviest fractions of the distillation column. According to [7] the average Sulphur content of HFO worldwide being 2.7% mass.

Reporting what the "Second IMO GHG Study", which has been carried out in 2009, HFO is the most used fuel in the world [2] thanks to its cheapness.

MGO is a light distillate fuel containing light aromatic hydrocarbons and no residual components, while MDO is a heavier distillate and may contain residual fuel oil. Furthermore, distillate fuels contain lower levels of sulphur, water, metals, ashes and carbon residues.

For further considerations, see Table 1-3.

LNG is colorless, odorless, flammable, ignitable by static electricity, extremely cold and volatile liquid. The boiling point is -161.5°C at normal conditions whereas the flash point is -187.8°C. By comparison to HFO tanks, LNG tanks ought to be about 2.5 times bigger by reason of smaller density and needed thermal shield [12].

LNG can be regarded as the best fuel for reducing non-GHGs emissions; indeed, burning it results in no SO_x and negligible NO_x and PM emissions. For what GHGs emissions are

concerned, thanks to its higher hydrogen-to-carbon ratio, LNG is less CO_2 intensive than oil.

Table 1-3 Fuel type and relative characteristics [13].

Fuel Type	Characteristics
Marine Gas Oil (MGO)	Light distillate fuel, low viscosity, low levels of impurities
Marine Diesel Oil (MDO)	Heavier distillate, may contain some residual components
Intermediate Fuel Oil (IFO)	Heavy fuel oil that might contain distillate fuel
Heavy Fuel Oil (HFO)	Residual fuel with the highest viscosity and highest levels of impurities

On the other hand, the ‘‘methane slip’’, which is the unburned methane emitted from its combustion, is important to be looked at since it has great a great impact on the atmosphere. That’s because CH_4 has 25 times higher global warming potential (GWP) than CO_2 over a 100-year perspective [14]. More than 90% reduction of the methane slip may occur with an oxidation catalyst, but this hasn’t been tested so far [15].
Along with the methane slip issue, other considerations have to be done when considering the possibility to use LNG as fuel.
One of the most important problem concerned to the LNG’s use seems to be LNG market: lack of much usable supply chain for distributing the fuel [16]. Besides that, there are also technical problems, which the shipping sector has to be confronted. Firstly, the cryogenic temperature associated with LNG systems creates a number of generalized safety considerations for bulk transfer and storage. Most importantly, LNG is a fuel that requires intensive monitoring and control because of the constant heating of the fuel, which takes place due to the extreme temperature differential between ambient and LNG fuel temperatures. Even with highly insulated tanks, there will always be a continuous build up of internal pressure and a need to eventually use the fuel vapor or safely vent it to the atmosphere. When transferring LNG, considerable care has to be taken to cool down the transfer lines in order to avoid excessive amounts of vapor from being formed. The constant vaporization of the fuel also has an interesting effect on the properties of the fuel: the methane in the fuel will boil off before some of the other hydrocarbon components such as propane and butane. Therefore, if LNG is stored over an extensive period of time without withdrawal and replenishment the methane content will continuously decrease and the actual physical characteristics of the fuel will change to some extent.

1.4 Companies’ point of view

In 2013, the shipping company Maersk published a materiality matrix, reported in Figure 1-5, showing which Environmental, Social and corporate Governance (ESG) issues are prominent to the business and to stakeholders (i.e. employees, suppliers, customers, communities etc.).

From Figure 1-5, it can be seen that the fourth most important aspect to the business, i.e. to the company, is related to SO_x. Other sustainability issues such as CO_2 emissions, energy consumption and NOx emissions rank fifth, seventh and eleventh, respectively. It is expected that, as soon as regulations on NO_x become more stringent, NO_x will rank among the top five most mattering sustainability issues. Other companies releasing a materiality matrix, such as Pacific Basin, are making similar observations.

1.4.1 Innovative solutions and strategies reviews

As a consequence of the forthcoming limits and regulations, ship-owners will have to adopt new strategies and solutions in order to be IMO compliant. In order to respect EEDI and SEEMP, ships have to be more efficient in terms of fuel consumption. The minor fuel consumptions could bring a reduction also to SO_x emissions. Along with ship's efficiency improvement, other interventions have been made to meet with the new and stricter non-GHGs emissions limit values.

One measure to overcome the GHGs problem is to enhance the efficiency of engines. Technologies exist that can help ship engines reduce emissions by potentially 40% [17]. At present, Wärtsilä, Rolls-Royce, MAN and Caterpillar, are those shipping companies which can be considered the best in the market to benefit from the new regulations on shipping emissions.

The EEDI will require ship builders to pay greater attention to ship's energy efficiency. As many studies confirmed, the best way to improve the ship's energy efficiency is recovering the waste heat produced by the engines. The most studied waste heat recovery (WHR) systems are cogeneration systems, trigeneration systems, Organic Rankine cycle, combined cycle.

As already outlined above, using low-sulphur fuel is the easiest method to overcome the SO_x issue. Despite being the easiest method, switching kind of fuel could be that much expensive that other solutions could be much more feasible.

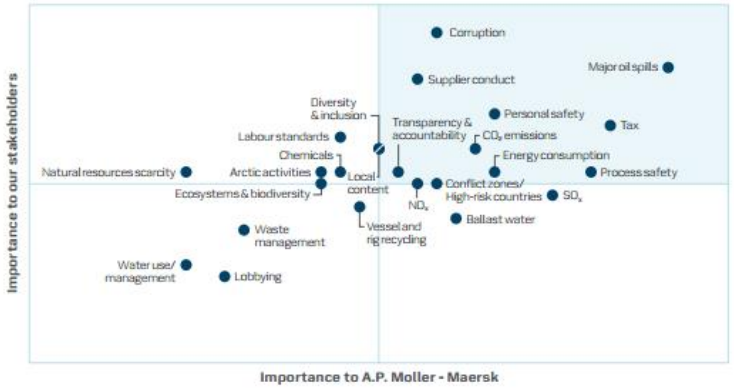

Figure 1-5 Materiality matrix of the most important issues to the stakeholders [18]

In 2012, Lloyd's Register, a voluntary association of ship owners, ship builders, engine builders, and insurance underwriters, made a survey asking 14 of the world's leading

shipping companies about their intention on implementing technologies to mitigate SO_x emissions [19]. What emerged are four types of solutions:

- Using MGO
- Using dual-fuel usually made of natural gas and diesel
- Using scrubbers
- Using LNG.

Among these, employing low-sulphur fuel is currently considered the best short-term solution for mitigation, with scrubbers being a better in the medium term, and dual-fuel/ LNG being considered as longer-term solutions [19], as it can be seen in the graph below. Despite of being a possible achievable solution, using LNG has problems concerning safety (high flammability and toxicity [8] as well as lack of infrastructures, as already mentioned above. Currently, the most developed network of LNG-fuelled ships and LNG bunkering is in Norway, whose flag is flown by 22 of 23 LNG ships operating in SECAs [20].

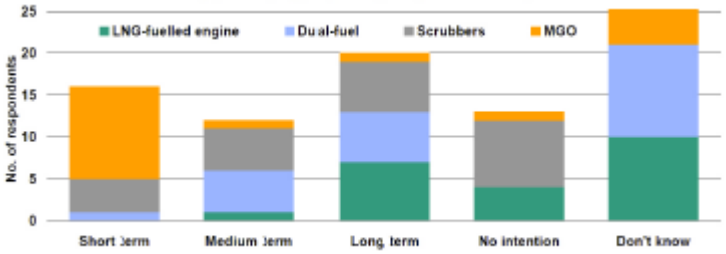

Figure 1-6 Owner survey in order to meet the new emissions regulations [19]

From Figure 1-6, it can be concluded that two alternatives are at hand to cut down SOx emissions: either equipping ships with a DeSOx system called “scrubber” or substituting the currently used fuel with a sulphur-free one, for instance MGO.

To cut down NOx emissions, switching type of fuel would not dispense ships from having to install a specific abatement device, even if there is an ongoing evolution of combustion systems of diesel engines. Selective Catalytic Reduction (SCR) systems are the most frequently used, this due to their capability to achieve such an high decrease in NOx emissions to comply with the Tier III NOX standards, as shown in the graph reported in Figure 1-7 [21].

Abatement devices, along with their auxiliaries, occupy room and increase the overall weight of the ship; as well as worsen the fuel consumption due to the bigger electric load.

Being saving space and weight a big issue for the maritime sector, a completely different solution could be taken into account, namely the use of MGO to get SOx free emissions and the consequent use of Gas Turbines (GTs) in place of ICEs. This drastic modification of the power generation system aims at reduce weight and increase room.

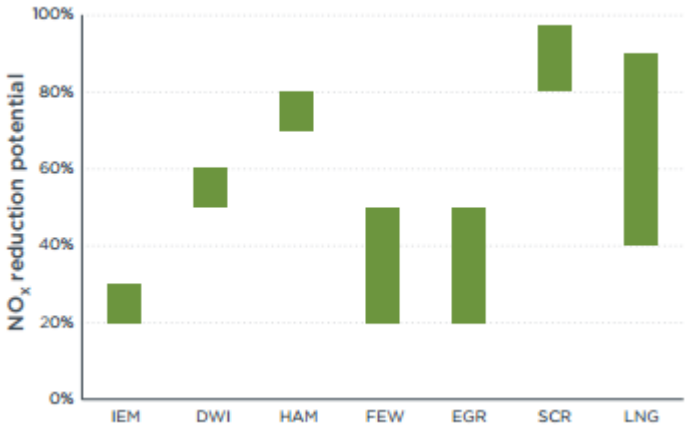

Figure 1-7 Shipping NO_x reduction potential. IEM: Internal Engine Modification, DWI: Direct Water Injection, HAM: Humid Air Motors, FEW: Fuel Water Emulsion, EGR: Exhaust Gas Recirculation, SCR: Selective Catalytic Reduction, LNG: Liquefied Natural Gas [21].

Adopting MGO fueled GTs instead of using ICEs means relying on fuel and combustion system characteristics sufficient to get pollutant emissions level compliant with the IMO regulations.

Moreover, due to the high rotational speed at which GTs usually operate, the generator paired to them is not as big as that of an ICE; meaning a further reduction in weight and space occupied. Finally, as shown in a recent industrial research project [22], these power generation and conversion system are well coupled with a power grid working in Medium Voltage Direct Current (MVDC). The choice of MVDC grids to power a large ship is a novel and interesting solution that is currently under investigation by many ship designers. That would enhance the electrical grid dynamic behavior during sudden power demand, achieving a better voltage control using controlled power converters and storage systems. It wound also improve the network quality of service and fault tolerance, as the DC grid is independent of frequency, and is assisted by storage systems; enhance the power control in different modes of operation, by exploiting the Direct Current (DC) distribution power converters to feed the variable-speed motors.

As can be easily foreseen the drawback of this solution is the negative gap that is found in the energy conversion efficiency of GTs with respect to ICEs, and in the higher cost of MGO with respect to HFO. In order to evaluate the technical and economical feasibility of this solution it is mandatory to be able to quantify the positive aspects coming from room and weight savings against the effective increase of fuel consumption. This evaluation is not trivial, since a ship is a closed and complex energy system, which operation profile might be extremely variable, and where energy recovery strategies are always implemented in order to reduce the waste heat by a partial cogeneration of the thermal loads. With particular regard to this latter aspect, it is also important to consider that thanks to the high temperature of GTs exhaust gas flows, a higher energy recovery can be achieved, hence reducing the initial efficiency gap between GTs and ICEs intended as prime movers.

As today, not that many studies have been conducted about the adoption of Gas Turbines as prime movers. However, there are a few examples of existing cruise ships having this configuration: one of them is the ship "Millennium" launched in the year 2000. The Millennium has a power plant consisting in a combined cycle of two 25MW "LM2500+" gas turbines burning MGO, followed by a 9MW steam turbine, which is powered by the GT's exhaust flows heat. As for the higher cost of MGO, if compared to a similar ICEs engined ship, the adoption of GTs resulted in a reduction in fuel consumption, pollutant emissions, as well as a notable saving of weight and volume. Furthermore, the reduction in weight meant the ship has a lower demand of propulsion power, allowing to install a smaller capacity engine. To give some numbers, fuel consumption is 7% lower [23], NOx and SOx emissions are 80% and 98% less respectively [24], and 50 [23] more cabins have been fitted thanks to the smaller engine.

1.5 Thesis objective

The present thesis aims at quantifying the gap between new-IMO-regulations-fulfilling and the actual engines configurations employed on board of a cruise ship. Indeed, quantifying the gap existing between different engines' configurations, which could be employed on board, should result of help for ship-owners and designers in order to take the best solutions from three different points of view. Indeed, in the present work, the environmental, energetic as well as weight & volume aspects have been taken into account, on which the quantitative analysis has been focused. All these points of view, are extremely important for the maritime sector, in particular for cruise ships.

Cruise ships are particularly demanding, in terms of energy systems, due to the versatility of their energy needs. Cruise liners have a passenger capacity of a few thousand persons with a crew of several hundreds. The principal energy demands of such vessels are propulsion power, electricity for covering the hotel related loads and heat in the form of water or low pressure steam for heat driven auxiliary equipment and sanitary purposes.

A multitude of feasible engines' configurations as well as waste heat recovery options have been explored with the use of an optimization procedure.

Optimization methodologies have been widely used for the design of land based systems in the energy production and process industry sectors. However, there are only a few optimization studies regarding marine energy systems (e.g. [25],[26]).

A real cruise ship's operation profile has been used as case study but the methodology followed in the present thesis can be applied to other real case studies.

Scope of the optimization problem is minimizing the amount of fuel burned during the whole cruise. Environmental results are determined consequently.

The optimization problem under consideration is a particularly difficult one, since it includes non-linear relations and constraints. This problem falls under the general category of Mixed Integer Non-Linear Programming (MINLP) problems.

Part I

Methodological approach and model description

Chapter 2

CASE STUDY

The cruise ship, taken as reference and shown in Figure 2-1, is the hull C.6194 of Fincantieri S.p.A. having 66000 Dead Weight Tonnages (DWT)[1]. An Integrated Power System (IPS) based on a diesel-electric propulsion system characterizes this project.

Figure 2-1 Reference cruise ship, the hull C.6194 of Fincantieri S.p.A.

Firstly, a description of what consists both diesel-electric propulsion system and IPS is given below in order to provide a better ship's system knowledge.

2.1 Diesel-Electric propulsion

Electric propulsion systems were developed in the early 1900s with the scope to improve the coupling between prime movers and propellers working at different spinning velocity. In the electric propulsion system, each propeller is started by an electric motor in place of traditional diesel engine, a static converter is also employed to power the propeller and control its velocity.

In 1920, US Navy launched the "New Mexico" combat-vessel that could be considered the first application of a diesel-electric propulsion system. For what the civil sector is concerned, the British "Viroy of India" and the German "Patria" were the first. Despite

[1] Dead Weight Tonnage is a measure of how much mass a ship is carrying or can safely carry and it does not include the ship's weight. DWT is the sum of cargo, fuel, fresh water, ballast water, provisions, passengers, and crew weights.

of being highly used during the 2nd World War, this kind of propulsion was slowly abandoned, and only in the last two decades it has been taken back into consideration. An increase of ship's energy demands, a high ship's maneuverability, the capability to make rapid inversion maneuvers and the need to navigate in environmentally controlled seas are primary reasons, which led to the reevaluation of diesel-electric propulsion system as a good option for some kind of vessels, cruise ships above all.
Cruise ships can benefit from adopting diesel-electric propulsion system for these reasons:

- Low noise and vibrations
- Maximum pay-load capacity and optimal utilization of available space by reduced volume and decentralized arrangement of components of the propulsion system
- Cost-effective operation due to the possibility to match the number of supplying generators according to the power demand so that loads of the diesel generator sets are prevented
- Redundant configuration which improve reliability and ship's safety
- Flexible use of the torque-speed characteristic
- Capability of changing speed and reversals at maneuver and positioning
- No interference of the mains due to inadmissible harmonics
- Reduced emissions of NO_x, SO_x, CO, HC and soot as well as reduced fuel consumption: the diesel motors operate with constant speed in the optimal operational range as well as at partial load
- High degree of automation
- Reduced maintenance expense and spare parts demand compared with diesel mechanical driven ships: fewer diesel motors are needed as well as cylinders.

On the other hand, this kind of propulsion requires bigger economical efforts because of all the electronic devices and regulation systems it needs.

2.1.1 IPS electric propulsion

Based on diesel-electric propulsion, IPS's main goal is to distribute the electric power through a single power grid to satisfy both the propulsion and the ship's electric demand. IPS provides a better structural efficiency than standard electric configuration thanks to the possibility to regulate the alternators regime following the loads of diesel engines employed on board.
Benefits from adopting such a system are those owing to diesel-electric propulsion but, highlighting the issue concerning ship room's organization and arrangement, it can be said that the possibility to spatially separate propellers and prime movers is fundamental. Indeed, due to the absence of an only shaft power, room for "host payloads" can be increased. Moreover, the lack of electric generators for on-board purposes, which are now satisfied by the same power plant used for propulsion demands, increases furthermore payload's room as well as reducing the weight of the ship.

The Figure 2-2 shows the difference between the two configurations: (a) standard, (b) IPS.

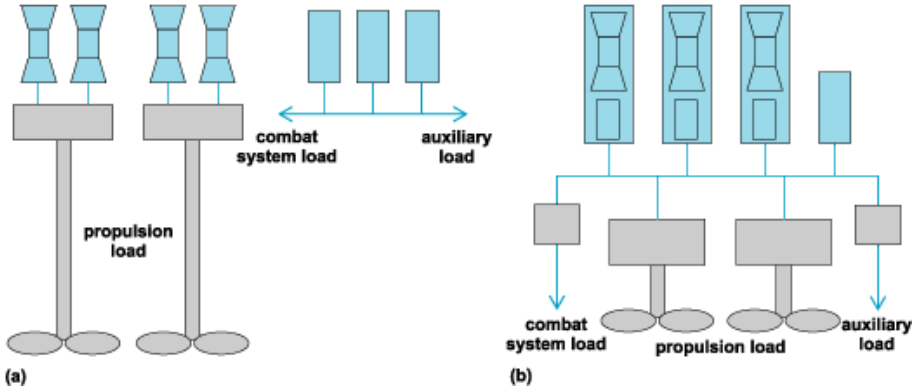

Figure 2-2 Diesel-elecctric propulsion system configurations: (a) standard, (b) IPS

2.2 The Hull C.6194

The hull under examination is used in a touristic cruise between Barcelona and Venice. Fincantieri S.p.A. has supplied the documentation reporting the real operation profile within a research project in which Department of Electric, Mechanic and Management Engineering of the University of Udine collaborated as a partner [22].

To analyze properly the operation profile, the whole cruise has been divided into three phases: harbor, maneuvering and navigation.

Based upon data of 12 journeys connecting two harbors it is safe to say that Harbor and Maneuvering are the more time-consuming, indeed time spent in those two phases accounts for 46% and 47% of the whole cruise respectively. These figures come from a preliminary operation profile's study phase.

Each phase is characterized by a specific electric and propulsive demand. Moreover, along with the electric and propulsive ship's request, total thermal loads are obviously analyzed.

It has to be said that electric and thermal loads vary also with season. Design data are given (by the constructor) for summer and winter, which are characterized by extreme sea and external air temperatures. In order to resemble real operational conditions, an intermediate season has been also taken into account, named autumn, and characterized by moderate temperatures, see Table 2-1.

2.2.1 Electric load

The electric load is split between Propulsion and Non-Propulsion Electric Load, which is also known as Accommodation Electric Load. As can be easily argued, Propulsion load changes only with the cruise phase (and it's obviously equal to 0 in harbor condition), while Non-propulsion electric load vary both with cruise phase and season. For what the last aspect is concerned, intermediate season's Non-Propulsion Electric Load (in particular the chilling load) has to be determined.

Table 2-1 Air, sea and internal temperatures for the different season considered [°C].

		t_{air}	t_{sea}	t_{in}
Season[2]	Winter	-10	0	18
	Summer	45	32	
	Autumn	18	16.5	

It seems quite clear that Propulsion demand is strictly linked to the navigation speed. The correlation is illustrated in the Figure 2-3, where, for sake of clarity, 1 knot corresponds to 1.85 km/h.

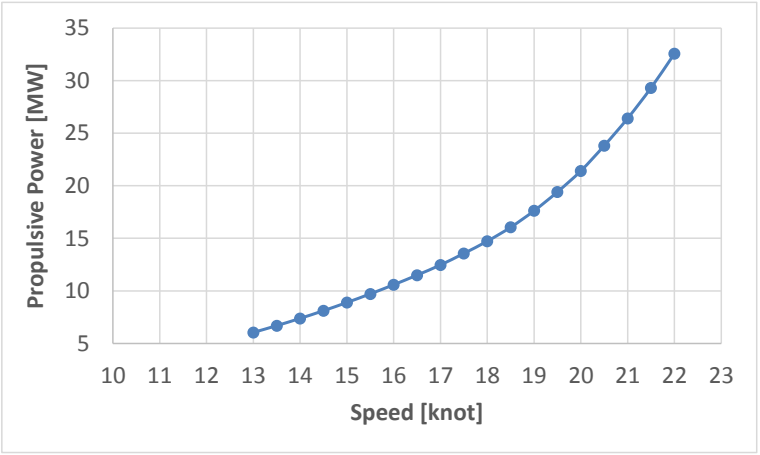

Figure 2-3 Speed and Propulsive Power demand correlation. Data obtained from [27].

For the cruise under study, the speed requested for the different navigation phases is reported in Table 2-2.
For safety purposes, a "sea margin" factor of 15% of the Propulsive Power demand is also taken into account. In this way, the Power Demand that has to be satisfied for propulsive purposes is given by Eq. (2-1):

$$Propulsive\ Power\ Loads = Propulsive\ Power \times (1 + Sea\ Margin) = Propulsive\ Demand \times 1.15 \quad (2\text{-}1)$$

Non-propulsion demand is made of auxiliary loads and, just for maneuvering phase, tunnel thrusters' loads. The former include services inherent to hull and deck operations, safety devices, engine room's requirements, galley demands, accommodation and lightening facilities. In addition to the above-mentioned "items", Auxiliary loads account also for chilling loads whose variations, due to seasonal changes, involve the main differences in Non-propulsion loads during the year.

[2] For sake of brevity, here after, Winter, Summer and Autumn will be recalled as W, S and A respectively.

Table 2-2 Propulsive Power requests during the navigation phase for the reference cruise ship [27].

Journey	Harbor		Journey Duration [h]	Speed [knot]	Propulsive Power [MW]
	Departure	Arrival			
1	Barcelona	Sète	9	17.7	13.5
2	Sete	Marseille	10	8.7	2.3
3	Marseille	Villefranche	12	8.3	2.1
4	Villefranche	Portofino	11	9.4	2.6
5	Portofino	Livorno	11	6.9	1.6
6	Livorno	Olbia	10	18.7	16.5
7	Olbia	Civitavecchia	11	13.1	5.4
8	Civitavecchia	Amalfi	10	17.7	13.6
9	Amalfi	Sorrento	1	13	5.3
10	Sorrento	Corfu	36	12.7	5
11	Corfu	Dubrovnik	12	19.1	18.2
12	Dubrovnik	Venezia	18	19.2	18.4

The reference cruise ship has four 800 kW compressors each, whose Coefficient Of Performance (COP) is equal to 4.9, to cover the chilling load [27].
The overall Non-propulsion electric load and the chilling load are reported in Table 2-3 and in Table 2-4 respectively, where the differences due to seasonal and cruise's phase variations are highlighted. Autumn's chilling load, which wasn't considered in the Fincantieri's reporting documentation, has been determined as the average between those relative to winter and summer.

Table 2-3 Overall Non-propulsive electric load for every cruise's phase and season [MW] [27].

	Harbor	Maneuvering	Navigation
W	7.5	11.7	9.3
S	8.7	12.9	9.9
A	8	12.3	9.7

Table 2-4 Chilling load [kW] [27].

	Harbor	Maneuvering	Navigation
W	310	310	1530
S	1550	1550	2184
A	930	930	1856

The Diesel Brake Power (DBP), namely the overall electric power that has to be fulfilled by the diesel engines employed on board, is the sum of Non-propulsive and Propulsive load. But, to be properly determined: alternator, electric motor, frequency converter

and propulsion transformer efficiencies have to be taken into account. Because of the absence of Propulsive loads in harbor, the formula to calculate DBP is different if harbor or maneuvering/navigation is considered, as reported in Eq.(2-2) and in Eq.(2-3) respectively:

Harbor:

$$DBP = \frac{Non\ propulsive\ loads}{\eta_{alt.}} \qquad (2\text{-}2)$$

Navigation/Maneuvering:

$$DBP = \left[\frac{Propulsive\ Power\ Loads}{(\eta_{elec.mot.} \times \eta_{freq.conv.} \times \eta_{prop.trans.})} + Non\ propulsive\ loads\right] \times \frac{1}{\eta_{alt.}} \qquad (2\text{-}3)$$

where:

- $\eta_{alt.}$ and $\eta_{elec.mot.}$ are equal to 0.97
- $\eta_{freq.conv.}$ and $\eta_{prop.trans.}$ are equal to 0.99

Figure 2-4 shows the Diesel Brake Power (corresponding to colored solid lines and labeled as EL in the graph) variation during the whole cruise in which hours of navigation add up, have been taken as *x-axis* reference. The colored dashed lines and the black solid line are representative of the Non-propulsive Loads (npep) and the Propulsive Power Loads (EL_prop) respectively.
Given that DBP is the sum of Propulsive Power Loads and Non-propulsive Loads, follows that power demand in summer is the highest due to the biggest Non-propulsive Loads demand.
Moreover, the Figure 2-4 shows the base load (approximately one fourth of the peak load), at which the ship operates for the 42% of the whole cruise, which represents also the minimum working load.
In terms of propulsion system optimization, this operational condition is quite heavy. To maximize the energy conversion efficiency, prime movers (PMs) need to be operated at maximum efficiency regimes as long as possible; condition which is usually next to its nominal power. It is well known that having an engine providing maximum efficiency levels for all these different loads, is not technically possible. To overcome this, and in order to obtain the highest energy conversion efficiency as possible, an option is splitting the installed power on more small engines. This way, it is possible to properly cover the electric load thanks to, not only the engine load modulation, but also the possibility to decide which and how many engines to switch on.
To properly satisfy all these loads, the ship under exam is equipped with two kinds of ICEs:

- 2*8.4 MW, namely WÄRTSILÄ8L46C
- 2*12.6 MW, namely WÄRTSILÄ12V46C

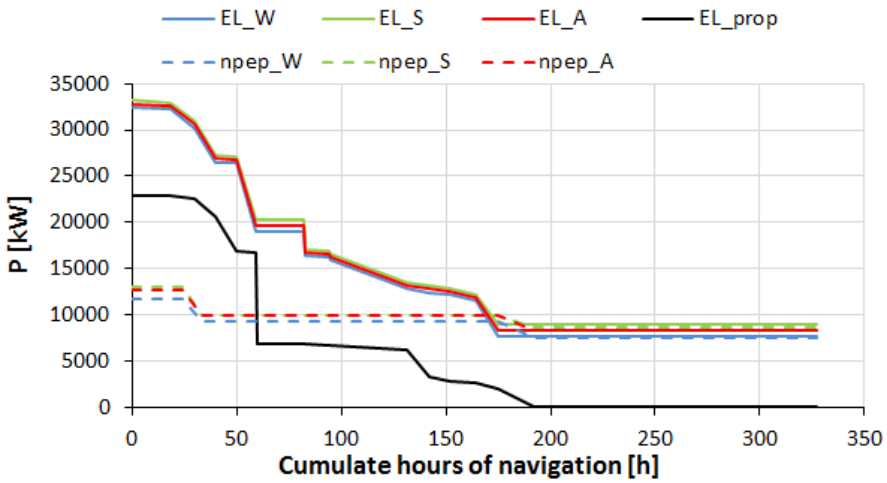

Figure 2-4 Variations of Diesel Brake Power during the cruise. Data obtained from [27].

This way the total power installed on board is 43 MW. For a complete analysis of these kind of ICEs, lectures should refer to 3.1.1.
Having introduced the concept of DBP, it considers worthwhile making readers acknowledged of another important parameter, namely the Maximum Continuous Rating (MCR). In general, it indicates the maximum power supplied by an engine. Nevertheless, in the literature it is easier to find the "%MCR" term, which stands for the percentage of available power used. This means that %MCR is the DBP, compared to the total power available, resulting from switching on one or more engines, as reported in Eq. (2-4):

$$\%MCR = \frac{DBP}{Engines'\ total\ available\ power} \qquad (2\text{-}4)$$

In the present work, %MCR has been used.

2.2.2 Thermal load

The considered cruise ship has an overall thermal load composed by three macro-poles:

- Tanks Heating (TH)
- E.R. Users (E.R.)
- Accommodation (ACC.)

"Tanks heating" and "E.R. Users" loads are thermal energy demands of all the devices handling fuel and lubricants. They are directly proportional to the amount of fuel burned. In particular, "Tanks heating" thermal load is necessary to keep HFO, which is burned in the reference ship's engines, at a constant temperature of about 50°C, at which its viscosity is kept low enough to be pumped into the engine.
"Accommodation" thermal load includes thermal loads deriving from "hotel" services. These can be divided in five main sub-poles:

- Air pre- and re-heating,
- Water heating,
- Swimming Pool heating,
- Galley purposes,
- Laundry services.

It's clear that the different ambient conditions occurring during the year cause thermal loads to change. In particular, calculations to determine the thermal load for the new intermediate season have to be made, similarly to what has been done for the chilling load.

For example, autumn "Tanks heating" thermal load has been determined using the Eq. (2-5), whose formula is based on the fact that fuel's tanks are placed below the "sea-line" and therefore they must be heated accordingly to the sea temperature in order to prevent fuel from the viscosity's increase. The above-mentioned equation is reported below:

$$Ct_A = Ct_W * \frac{(t_f - t_{sea,A})}{(t_f - t_{sea,W})} \qquad (2\text{-}5)$$

where:

- Ct_W is the winter thermal load for the tanks heating [MW]
- t_f is the temperature at which the fuel has to be held (app. 50°C)
- $t_{sea,A}$ is the sea temperature in autumn [°C]
- $t_{sea,W}$ is the sea temperature in winter [equal to 0°C, see Table 2-1].

For "E.R. Users", the assumption to maintain the same thermal load occurring in winter has been carried out.

For what "Accommodation" loads are concerned, a distinction between Air pre-heating and the others has to take place, since the former is basically based on the external and internal air temperatures difference. Therefore, Eq. (2-6) has been employed:

$$Ct_A = Ct_W * \frac{(t_{in} - t_{air,A})}{(t_{in} - t_{air,W})} \qquad (2\text{-}6)$$

where

- Ct_W is the winter thermal load for pre-reheating [MW]
- t_{in} is the internal air temperature [°C]
- $t_{air,A}$ is the external air temperature in autumn[°C]
- $t_{air,W}$ is the external air temperature in winter [°C]

For the remaining components of the "Accommodation" thermal load, has been taken an average between winter and summer.

Because of maneuvering's scarce importance with respect to time-consume (the maneuvering phase represents just the 7% of the whole cruise duration), Table 2-5 shows thermal loads, for each macro-pole, just for harbor and navigation. Furthermore, in Table 2-5, it can be noted not only differences between harbor and navigation but also differences linked to seasonal variations.

Since thermal loads due to Accommodation are the most important, Table 2-6 reports thermal loads dividing for the various items.
In Figure 2-5 total thermal loads for the different season is shown.

Table 2-5 Reference cruise ship's total thermal load [MW] [28].

	Navigation			Harbor		
	W	S	A	W	S	A
Tanks heating	0.8	0.3	0.6	0.7	0.3	0.5
E.R. users	1.1	1.2	1.1	0.9	0.9	0.9
Accommodation	10.9	7.5	6.3	10.9	7.5	6.3
Total Ship's Consumption	12.8	8.9	7.9	12.5	8.7	7.7

Table 2-6 Reference cruise ship's accommodation thermal load [kW] [28].

	Navigation			Harbor		
	W	S	A	W	S	A
Pre-Re Heating	5272	1932	659	5272	1932	659
Hot Water	3086	2374	2730	3086	2374	2730
Galley User	817	817	817	817	817	817
Swimming	81	811	446	81	811	446
Laundry	1616	1616	1616	1616	1616	1616

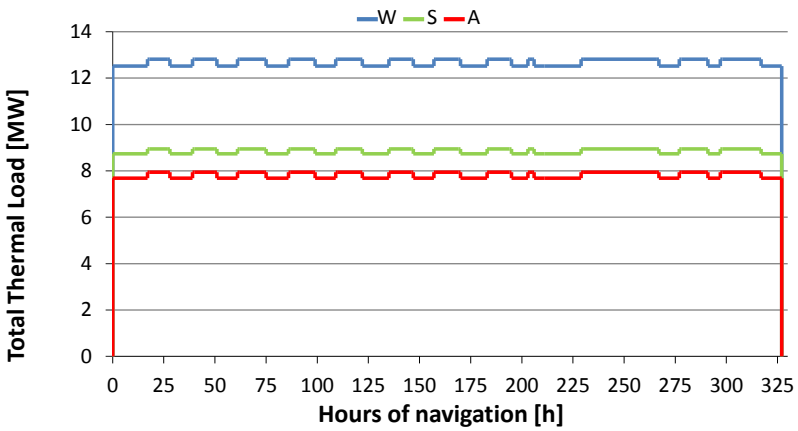

Figure 2-5 Total Thermal load for each season. Data obtained from [28].

Quite foreseeably, winter thermal load is higher than in autumn and summer but, as described by the graph in Figure 2-5, the trend at which it varies during a whole cruise is the same regardless the season. Those variations happen at the same time because they depend on the ship's being in navigation or not. In particular, navigation requires a higher energy consumption to supply "Tanks heating" and "E.R. Users". Though the

moment when the variation happens is the same, the variation itself is not: because each season requires a different thermal load to navigate.

2.2.2.1 Steam production

Thermal loads are satisfied by a steam flow at 182°C and 10.5 barg. Currently, steam is produced by the engines' exhaust gas flows recovery.

In the model ship used in our survey, thermal energy is recovered by utilizing the energetic content of exhaust gas flows. High temperature exhaust fumes are redirected into heat exchangers: Exhaust Gas Boilers (EGBs). Thanks to that, it will be possible to generate steam at 180°C. If the only cogeneration done by EGB will not be sufficient, their employment will be coupled by the use of Oil Fired Boilers (OFBs). The ship examined in this study has two OFBs producing steam at a capacity of 10 t/h, burning HFO with an efficiency of 90% [27].

2.2.2.2 Fresh water production

Another significant thermal load derives from the production of fresh drinking water (FW).

In cruise ship's sector, there are two main ways to product fresh drinking water on board:

- Low pressure MultiStage Flash steam generators (MSF), whose principle is based on boiling the sea-water and collecting the resulting water vapor
- Reverse osmosis (RO) devices employing the natural process that occurs due to osmotic pressure between two substances divided by a semi-permeable membrane.

The first method uses either heat coming from the high temperature engine's cooling water circuit or steam whereas the second one requires electric energy to work. In this sense, MSF can be considered as part of a cogeneration system without requesting any other electric energy.

In the reference cruise ship, two MSF generators are used with a fresh water's production capacity of 50 t/day and a consumption of 0.144 kWh/kg_{FW} [28]. The high temperature engine's cooling water circuit provides the necessary heat and when not enough, OFB are used.

Assuming a fresh water demand of 260 l/day*person and considering 2100 people on board, the production needed is 22750 kg_{FW} every hour. Along with fresh water production, a 22000 l stocking capacity tank is provided in order to have no fresh water's waste [28].

Since MSF generators are adopted in the reference cruise ship, its operation principle is schematized in Figure 2-6.

After leaving the first stage condenser (3), the seawater flows through the brine heater (1), where the heat input to the plant causes a temperature increase. The seawater leaves the brine heater (1) and enters the first flash chamber (2). At this point the pressure of the incoming seawater is suddenly reduced, by means of an orifice, below its equilibrium vapor pressure resulting in explosive boiling or evaporation (flashing). The pure vapor produced is then condensed giving up its latent heat to preheat the incoming seawater (3). If this process is repeated over a large number of effects, at

successively lower pressures and temperatures, large distillate production rates at reasonable performance ratios can be achieved. Before being supplied, the obtained distillate undergoes sanitary treatments such as chlorination, neutralization, remineralization, pH correction.

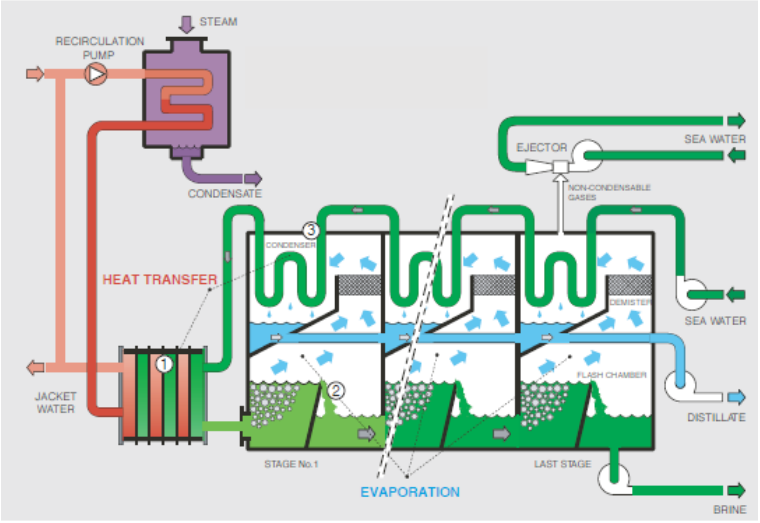

Figure 2-6 Scheme of the operation principle of a MSF fresh water generator.

Chapter 3

COMPONENTS DESCRIPTION

3.1 Prime movers

As already mentioned, all the solutions, which have been considered, are based either on internal combustion engines or gas turbines. Analysis of these two kind of engines have been carried out to extrapolate all the useful information required to achieve the thesis's scopes. In particular, the trade-off between engines' efficiency and loads, the quality and quantity of the waste heat recoverable through EGB as well as engines' weight and volume have to be analyzed and determined.

3.1.1 Internal engine combustion (Wärtsilä W46)

In the reference cruise ship, as already mentioned in Chapter 2, 4-stroke-turbocharged-intercooled diesel engines are employed. Despite of having a different cylinder configuration and power output, the two type of engines are characterized by the following data [29]:

Nominal speed:	514	[rpm]
Bore:	460	[mm]
Stroke:	580	[mm]
Maximum Continuous Output:	1050	[kW/cyl]

Being the ship's efficiency determination one of the major scope of the thesis project, engines efficiency's trend respect to engines' loads have to be properly analyzed.
From data reported by [29], the graph shown in Figure 3-1 has been extrapolated. It represents the increase of fuel oil consumption's in term of delta Specific Fuel Oil Consumption (dSFOC), it means that the graph depicts how much the fuel oil consumption increases if engines work under not optimal load conditions. It can be noted that the minimum fuel oil consumption, i.e. maximum efficiency, happens for an engine's load equal to 80%, which is the engines' load design point. This design choice has two positive effects, especially for what the ships sector is concerned:

- Possibility to rely on an huge power margin to be used in emergency case

- Capability to have a limited variation of specific fuel oil consumption for a big engine's load variation (for example, it can be inferred that even if an engine's load variation between 50 and 100 % occurs, dSFOC does not increase above 5 g/kWh).

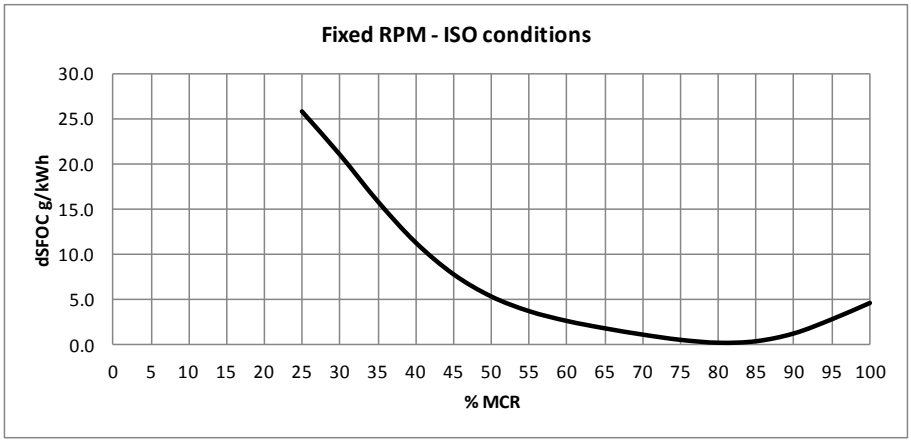

Figure 3-1 Behavior of dSFOC respect to engine's load variation. Data obtained from [29].

As a consequence, engines actually employed have good working flexibility maintaining a good efficiency. Indeed, if the choice had have been to maximize the efficiency for the 100% load, a +5g/kWh dSFOC would have been reached at 70% load, reducing the actual modulation range which is characterized by a +1g/kWh at 70% load.
Along with dSFOC, other dSFOC have to be analyzed. They are related to the water and lubricating oil pump power demand, as reported in Figure 3-2 and in Figure 3-3 respectively.

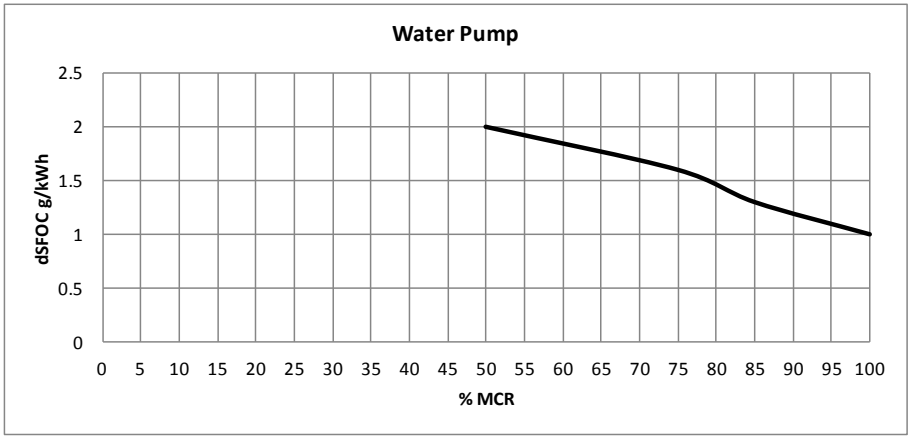

Figure 3-2 Water pump dSFOC [29]

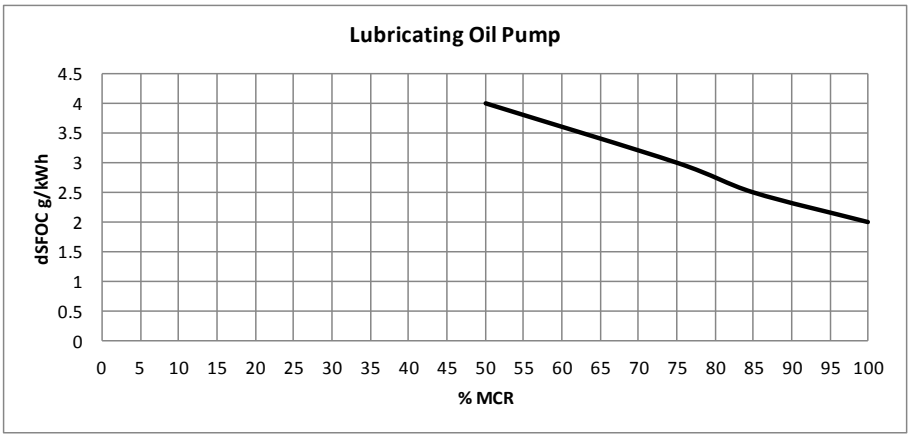

Figure 3-3 Lubricating oil pump dSFOC [29]

Based on data reported in Figure 3-1, Figure 3-2 and Figure 3-3 and considered a minimum specific fuel oil consumption ($SFOC_{iso}$) of 172g/kWh under ISO[3] condition [29], trend of the total specific fuel oil consumption respect to engine's load can be obtained, see Figure 3-4.

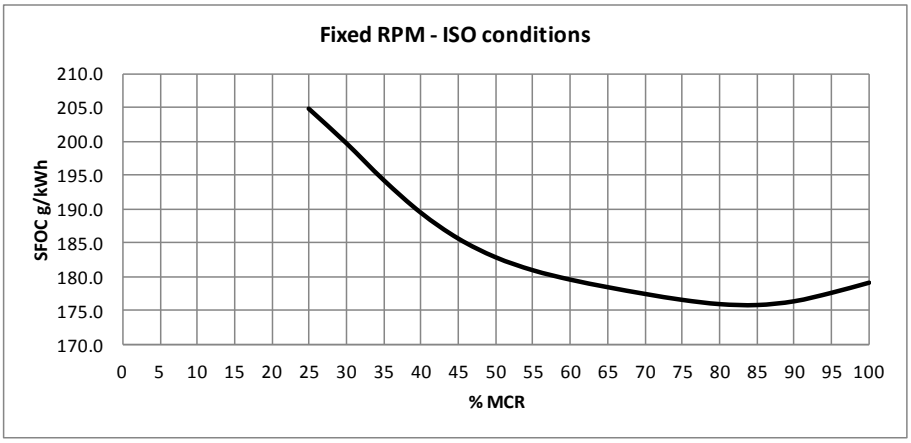

Figure 3-4 Behavior of SFOC respect to engine's load variation. Data obtained from [29].

Furthermore, considering HFO's lower heating value equal to 42700 kJ/kg, it is possible to determine the selected diesel engines' efficiency in relation to loads, see Figure 3-5. Along with these analysis, evaluation of how much heat can be recovered by the exploitation of ICEs' exhaust gas has to be made in order to properly calculate the global ship's energy efficiency.
On board employed ICEs have three kinds of thermal flows that differentiate from each other by the thermal level at which they are available.

[3] ISO conditions are T=15°C and p=1.013 bar

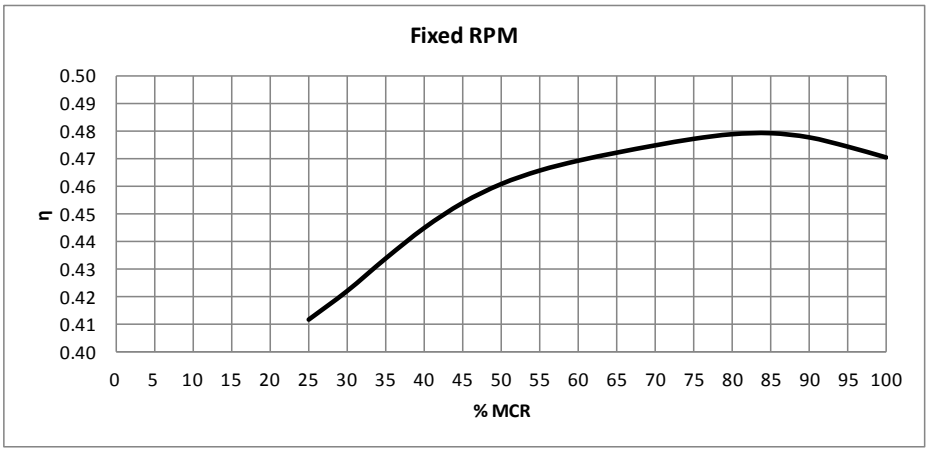

Figure 3-5 Behavior of efficiency respect to engine's load variation. Data obtained from [29].

In particular, there can be distinguished three enthalpy content flows linked to:

1. Engines' exhaust gas
2. High temperature circuit (both jacket water and air)
3. Low temperature circuit (both lubricating oil and air)

which are ordered by their thermal level, from the highest to the lowest.
The first one depends directly on both mass flow and temperature of engine's exhaust gas. The variation of these two parameters under different engines' load conditions is reported in Figure 3-6 and in Figure 3-7 respectively.

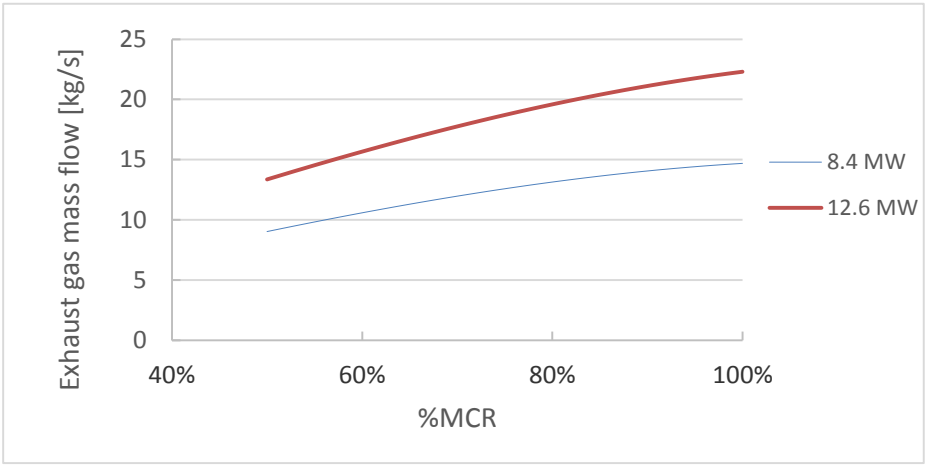

Figure 3-6 Reference ICEs' exhaust gas gas mass flow variation respect to %MCR [29].
(8.4 MW=W8L46C and 12.6=W12V46C).

For what the second enthalpy flow is concerned, the reader should refer to the graph reported in Figure 3-8.

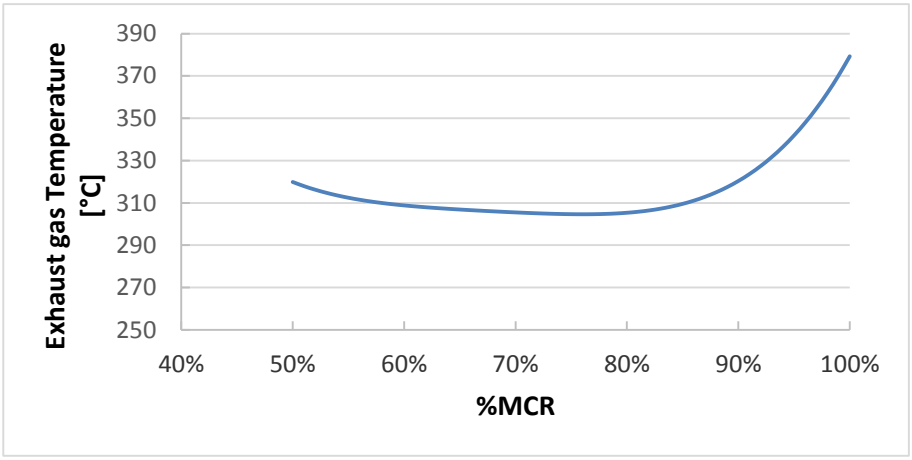

Figure 3-7 Reference ICEs' exhaust gas temperature variation respect to %MCR [29].

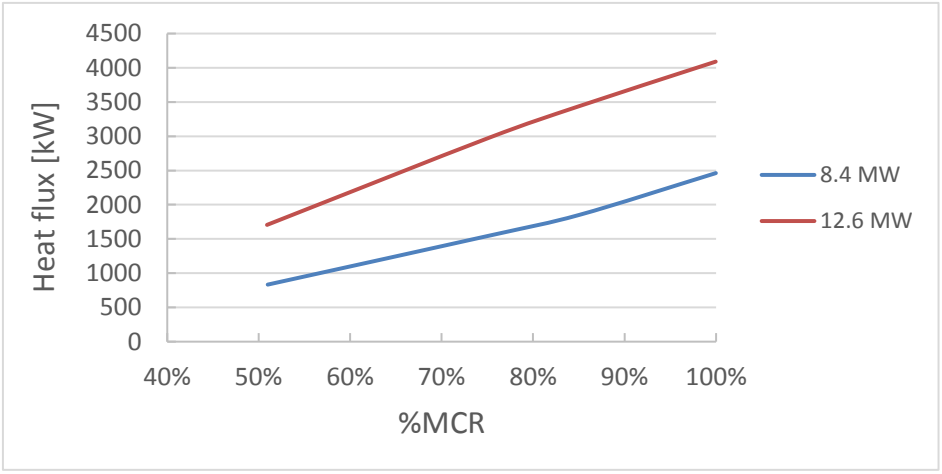

Figure 3-8 Thermal power recoverable from high temperature circuit variation respect to %MCR [29]. *(8.4 MW=W8L46C and 12.6=W12V46C).*

This kind of thermal flow is available by means of water flow having circuit's inlet/outlet temperatures of 90 and 70°C respectively [29].

The heat recoverable from the exploitation of the third enthalpy flow, namely the low temperature circuit, is depicted in Figure 3-9. Thermal flows are available through water flow having a temperature's variation from 40 to 80°C [29].

Given the different thermal level at which these flows are available, it follows that they suitable for different purposes.

The first heat flux has been used to cover the highest thermal load, thus the steam production; meanwhile the second one can be used to cover the other ship's thermal load, meaning the thermal load required for fresh water production. Actually, in the reference cruise ship, the third flow is not used [28].

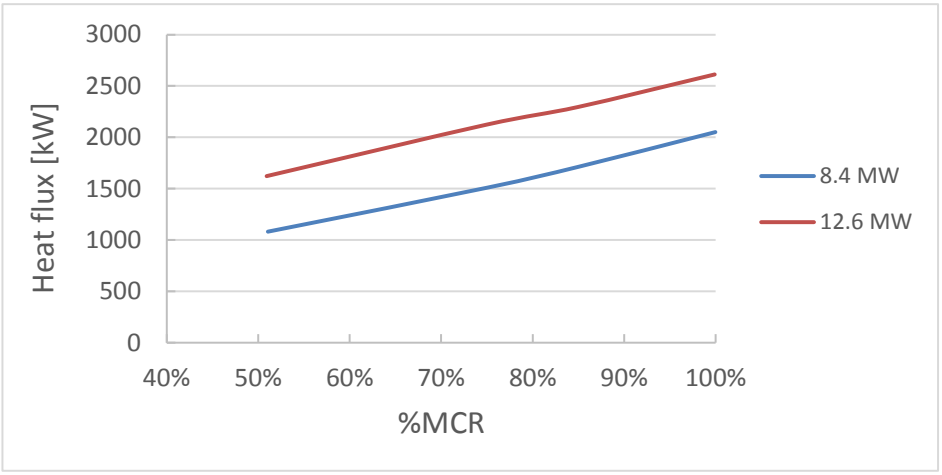

Figure 3-9 Thermal power recoverable from low temperature circuit variation respect to %MCR [29]. *(8.4 MW=W8L46C and 12.6=W12V46C).*

Other important information about these engines regard their weight and volume occupied. These data are available from [30] and reported in Table 3-1.

Table 3-1 Weight and volume occupied (and dimensions) of the actually employed ICEs [30].

	WÄRTSILÄ8L46C	**WÄRTSILÄ12V46C**	
Weight	95	169	[ton]
Volume occupied (dimensions)	169.5 (10x3.2x5.3)	234 (10.2x4.5x5.1)	[m^3 (m)]

3.1.2 Gas Turbines

Since engines have always been engineered and sized to optimally cover the ship's electric load, to this day it is possible to find many ICE fitting any ship's demand, this, unfortunately is not possible for gas turbines. Therefore, to be able to conduct the best simulation possible, it has been thought to choose two GTs having the most similar power output range [to the original ICE's] even if they weren't initially supposed to be installed on a ship. A survey has been carried out in order to find out the most suitable gas turbines for this application. Siemens SGT-300 and Siemens SGT-400 have been selected whose nominal data are reported in Table 3-2.

Figurative schemes of these gas turbine are shown in Figure 3-10 while in Figure 3-11 it can be seen schemes of GT's geometry where the major components are highlighted, in particular: Compressor (C), Combustion Chamber (CC), High and Low Pressure Turbine (HPT and LPT respectively), Power Turbine (PT) and Generator (G).

Along with nominal data, also known as "design-mode" data, part-load values should have been provided in order to have a complete trade-off between GT's loads and other parameters, such as efficiency, fuel consumption, exhaust gas mass flow and so on.

Table 3-2 Selected Siemens Gas turbines' technical Data

	Siemens SGT-300 [31]	**Siemens SGT-400** [32]	
Power output	8.6	13.5	[MW]
Efficiency	34.6	36.2	%
Pressure Ratio	13.3	16.8	[-]
Exhaust Gas Mass Flow	29	39.4	[kg/s]
Turbine Outlet Temperature (TOT)	498	555	[°C]
"Core" speed	14010	14100	[rpm]
"Power Turbine" speed	11500	9500	[rpm]
Axial Compressor's stages	10	11	[-]
Turbine's stages	4	4	[-]
Inlet pressure drop	0.9	0.98	%
Outlet pressure drop	1.9	1.9	%
Power unit electric efficiency	97	97.2	%
Shaft	1		[-]
NOx emission	15		[ppmV]
CO emission	10		[ppmV]

These data are not available from the above-cited literature and therefore it has been taken advantage by the use of a commercial software, THERMOFLEX provided by Thermoflow Inc.

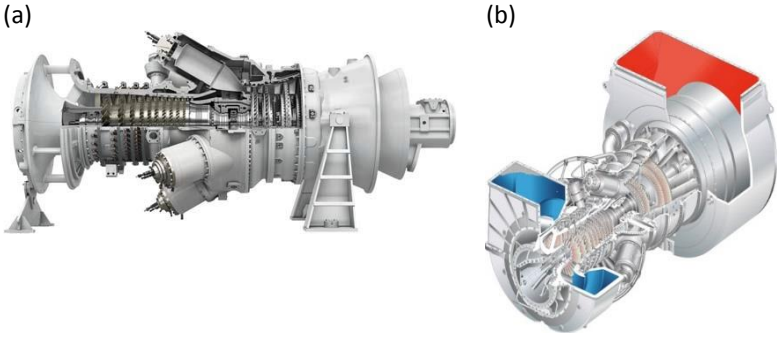

Figure 3-10 Figurative scheme of (a) Siemens SGT-300 [31] *and (b) Siemens SGT-400* [32].

Briefly, THERMOFLEX is a modular program with a graphical interface that allows the user to assemble a model from icons representing more than 150 [33] components.
The program covers both design and off-design simulation, and models all types of power plants, including combined cycles, conventional steam cycles, and repowering.
Simulations carried out with THERMOFLEX's aid are based on a "component matching" method, indeed GT's behavior is inferred by that of elementary components which are properly modeled either from some equations or characteristic maps, where possible.

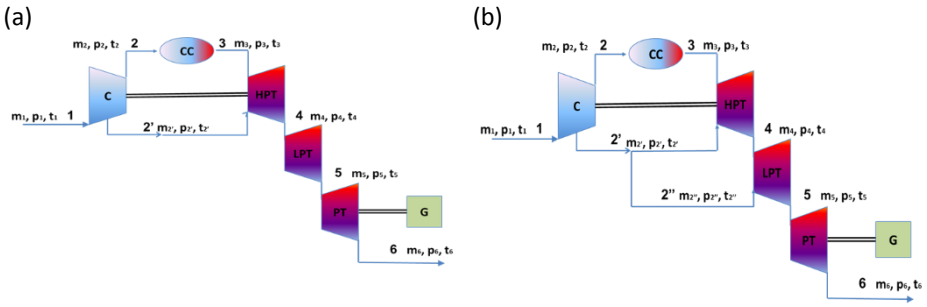

Figure 3-11 Selected Siemens GTs' geometry (a) SGT-300 [31] *and (b) SGT-400* [32] *where m_i, p_i, T_i stands for mass flow, pressure and temperature related to the i-th thermodynamic point.*

Typically, four conditions have to be respect for the system resolution:

1. Thermodynamic balance
2. Continuity equation
3. Pressure drop compatibility
4. Shaft's mechanical balance

For what the fuel is concerned, it is well worth to report that in all the conducted simulations natural gas has been the hypothetic fuel of choice, having a lower heating value of 50047 [kJ/kg] under ISO[3] conditions.

Firstly, THERMOFLEX has been validated using the nominal data for the selected Siemens gas turbines: simulations have been carried out in order to obtain results to match the nominal data available. Namely it has been searched fuel consumption, turbine inlet temperature etc. so that to match perfectly the nominal data reported in Table 3-2.

Simulation's results in design mode are so good that model based point had very little discrepancy from the reported ones, as shown in Table 3-3.

In Table 3-4, other parameters performed by the design mode simulation are reported.

The next step was the simulation in off-design.

A series of simulations has been carried out varying both the fuel flow rate and the IGV Compressor aperture. This was necessary since the Turbine can be controlled through these two "control parameters", and the machine's performance has to be evaluated at the variation of both of them.

Table 3-3 Differences, in terms of Δ%, between data obtained by design mode simulation and available data for Siemens SGT-300 [31] *and Siemens SGT-400* [32].

	Siemens SGT-300	Siemens SGT-400
Exhaust gas mass flow	-7.48	-0.3
Turbine Outlet Temperature "TOT"	-0.02	-0.25
Electric power output	+0.8	-0.1
Electric Efficiency	-0.028	-0.35
Net heat rate	-0.09	0.38

Table 3-4 Other parameters obtained by design mode simulation carried out with Thermoflex

	Siemens SGT-300	**Siemens SGT-400**	
Fuel mass flow	0.5	0.7498	[kg/s]
Compressor Outlet Temperature	375.9	421	[°C]
Turbine Inlet Temperature "TIT"	1100	1290	[°C]
Stator Blade Metal Temperature	815	830	[°C]
Rotor Blade Metal Temperature	810	825	[°C]

In particular, it has been maintained a fixed Inlet Guide Vanes (IGV) value, while changing the fuel flow rate (thus the TIT): this means that every combination consists of a value for the IGV and one for the TIT, with the first always different and the second remaining fixed. Each of the combinations has its own power output and efficiency. From all the resulting combinations, the most efficient one has been chosen bringing with it the related power output. This way it was possible to draw the curve of the "efficiency-%MCR" graph (or SFOC-%MCR), as well as other graphs describing other parameters: exhaust gas mass flow, exhaust gas temperature, and so on. Consequently, the relation between these parameters at the load's variation could be found. The relations between "efficiency-%MCR" and "exhaust gas mass flow-%MCR" are shown in Figure 3-12 and Figure 3-13 respectively.

Ship's electric load needs to be covered at the best possible efficiency. For ICE, as already said, using more smaller engines instead of a big one, provides the possibility to cover a wider range of electrical loads with engines working at maximum efficiency for most of the time. In the case of GTs, said solution is even more justified since GTs's efficiency curve is narrower than that of an ICE (compare Figure 3-5 and Figure 3-12). Substituting ICEs with GTs therefore, means that the number and the capacity of GTs to be installed has to be carefully calculated in sight of the ship's electric load. Moreover, having to adapt to what the market has to offer, the decision is rendered even more difficult.

Given the ship's electric loads reported in Chapter 2, the selected gas turbines would not work at optimal conditions because of their higher power output than the ICEs's. To overcome this issue, the depowering of the selected GTs to meet the ship's electrical needs has been made.

This meant to use the data resulted from both the simulations as a starting point on which to make some modifications in order to get better fitting to the purpose GT's.

The new technical data and the related performance of the GTs therefore consist mostly in a lower power output. The size coefficient has been determined so that gas turbines could operate mostly with a load above 95%. Decreasing SGT-300's power output by 3% and SGT-400 by 21%, two new gas turbines have been created characterized by 8.3 MW and 10.6 MW respectively. For sake of brevity, from here on out, the new gas turbine will be named as "Type A" and "Type B" respectively.

All the nominal parameter have been scaled accordingly, see Table 3-5. This manner, the overall power installed would be almost equal to 38 MW instead of the actually 42 MW installed with the ICEs' use.

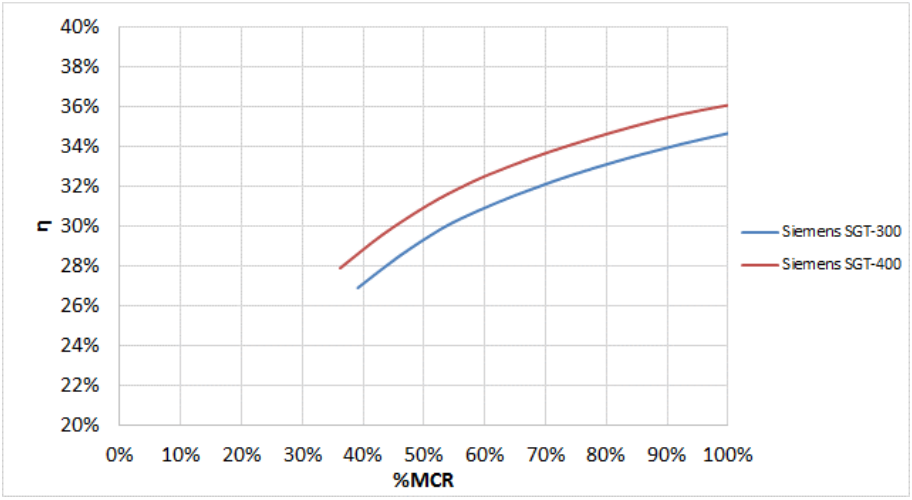

Figure 3-12 Efficiency Vs. %MCR of the selected GTs [data obtained from Thermoflex's simulations].

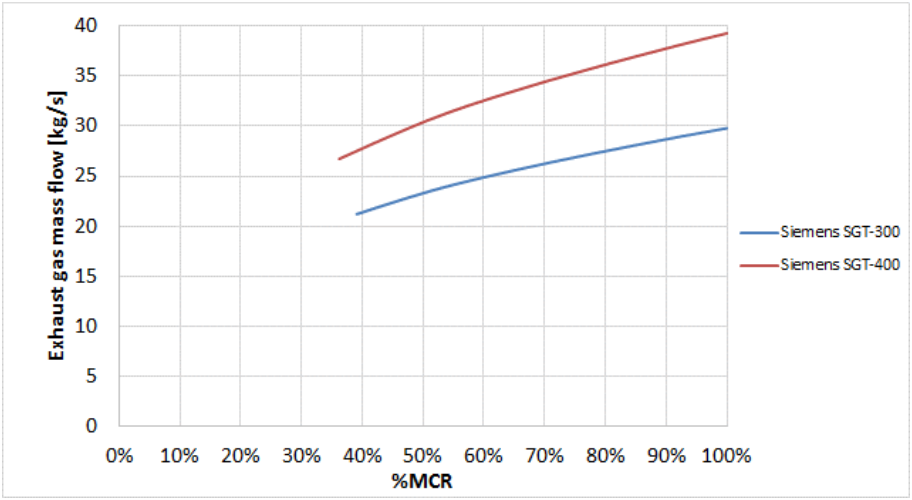

Figure 3-13 Exhaust gas mass flow Vs. %MCR of the selected GTs [data obtained from Thermoflex's simulations].

In order to have the same power installed on board, the employment of one more gas turbine, having a power output equal to 5MW, has to be considered just for safety purpose.

The use of GTs instead of ICEs allows to use MGO as fuel, as already reported in Chapter 1. Since MGO and CH_4 have different Lower Heating Value, 43154 and 50047 kJ/kg respectively, the results provided by THERMOFLEX's simulations ought to be corrected. Likewise to ICEs, in Table 3-6 weight and volume occupied of the new gas turbine are reported.

Also these values have been determined from a linear regression of those of the original Siemens gas turbines.

Table 3-5 Characterizing parameters of real GTs and Virtual ones.

Parameters	**Siemens SGT-300**	**Siemens SGT-400**	**Type A**	**Type B**	
Nominal Power	8.7	13.5	8.3	10.6	[MW]
Air mass flow	29.99	38.90	28.6	30.5	[kg/s]
Exhaust gas flows	26.98	39.28	26.1	31	[kg/s]
TOT	497.7	545.3	497.7	545.3	[°C]
TIT	1100	1290	1100	1290	[°C]
rpm	14010	14100	14010	14100	[-]
η (@100 %MCR)	34.65	36.07	34.65	36.07	
η (@ 90 %MCR)	33.94	35.44	33.94	35.44	
η (@ 80 %MCR)	33.09	34.62	33.09	34.62	

Table 3-6 Weight and volume occupied of the new gas turbines

	Type A	**Type B**	
Weight	30	38	[ton]
Volume occupied	79	81	[m^3]

It is well worth reminding that to properly account the overall prime movers' weight and volume also that of the extra gas turbine has to be considered. Therefore, further 18.5 tonnes and 75 m^3 have to be added to the values reported in Table 3-6.
For sake of clarity, it has to be pointed out that it has not been considered the effects on the GTs' efficiency-%MCR curve caused by the ambient conditions' variations.

3.2 Exhaust Gas Boilers

The reference cruise ship's thermal loads are covered by the production of steam at 10.5 bar and 182.5 °C, see Chapter 2. To limit the ship's fuel consumption, cogeneration has been put into force. In practice, specific heat exchangers, called Exhaust Gas Boilers, are used in order to make steam recovering prime movers' exhaust gas.
Technical data and specification for employed EGB have been supplied by [28]. It is clear that the amount of steam produced depends on engine's type and load: nominal steam production is referred to ICE's nominal load, namely 80%. In Table 3-7 Technical data of the actually EGBs' employed on board are reported.
These data are relative to ICEs and therefore, if solutions based on GTs are considered, using the same EGBs would be wrong due to the different enthalpy flows of the prime movers' exhaust gas. To overcome this issue, it is necessary to model EGBs' mode of operation. Furthermore, modeling EGB's working behavior is useful to find out other heat exchangers' typical parameters, such as pinch point, approach point, global heat transfer coefficient and their variation respect to engines' load.

Table 3-7 EGB's technical data [28].

	WÄRTSILÄ8L46C				WÄRTSILÄ12V46C				
Engine load	100	80	70	50	100	80	70	50	%
Nominal gas flow rate	14.7	13.1	12	9	22.4	19.6	17.8	13.3	[kg/s]
Engine turbocharger gas outlet temperature	379	305	306	320	379	305	306	320	[°C]
Gas outlet temperature	216	199	197	192	216	199	197	192	[°C]
Feed water temperature	92.5								[°C]
Minimum saturated steam production	1.07	0.61	0.57	0.51	1.63	0.92	0.85	0.75	[kg/s]
Steam working pressure	10.5								[bar]
Gas side pressure drop	2.3	2.4	2	1.1	5.2	5.4	4.4	2.5	[mbar]
Weight	9				12				[ton]
Volume	18				24				[m^3]

EGB's working simulations are carried out with THERMOFLEX, which implements the mass and energy conservation. Results of these simulations will be analyzed in detail in Chapter 4.

3.3 Chilling devices

In the studied cruise ship, traditional chilling devices are used, meaning that four compressors are employed on board to cover the ship's chilling load, as already mentioned in Chapter 2.

For what the compression chillers are concerned, data supplied by [27] are used, see Table 3-8.

Instead of using these devices, absorption machines can be used to satisfy the chilling requirements.

For sake of clarity, it follows a brief description of the absorption chillers' working principle.

Table 3-8 Main data of the used compression chillers [27].

	Compression chiller	
Electric power demand	800	[kW]
COP	4.9	[-]
Volume	42	[m^3]
Weight	18	[ton]

Absorption chillers work with a mixture of two fluids: the fluid with the lowest vapor pressure is the solvent and the fluid with the highest vapor pressure is the solute. Usually the couple of fluids used can be water (solvent) and ammonia (solute) or lithium bromide (solvent) and water (solute). Absorption chillers can use directly the prime mover's exhausted gases or steam produced in some way.
Four main parts constitute the absorption chiller:

1. evaporator, is the heat exchanger in which the refrigerant absorbs the heat from the source at low temperature and becomes vapor. Considering that the refrigerant it is at low pressure, its boiling point is low and evaporates absorbing heat from the stream which needs to be cooled;
2. absorber, is the device in which the vapor, produced in the evaporator, turns back into a liquid solution at constant pressure. The solute is absorbed by the liquid mixture coming from the generator. The absorption process takes place here because of the affinity between solute and solvent, producing heat. The pump raises the pressure of the rich solution coming from the absorber
3. generator, receives this mixture and separates solute from solvent in a process similar to distillation using the heat source available.
4. condenser is the heat exchanger in which the vapor, produced from the generator, condenses releasing heat to the environment.

The scheme of the absorption chiller working principle is reported in Figure 3-14.
The cooling effect is usually provided between 7 °C and 12 °C when water is used as refrigerant. When temperatures under 0 °C are required, mixtures of glycol-water or other mixtures are used.

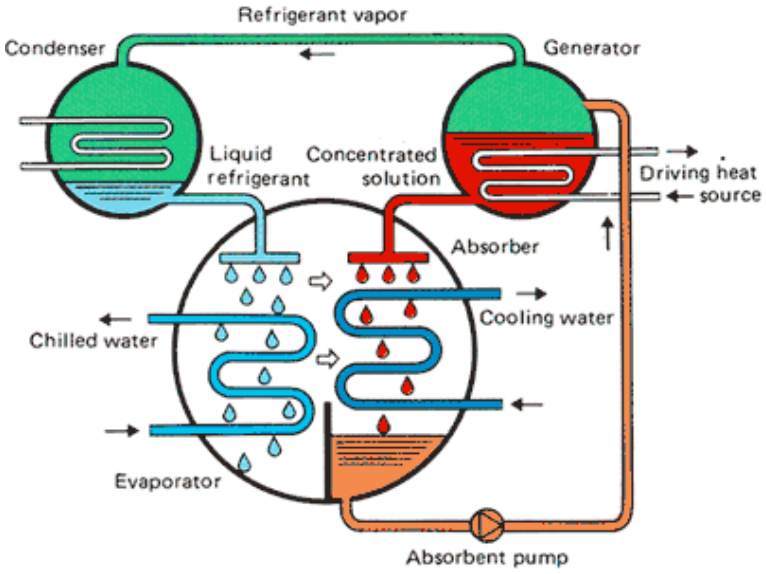

Figure 3-14 Figurative scheme of the absorption chillers working principle.

The main advantage coming from the absorption chillers use is linked to the possibility to further recover prime mover's exhaust gas (trigeneration system) instead of requiring extra electric power to start the chilling compressors. Along with this energetic aspect, another one should be taken into account when considering this thesis's specific application and it is the noise level. Absorption chillers are characterized by a lower noise level than compression chillers thanks to the fact that the former are static machines having much lower moving parts.
The choice to use a double effect steam driven absorption machines has been done.
In particular the "SD 80A TCU" model produced by THERMAX Inc. has been chosen.
In Table 3-9 the main characteristics of this machine are reported.

Table 3-9 Main data of the selected absorption chiller machines [34].

	SD 80A TCU	
Cooling Capacity	5156	[kW]
COP	1.4	[-]
Volume (dimensions)	130 (8.3x3.6x4.5)	[m^3 (m)]
Working weight	58.5	[ton]

3.4 Exhaust gas after-treatment devices

As mentioned in Chapter 1, nowadays SCR and scrubber are the most feasible options to meet IMO threshold limit values. In the following paragraph, operating principles and characteristics of both of them are highlighted and briefly described.

3.4.1 Selective Catalytic Reduction (SCR) for NOx reduction

In the 1950s, it was discovered that ammonia could be used to catalytically remove NOx from lean exhaust gases [35].
Firstly used to control NO_X emissions from stationary sources, SCR systems came out to be a good option for diesel NOx emissions reduction in a variety of mobile applications, such as heavy-duty trucks and buses, diesel passenger vehicles, and off-road applications. Nowadays, cumulative capacity of vehicles and power plants that take advantage by SCR systems' employment is about half million megawatts worldwide [21].
SCR functions by combining ammonia (NH_3), typically derived from an aqueous solution of urea, with a catalyst mounted on a ceramic monolith, to reduce NO_X, forming nitrogen (N_2) and water (H_2O) without the production of any liquid or solid by-products. Eq. from (3-1) to (3-3) are the principal reactions that occur in a generic SCR device:

$$(NH_2)_2CO + H_2O \rightarrow 2NH_3 + CO_2 \quad (3\text{-}1)$$
$$4NO + 4NH_3 + O_2 \rightarrow 4N_2 + 6H_2O \quad (3\text{-}2)$$
$$6NO_2 + 8NH_3 \rightarrow 7N_2 + 12H_2O \quad (3\text{-}3)$$

Undesirable processes occurring in SCR systems include several competitive, nonselective reactions with oxygen, which is abundant in the system. These reactions

can either produce secondary emissions or, at best, unproductively consume ammonia. Partial oxidation of ammonia, given by Eq. (3-4) and (3-5), may produce nitrous oxide (N_2O) or elemental nitrogen, respectively. Complete oxidation of ammonia, expressed by Eq. (3-6), generates nitric oxide (NO).

$$2NH_3 + 2O_2 \rightarrow N_2O + 3H_2O \quad (3\text{-}4)$$
$$4NH_3 + 3O_2 \rightarrow 2N_2 + 6H_2O \quad (3\text{-}5)$$
$$4NH_3 + 5O_2 \rightarrow 4NO + 6H_2O \quad (3\text{-}6)$$

Ammonia can also react with NO_2 producing explosive ammonium nitrate (NH_4NO_3), Eq.(3-7). This reaction, due to its negative temperature coefficient, occurs at low temperatures, below about 100-200°C. Ammonium nitrate may deposit in solid or liquid form in the pores of the catalyst, leading to its temporary deactivation [36].

$$2NH_3 + 2NO_2 + H_2O \rightarrow NH_4NO_3 + NH_4NO_2 \quad (3\text{-}7)$$

Ammonium nitrate formation can be avoided by making sure that the temperature never falls below 200°C. The tendency of NH_4NO_3 formation can also be minimized by supplying into the gas stream less than the precise amount of NH_3 necessary for the stoichiometric reaction with NOx (1 to 1 mole ratio).
Moreover, when the flue gas contains sulfur, as is the case with diesel exhaust, SO_2 can be oxidized to SO_3 with the following formation of H_2SO_4 upon reaction with H_2O. These reactions are the same as those occurring in the diesel oxidation catalyst. In another reaction, NH_3 combines with SO_3 to form $(NH_4)_2SO_4$ and NH_4HSO_4, Eq. (3-8) and (3-9), which deposit on and foul the catalyst, as well as piping and equipment. At low exhaust temperatures, generally below 250°C, the fouling by ammonium sulfate may lead to a deactivation of the SCR catalyst [37].

$$NH_3 + SO_3 + H_2O \rightarrow NH_4HSO_4 \quad (3\text{-}8)$$
$$2NH_3 + SO_3 + H_2O \rightarrow (NH_4)_2SO_4 \quad (3\text{-}9)$$

The SCR process requires precise control of the ammonia injection rate. An insufficient injection may result in unacceptably low NOx conversions. An injection rate which is too high results in release of undesirable ammonia to the atmosphere. These ammonia emissions from SCR systems are known as ammonia slip. The ammonia slip increases at higher NH_3/NOx ratios. According to the dominant SCR reaction, Eq. (3-2), the stoichiometric NH_3/NOx ratio in the SCR system is about 1. Ratios higher than 1 significantly increase the ammonia slip. In practice, ratios between 0.9 and 1 are used, which minimize the ammonia slip while still providing satisfactory NOx conversions. Figure 3-15 presents an example relationship between the NH_3/NOx ratio, NOx conversion, temperature, and ammonia slip [35]. The ammonia slip decreases with increasing temperature, while the NOx conversion in an SCR catalyst may either increase or decrease with temperature, depending on the particular temperature range and catalyst system, as will be discussed later.

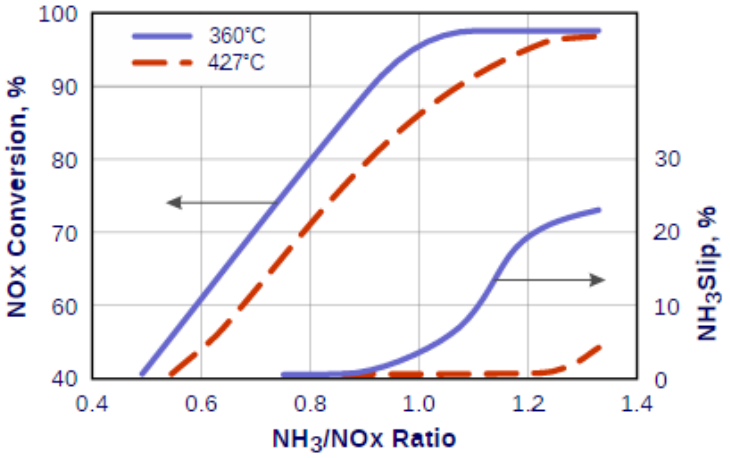

Figure 3-15 NOx conversion and ammonia slip for different NH3/NOx ratios V2O5/TiO2 SCR catalyst, 200 cpsi [35].

3.4.1.1 SCR in the maritime sector

For what the maritime sector is concerned, MAN B&W and Wärtsilä were the first companies that tested in the 1990s the feasibility of employing SCR on board. According to what [21] reported, in 2013 over 500 SCR's applications have been numbered in the marine sector for a total of 1250 SCR systems being installed in the past decade. Moreover, SCR's employment does not depend the kind vessel nor the engine type nor the fuel; but the largest category that uses SCR is "carriers" including Roll on/Roll Off passengers (RoPax), Roll on/Roll Off (RoRo), cargo, ferry, high speed catamaran, container vessel, RoRo cargo, cruise ferry, tanker, Liquid Petroleum Gas (LPG) tanker and chemical tanker [21].

SCR's NOx reduction efficiency is very high achieving 90% at temperatures above 300°C as reported in [38]. Despite of this high efficiency, it should be pointed out that there are three technical aspects to take into consideration and they are reported in [39]. The first matter of concern regards the low temperature operation happening when the engine load is low, for example below 25%. Low temperatures involve both an unoptimality SCR's operation and the possible formation of ammonium sulphates, whose deposition on the catalyst layer causes lower NOX reduction and higher back pressure. Therefore, a minimum exhaust gas temperature should be maintained depending on the type of fuel: 270-300°C for low sulphur fuel (i.e. 0.1% S on weight) and above 300°C for fuels with higher S content [39]. The second issue regards catalyst's deterioration by poisoning and fouling by soot, ash and ammonium sulphates resulting not only in a minor NOx's cutting down but also in an ammonia slip increase. In [40] different strategies and technologies to avoid deterioration are presented such as: using the SCR only in ECAs, using low sulphur fuels of 0.1 wt% S or lower in combination to SCR, turning off the system at predetermined low exhaust gas temperatures.

The problem linked to ammonia slip is the last aspects on which attention has to be focused. Even if, at present, the ammonia is not a controlled parameter under MARPOL

Annex VI, it is recommended to respect the limit of 10 ppm imposed by the Euro 6 legislation for heavy-duty diesel engines [41].
Brynolf et al. in their paper reported the results, in term of NO_x and NH_3-slip emissions, obtained within the program promoted by Swedish Maritime Administration in order to achieve Tier II and Tier III threshold limit values [39]. NO_x measurements have been done for vessels operating on different marine fuels, with a sulphur content up to 2 wt%. The instrument was designed as a financial incentive to encourage reduced NO_x emissions from vessels, by offering a stepwise reduction in the fairway due as a function of the NO_x emission as gNO_x/kWh from the vessel [39]. The stepwise function started at 12 gNO_x/kWh and reached a maximum reduction at 2 gNO_X/kWh. The result reported in [40] is shown in Figure 3-16 where it can be noted that the majority of the measured NO_x emissions were below the IMO Tier III level and the majority of all measured ammonia slips were below 20 ppm. Furthermore, it isn't observed any correlation between NO_x levels both the magnitude of ammonia slip and the fuel Sulphur content, which instead determines the SCR's working minimum exhaust gas temperatures.

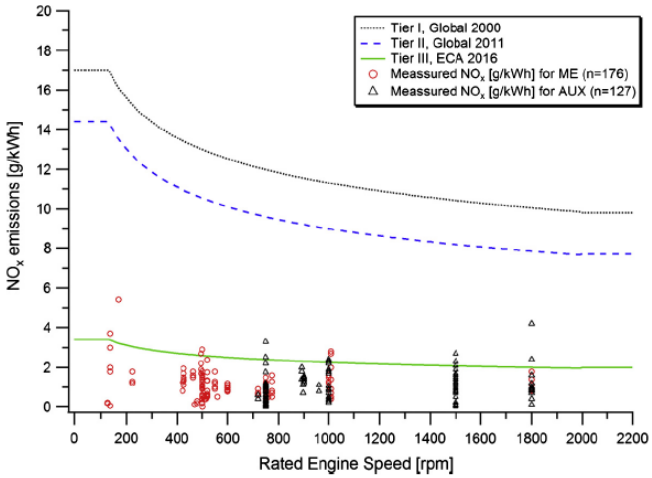

Figure 3-16 IMO NOX emission regulation and measured NOX emissions in accordance with Swedish environmental differentiated fairway dues [40].

3.4.1.2 SCR system on board of Hull C.6194

Every engine has its own SCR reactor that consists of an inlet and an outlet cone, catalyst layers, a steel structure for supporting the catalyst layers and a soot blowing unit.
SCR comprises many units that make it a very complex system:

- Reactor housing
- Catalyst elements, mainly Vanadium pentoxide (V_2O_5), are posed in a honeycomb structure to increase the catalytic surface. Notwithstanding all the operations made for preventing catalyst from solids deposit formation and clogging, the efficiency of the catalyst decreases with time, mainly due to

thermal load and small amounts of catalyst poisons. When the catalytic activity has decreased too much, the catalyst elements must be changed

- Soot blowing unit operates automatically at a preset interval and is controlled by the control unit
- Urea injection and mixing unit. The reducing agent is sprayed into the exhaust gas duct and mixed with the exhaust gas before it enters the reactor. The urea injection is performed using compressed air. After the injection of reducing agent, the exhaust gas flow passes through a mixing duct where the urea transforms into ammonia and mix homogeneously before it reaches the reactor with the catalyst elements.
- Urea dosing unit defines the correct urea dosing rate for the injection. The dosing unit also supplies air to the soot blowing unit.
- Control and automation unit receives the engine load and speed signal, and adjusts the urea dosing accordingly. When the engine load increases, the urea dosing is also increased to maintain an efficient nitrogen oxide abatement.
- Urea pump unit transfers urea from the tank to the dosing system and maintains a sufficient pressure in the urea lines. The unit has full redundancy so that failure of one pump will not stop the SCR system operation.
- Air unit is the connection point for compressed air supply to the SCR system. The unit distributes air to the dosing units. The unit includes a filter element, pressure regulators and an outlet pressure transmitter.
- Urea tank.

The described units and their connections are depicted in Figure 3-17.
The process can be summarized in these following steps:

1. The pump unit ⑤ transfers urea from the storage tank ④ to the dosing unit ⑥
2. The urea injector ⑧ sprays the urea solution into the exhaust gas duct.
3. The exhaust gas ⑦ flows through the mixing pipe ⑧ to the reactor ⑨, where the NOx reduction take place over catalyst elements.

The reactor is equipped with a differential pressure transmitter for monitoring the condition of the catalyst elements as well as upstream and downstream temperature transmitters for monitoring the exhaust gas temperature:

- pressure drop over the SCR system is normally designed to be below 15mbar at 100% engine load [42].
- the working temperature of the SCR system is dependent on the fuel sulphur content and fuel type. The trade-off between the minimum and the maximum recommended exhaust gas temperature and the sulphur content of the fuel oil in order to achieve good efficiency and durability is shown in Figure 3-18.

For what the urea consumption is concerned, it is directly proportional to the NOx reduction amount over the SCR catalysts.
The expected urea consumption can be calculated according to the formula (3-10):

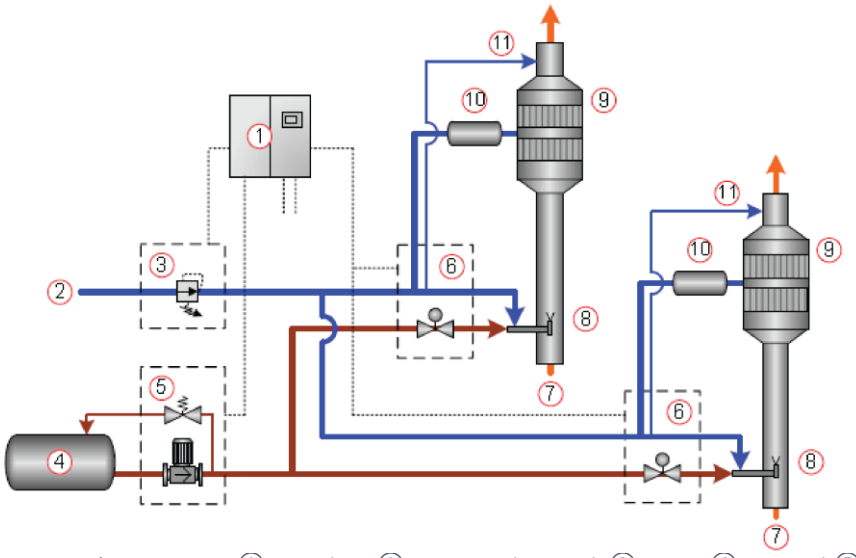

Figure 3-17 SCR's units process: ① Control unit ② Compressed air supply ③ Air unit ④ Urea tank ⑤ Pump unit ⑥ Dosing unit ⑦ Exhaust gas from the engine ⑧ Injection and mixing unit ⑨ Reactor with catalyst elements ⑩ Soot blowing unit ⑪ NOx sensor purge

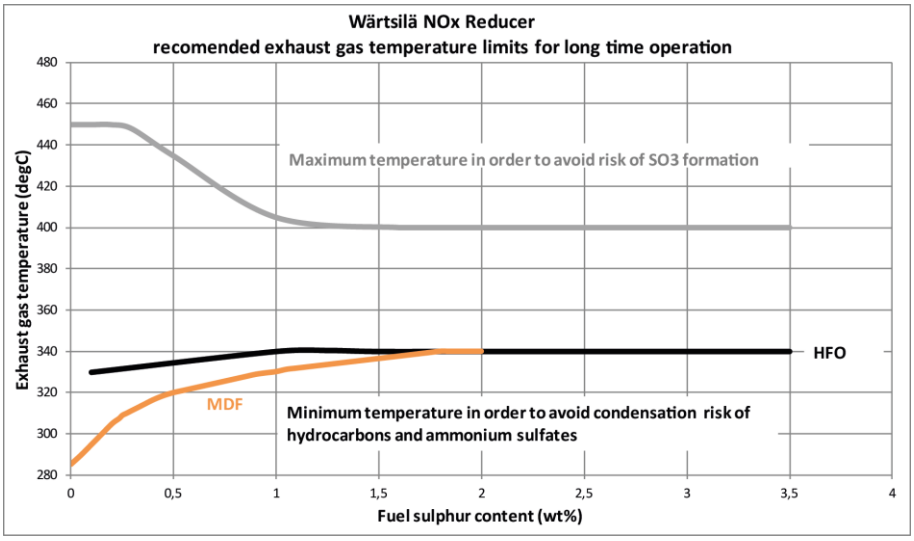

Figure 3-18 Trade-off between fuel's Sulphur content and exhaust gas temperature required for SCR [42].

$$\dot{V}_{urea} = \frac{P_{engine} \times \dot{m}_{NO_2} \times \frac{MM_{urea}}{2 \times MM_{NO_2}} + P_{engine} \times 0.1}{10 \times C_{urea} \times \rho_{urea}} \quad \text{[l/h]} \qquad (3\text{-}10)$$

where:
$\dot{V}_{urea}$, urea solution consumption [l/h]
P_{engine}, engine power output [kW]
$\dot{m}_{NO_2}$ NO_x (as NO_2) from engine - NO_x after SCR [g/kWh]
MM_{urea}, urea ($(NH_2)_2CO$) molar mass [g/mol] (=60.07)
MM_{NO2}, NO_2 molar mass [g/mol] (=46.01)
C_{urea}, urea solution concentration [weight-%]
ρ_{urea}, urea density [kg/l] ≈ 1.1
For what the power demand, weight, room occupied, efficiency and other technical data related to the SCRs employed on board of the reference cruise ship, see Table 3-10. The used solution has a 40% of urea concentration on weight.

Table 3-10 SCR employed on board of the reference cruise ship technical data [43].

	Engine type		
	W12V46C	W8L46C	
Weight (SCR+urea tank+auxilieries)	7.5	3.9	[ton]
SCR's dimension	4.5x3.25x2.95	3.8x2.65x2.25	[m^3]
Urea tank and auxilieries' dimension	10.5	7.2	[m^3]
Urea consumption	195	132	[l/h]
Urea tank temperature	n.a	n.a	[°C]
Compressed air mass flow	130	90	[m^3/h]
Compressed air pressure	8	8	[Pa]
Auxilieries' power demand	15	10	[kW]
Temperature difference between SCR's in and out	negligible	negligible	[K]

According to [43], SCR's efficiency is considered to be equal to 85% regardless the engine loads (i.e. exhaust gas' temperatures, mass flow, NOx content…).
An other important consideration regarding the SCR's location has to be done. In the reference cruise ship, SCR's are considered to be placed immediately after the engines. This choice has been made in order to have always an exhaust gas temperature high enough to avoid the risk of hydrocarbons' condensation and ammonium sulphate formation and at the same time to achieve/maintain a good efficiency.
The possible catalyst deterioration caused by high temperatures and the passage of very dirty exhaust gas is a consequence to take into account only when economic point of view is examined. Indeed, if the latter aspect is considered, the catalyst layers' replacement, due to their worsening, represents a cost that has to be contemplated.

3.4.2 Scrubbers for meeting SOx emission reduction

Since using a different kind of fuel instead of HFO is expensive, see Chapter 1, the methodology that is the most affordable to meet Sox emission reduction is the employment of scrubbers on board. Scrubbers have to be efficient enough to ensure SOx emissions levels comparable to those obtained by switching type of fuel. Therefore, an abatement efficiency of 95% is required.

Scrubbers are systems capable of cleaning exhaust gas flows containing SO_x. The working principle is very simple and it is based on a chemical reaction involving SO_x and an alkaline water made of water and a cleaning agent, namely limestone or hydrated lime. After scrubbing, the cleaned exhaust is emitted into the atmosphere. All scrubber technologies create a waste stream containing the substance used for the cleaning process plus the SOx and PM removed from the exhaust. SOx (SO_2 plus SO_3) gases are water soluble. Once dissolved, these gases form strong acids that react with the natural alkalinity of the seawater, or the alkalinity derived from the added substances, forming soluble sodium sulfate salt, which is a natural salt in the seas. In addition, the PM in the exhaust will become entrapped in the wash water, adding to the sludge generated by a scrubber.

The process is regulated by the following chemical reactions for both SO_2 and SO_3 contained in the diesel engines' exhaust gas:

$$SO_2 + H_2O \rightarrow H_2SO_3 \quad (3\text{-}11)$$

$$SO_3 + H_2O \rightarrow H_2SO_4 \quad (3\text{-}12)$$

$$CaCO_3 + H_2SO_3 \rightarrow CaSO_3 + H_2O + CO_2 \quad (3\text{-}13)$$

$$2CaSO_3 + O_2 \rightarrow 2CaSO_4 \quad (3\text{-}14)$$

Sulfurous gases in water are in a state of rapid oxidation: sulfur dioxide (SO_2) oxidizes to sulfur trioxide (SO_3), which dissolves in water to form sulfuric acid (H_2SO_4), Eq. (3-12). Also, upon dissolution in water, SO_2 forms the hydrate $SO_2 + H_2O$ or sulfurous acid H_2SO_3, Eq. (3-11), which dissociates rapidly to form the bisulfate ion HSO_3, which in turn is oxidized to sulfate.

There are two basic concepts commonly proposed for shipboard application of exhaust gas desulphurization systems, the dry scrubber-type and the wet scrubber-type. The basic principles for each concept are described in the following.

3.4.2.1 Scrubber in the maritime sector

First employment of scrubbers as SOx abatement devices in the maritime sector were in the late 1970s. Since then we assisted to an exponential growth of vessels equipped with scrubbers, going from nearly 0 to almost 90 fleet worldwide, considering both new ship and retrofitted ones [44]. Scrubbers are mostly used in RoRo, offshore service ships, cruise/passenger ships and gas carriers, as reported in Figure 3-19. The relatively large numbers of scrubbers fitted onto RoRo ships can be explained by the fierce competition with truck transport within this sector.

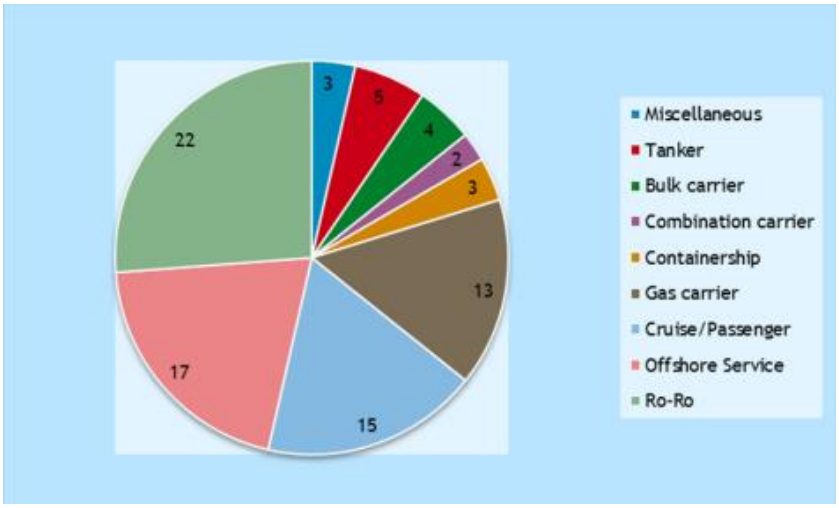

Figure 3-19 Distribution of exhaust scrubbers over ship types [44].

3.4.2.2 Scrubber on board of the Hull C.6194

In this work, two kind of scrubbers have been studied in order to evaluate which one could be the most suitable for an on-board application: both dry scrubbers and wet scrubbers have been considered.

A dry scrubber does not use water or any liquid to carry out the scrubbing process but exposes hydrated lime-treated granulates to the exhaust gas to create a chemical reaction that removes the SOx emission compounds.
The waste stream and generated sludge has to be processed as per the IMO guidelines [45] before discharge overboard, where allowed, or stored and discharged to shore as a waste substance.
Dry scrubbers require an on-board storage of the cleaning agent (lime products), as well as a storage and shore disposal of used reactant. This comes to be a disadvantage because weight and volumes represent a big issue on board of a ship. On the other hand, the heat released during the chemical reaction occurring in dry scrubbers, allows to use SCRs, which require a temperature higher than 300°C, after the scrubbers. This way, SCR can operate with a stream of exhaust gas flows not containing SOx component, reducing the probability of the formation of the, very dangerous for the catalyst, ammonium sulphate compounds. But, since weight and room occupied on board represent an issue of great importance, dry scrubber have not been considered as a feasible solution.

Wet scrubbers can be at open or closed loop: the former use seawater, and the latter use fresh water in combination with chemical additives. Contrary of what already seen for dry scrubbers, wet scrubbers decrease exhaust gas flows temperature. This means that they have to be collocated after the SCRs. This way the problem could be the formation of ammonium sulphate compounds. This can be easily avoided if exhaust gas flows temperatures are maintained above of 340°C, as mentioned before.

Using seawater scrubbers, allows to enhance the chemical reaction efficiency because of presence of the alkalinity compounds, which, as opposite to them, have to be added in closed loop scrubbers. Both scrubbers are very efficient and, in recent study, efficiencies up to 93% [46]. have been reached. It has to be underlined that the quality of seawater is extremely important for better efficiency. This means that seawater scrubbers can have different efficiency depending on the seawater quality. In addition, discharging acidic waste water in the sea, and power consumption for water intake purposes, are other big problems concerning the use of open loop scrubbers. Closed loop scrubber, lacking of these disadvantages, can reach high efficiency regardless the seawater alkalinity.
In this work, closed loop wet scrubbers have been chosen like in most of real applications.
Closed Loop Scrubber have an efficiency of 97% [47]. Such SO_x emissions could also be achieved, without the Scrubber, by switching to a fuel with lower sulphur content.
It has to be underlined that, in this study, only ICEs exhaust gas flows are treated with these devices, meanwhile exhaust gas flows deriving from OFB are released in the atmosphere without being cleaned.
For what the power demand, weight, room occupied, efficiency and other technical data related to the scrubber employed on board of the reference cruise ship, see Table 3-11.

Table 3-11 Scrubber employed on board of the reference cruise ship technical data [43].

	Engine type		
	W12V46C	W8L46C	
Weight (Scrubber)	16	10	[ton]
Weight (Auxilieries)	20	14.5	[ton]
Scrubber's dimension	3.2 diameter x 12.5	2.5 diameter x 12.5	[m^3]
Auxilierie's dimension	15	10	[m^3]
Power demand	8.5	8.5	[kW]

Part II

Model application

Chapter 4

OPERATION PROFILE SIMULATIONS

Achieving the target described in Chapter 1 necessary results in carrying out an optimization procedure, whose outcomes are a help to both cruise ships energy efficiency's engineers and ship-owners.
Therefore, it has been considered essential to briefly introduce the basic optimization principles.

4.1 Optimization model

The aim of an optimization model is to find the best feasible solution, which maximize or minimize a so-called objective function respecting some constraints imposed by the problem under exam.
A generic energy system's optimization is divided into three levels:

1. Synthesis that implies the components appearing in a system and their interconnections
2. Design that determines the technical characteristics (specifications) of the components and the properties of the substances entering and exiting each component at the nominal load (or "design point") of the system
3. Operation that, for a given system (i.e. the synthesis and design are known) under specified conditions, allows the optimal operating point to be reached, which is defined by the operating properties of components and substances in the system (speed of revolution, power output, mass flow rates, pressures, temperatures, composition of fluids, etc.).

The various methods that have appeared in the literature on the optimal synthesis of energy systems can be classified into three groups [48]:

(a) Methods based on heuristics and evolutionary search.
(b) Methods attempting to reach pre-determined targets, which have been identified by the application of physical rules.

(c) Methods starting with a superstructure, which is reduced to the optimal configuration.

In class (a), rules based on engineering experience and on physical concepts are applied to generate feasible configurations, which are subsequently improved by applying a set of evolutionary rules in a systematic way. Artificial Intelligence and Expert Systems have proven effective in generating appropriate configurations [48]. For each acceptable configuration, a figure of merit or performance indicator is evaluated (e.g., efficiency, cost, etc.) and the system with the best performance is selected. These kind of methods, because of their nature, do not guarantee that the found best solution coincide to the optimal one. Nevertheless, at least a near-optimal configuration has been obtained.

In class (b), principles from thermodynamics and other physical sciences are applied to obtain targets for the optimal system configuration. These targets can correspond to upper or lower bounds on the best possible configuration and provide vital information for improvement of existing configurations. In addition, many configurations are excluded from further investigation, thus reducing the search space for the best system. If the physical target is the optimization objective (e.g., minimization of energy utilization), then these methods provide the solution to the optimization problem. However, if the optimization objective is economic, e.g., minimization of the total cost, then these methods are not very appropriate. Attempts have been made to introduce economics at a second level, but the whole approach is mathematically non-rigorous and, consequently, the configuration obtained may be non-optimal [48].

In class (c), a superstructure is considered with all the possible (or necessary) components and interconnections. An objective function is specified and the optimization problem is formulated. The solution of the optimization problem gives the optimal system configuration, which, inevitably, depends on (and is restricted by) the initial superstructure. The main advantages of such an approach are that it can work with any objective function and that it automatically reveals the optimal system configuration. The difficulty with these methods is that the size of the optimization problem may be such that the available mathematical optimization algorithms may not be capable of a rigorous solution.

It should be noted that the distinction among the three classes may not be so clear. For example, the targets of class (b) can serve as heuristics or rules in class (a) and they can be embedded in the optimization procedures of class (c) to the benefit of the whole process.

Generally, the objective function of the complete optimization problem (i.e. synthesis, design, and operation) is written by means in the following equation:

$$\underset{x,w,z}{\text{minimize}}\, F(x, w, z) \qquad (4\text{-}1)$$

subject to the constraints:

$$h_i(x) = 0, i = 1,2, \dots, I \qquad (4\text{-}2)$$

$$g_j(x) \leq 0, j = 1,2, \dots, J \qquad (4\text{-}3)$$

where

- x, set of independent variables for operation optimization (load factors of components, mass flow rates, pressures and temperatures of streams, etc.),
- w, set of independent variables for design optimization (nominal capacities of components, geometry, mass flow rates, pressures and temperatures of streams, etc.),
- z, set of independent variables for synthesis optimization indicating whether the component exists in the optimal configuration or not; it may be a binary (0 or 1), an integer, or a continuous variable such as the rated power of a component, with a zero value indicating the non-existence of a component in the final configuration,
- $h_i(x)$, equality constraint functions, which constitute the simulation model of the system and are derived by an analysis of the system (energetic, exergetic, economic, etc.),
- $g_j(x)$, inequality constraint functions corresponding to design and operation limits, state regulations, safety requirements, etc,
- F, is the objective function and can be the fuel consumption, exergy destruction, annualized cost of owning and operating the system, life-cycle cost (including environmental considerations, if needed), etc.

Eq. (4-1) can be used also for multi-objective optimization problem provided that the various objectives are combined into one objective function by means of weighting factors.

If the system is completely specified, meaning that both the set of independent variables related to synthesis "z" and design "w" are given/imposed, the optimization problem turns out to be one of operation and the objective function expressed by Eq. (4-1) becomes Eq. (4-4):

$$\underset{x}{\text{minimize}}\, F_{op}(x) \qquad (4\text{-}4)$$

For what the specific application under exam is concerned, the amount of the possible options regarding the components' designs and synthesis, is restricted to some kind of engines' size and technology in order to respect the constraints imposed by the problem under exam. It follows that a complete three-levels optimization has not been carried out but rather an operational one[4]. Notwithstanding, an operation optimization has been considered not only a plus but also a necessity in order to improve the under exam cruise ship's energy efficiency with the aim of meeting IMO requests.

Thus, the optimization problem is one of operation.

[4] For sake of clarity, when dealing with GTs as prime movers, EGBs' design has to be provided. Hence, the optimization procedure turns out to be a mixed up one, which takes into account the EGBs' performance in the operation optimization procedure.

Because of the presence of both discrete and continuous variables as well as non-liner functions, the problem under exam falls under the general category of MINLP problems that combine the combinatorial difficulty of optimizing over discrete variable sets with the challenges of handling nonlinear functions.
Which methods among those reported in pag. 53 has to be adopted for the application under exam, is another issue to be solved. From a literary review focused on optimization in the maritime sector, it has been chosen to follow the same method used by Dimopoulos et al. in [49], which undergoes the class (a) of the methods described in pag. 53.
It is worth introduce the readers on what methods based on "heuristics and evolutionary search" consist of.

4.1.1 Evolutionary algorithms (EAs)

An evolutionary algorithm is an optimization method, which uses a mechanism inspired by biological evolution. Adopting Charles Darwin's quote "*the fittest survives*", the idea behind an evolutionary technique is that, for a given population of individuals, the environmental pressure causes natural selection leading to an increase of the population's fitness.
EAs were developed by Holland [50] in an attempt to simulate growth and decay of living organisms in a natural environment. Even though originally designed as simulators, EAs turned out to be a robust optimization technique denoting an ability to find the global optimum, or a near-optimal point, for any optimization problem [51].
Differently to optimization strategy adopted by the classical algorithms, which iterate from one solution point to the other as long as the goal has been reached, an evolutionary algorithm works with a solution points population, which is updated and "transformed" as the optimization process goes. Updating and transforming are made through particular operators that are mathematical representations of physical procedures, or laws of nature, that describe the growth and decay of living organisms in physical systems. The most used operators are "reproduction", "crossover" and "mutation".
Reproduction is based on one of the basic laws of evolution, which states that the most optimal species are multiplied more than others, while the less optimal species die out. Thus, with the application of reproduction on a population, a temporary new population is created, which consists of more copies of the more optimal solutions, while the less one tend to be dropped out. In correspondence with natural systems, a randomization is also inserted. Due to this randomization, sometimes solutions of higher optimality may not be reproduced as many times as those of lower optimality.
Next, to this temporary new population the crossover operator is applied. This operator emulates the evolution of species in natural systems. In a given population, this operator randomly couples two individuals and then interchanges the characteristics between the two individuals, giving birth to two new individuals (off-springs) which correspond to two new points in the optimization space.
Finally, to the so created individuals, the mutation operator is applied. This operator emulates the random mutation that exists in natural systems, and prevents loss of valuable information. This operator is applied on each individual and performs a

random alteration to its contents, giving birth to a new individual. The application of this operator ensures that even in the most extreme application cases the EA will continue converging to the optimal.
Summarizing, it can be said that sequentially applying EAs' operators on an existing population, a new one is created.
In Figure 4-1, schemes of what mutation and crossover consist are depicted.

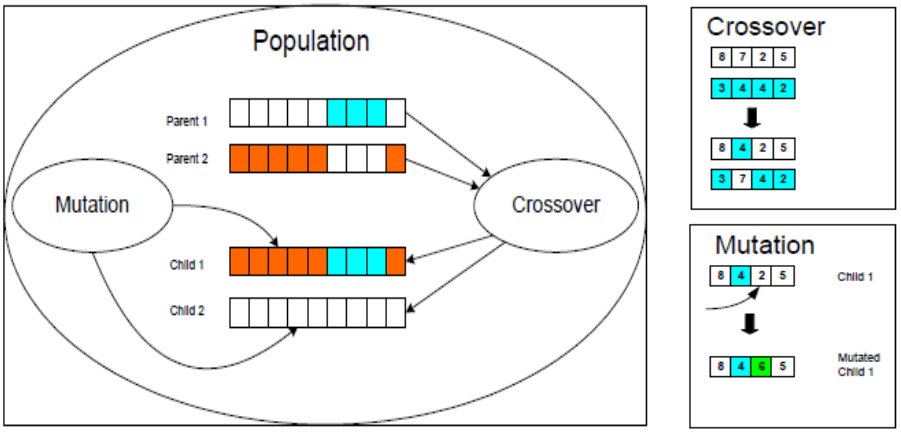

Figure 4-1 Figurative scheme of crossover and mutation [52].

A generic EA work following these steps and sub-steps:

1. Create a random initial population
2. Evaluate the individuals in the population and assign fitness
3. Repeat the generations until termination
    a. Select the most fit individuals (parents) from the population for reproduction
    b. Produce new individuals through Crossover and Mutation operators
    c. Evaluate the new individuals and assign fitness
    d. Replace low fitness members with high fitness members in the population
4. Output

These steps can be represented with the flowchart shown in Figure 4-2.
After initialization, each population's member is evaluated and assigned a fitness. For instance, while solving a single objective maximization problem, a solution point with a higher objective function value is better than a solution point with a lower one. As a consequence, individuals that have higher objective function value are assigned a higher fitness. After that, stopping criteria are checked.
If none of the stopping criteria is met, a new population is generated again and the process is repeated until one or more of the stopping criteria are met.

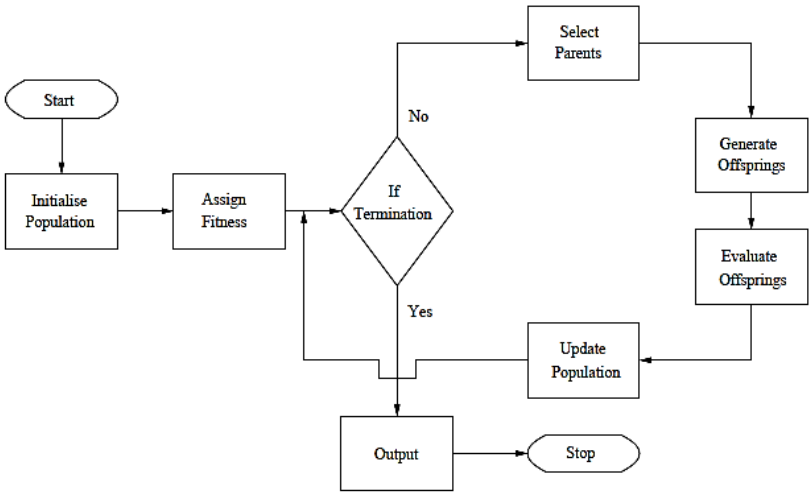

Figure 4-2 Scheme of a generic evolutionary algorithm [53].

A stopping criterion may be static or dynamic. For example, a static stopping criterion may allow an algorithm to run for a fixed number of iterations.
An example of a dynamic stopping criterion is to repeat the process until a certain percent of the solutions is within some percentage of the best solutions found. In some cases, a combination of several stopping criteria is used.

There are many software implementations of EA available from various sources. A more general implementation of EA is the C++ GALib by Wall [54].
Other software packages for EA are also available in EXCEL Solver (http://www.solver.com/),and MatLab (http://www.mathworks.com/products/gads/). In the present work, EXCEL Solver has been chosen to optimize engines' load and consequently the global ship efficiency.
For sake of brevity, readers should be referred to Appendix 1 to find out more on the parameters used within EXCEL Solver Add-In and its implementation using Visual Basic language.

4.2 Operation profile simulation

The aim of the optimization carried out in the present work is to ensure that the highest ship's energy efficiency is achieved within operation profiles simulated.
It is high time to introduce how global ship's energy efficiency is calculated for the cruise ship taken into consideration. In this context, the term "global" indicates that the whole cruise is considered meaning that what happens in each cruise's phase is held back. Eq. (4-5) provides how the global ship's efficiency has been determined and considered in this application:

$$\eta_{ship,global} = \frac{E_{el.} + E_{TH,ACC.} + E_{TH,FW}}{E_{fuel,global}} \qquad (4\text{-}5)$$

where

- $E_{el.}$ is the ship's global electric load (consisting of propulsive and accommodation electric loads) (expressed in [kJ])
- $E_{TH,ACC.}$ is the ship's global accommodation thermal load (expressed in [kJ])
- $E_{TH,FW.}$ is the ship's global thermal load for fresh water production (expressed in [kJ])
- $E_{fuel,global}$ is the global energy content of the burned fuel both in the prime movers and in the OFBs (expressed in [kJ])

The last term, $E_{fuel,global}$, can be determined by Eq. (4-6):

$$E_{fuel,global} = E_{fuel,global\_PMs} + E_{fuel,global_{OFBs}} \quad [kJ] \quad (4\text{-}6)$$

where the terms concerned the amount of fuel globally burned in PMs ($E_{fuel,global\_PMs}$) and in OFBs ($E_{fuel,global\_OFBs}$) is given by Eq. (4-7) and Eq.(4-8) respectively:

$$E_{fuel,global\_PMs} = \sum_{k=1} E_{fuel\_PMs_k} \quad [kJ] \quad (4\text{-}7)$$

$$E_{fuel,global\_OFBs} = \sum_{k=1} E_{fuel\_OFBs_k} \quad [kJ] \quad (4\text{-}8)$$

where the index k represents the k-th cruise's phase of which the whole cruise consists. It has to be said that among the useful effects, the thermal load linked to Tanks Heating and E.R. users have not been taken into account because it has been chosen to consider just those effects, which allow the ship to move and to provide facilities to the customers. On the other hand, in Eq. (4-5) the denominator is represented the overall amount of fuel burnt in PMs and hence also that amount used to satisfy the Tanks heating and E.R. users thermal loads.

Analyzing what the Eq. (4-5) suggests, it comes clear that the only way to enhance the ship's energy efficiency is lowering the overall amount of $E_{fuel,global}$ determined by Eq. (4-6).

Although the final result consists of determining $\eta_{ship,global}$ and $E_{fuel,global}$ with Eq. (4-5) and Eq. (4-6) respectively, $\eta_{ship,}$ and $E_{fuel,}$ have been calculated for each cruise's phase using the same equations.

Since OFBs work to satisfy thermal loads (Accommodation and fresh water production), $E_{fuel,global}$ burned in them depends on how much the waste heat, contained in prime movers' exhaust gas, is exploited to cover thermal loads.

At this moment, it is important to make readers aware of how the percentage of cogeneration is calculated, Eq. (4-9):

$$\%\, cogeneration = 1 - \frac{E_{TH,ACC.-OFBs} \times \eta_{OFB} + E_{TH,FW.-OFBs} \times \eta_{OFB}}{E_{TH,ACC.} + E_{TH,FW}} \quad (4\text{-}9)$$

where

- $E_{TH,Acc.-OFBs}$ is the accommodation thermal load covered by OFBs' use [kJ]
- $E_{TH,FW.-OFBs}$ is the thermal load for the fresh water production satisfied by OFBs [kJ]
- η_{OFB} is OFB's thermal efficiency.

Thermal loads satisfied by OFBs are determined by Eq. (4-10) and Eq. (4-11) for what concerns accommodation thermal loads and fresh water production thermal loads respectively:

$$E_{TH,ACC.-OFB} = E_{TH,ACC.} - E_{TH,ACC.-EGBs} \quad [kJ] \quad (4\text{-}10)$$

$$E_{TH,FW.-OFB} = E_{TH,FW.} - E_{TH,FW.-Cogen.} \quad [kJ] \quad (4\text{-}11)$$

where

- $E_{TH,ACC.-EGBs}$ is the accommodation thermal load covered by the exhaust gas waste heat recovery through EGBs [kJ]
- $E_{TH,FW.-Cogen.}$ is the thermal load for the fresh water production [kJ].

Thermal load for the fresh water production is fulfilled by two different ways respect to prime movers' typology:

- Internal Combustion Engine: exploitation of engines' High Temperature circuit, as already mentioned in ¶ 2.2.2.2 and in ¶ 3.1.1
- Gas turbines: exploitation of the remaining exhaust gas' waste heat content once having satisfied the accommodation thermal load, for further information see paragraph 4.3.

Generally, heat recovered by exhaust gas waste heat exploitation, $E_{TH,WHR}$, is proportional to exhaust gas' mass flow and temperature as reported in Eq. (4-12):

$$E_{TH,WHR} \propto (\dot{m}_g, T_g) \quad (4\text{-}12)$$

where

- $\dot{m}_g$ is the exhaust gas mass flow
- T_g is the exhaust gas temperature

These two fundamental parameters depend only on a single factor: %MCR that is calculated by Eq. (2-4) both for ICEs and GTs. The relations, which link %MCR and the above parameters are depicted in Figure 3-6 and in Figure 3-9 for what concerns the ICEs and GTs respectively. Along with that, also the amount of heat recovered by ICEs' high temperature circuit exploitation depends on %MCR, as already seen in Figure 3-8.

In conclusion, lowering $E_{fuel,global}$ burned means that in every cruise's phase the fittest %MCR has to be reached so that to achieve the best percentage of cogeneration in the reference cruise ship. In other terms, a sort of compromise between exhaust gas waste heat exploitation and OFBs' use is necessary.

Since prime movers are of different size, choosing which kind of engines should be switched on in order to provide the most suitable %MCR and hence the lowest $E_{fuel,global}$, is not trivial and therefore an optimization procedure is useful. Indeed, because of the

isolated nature of the cruise ship's energy system, for every cruise's phase electric loads have to be firstly satisfied not "tout court" but in such a manner that can also guarantee the global lowest $E_{fuel,global}$.
It can be said that, the question to which the optimization procedure intends to respond is:

"Given a cruise's phase, having a specific electric and thermal loads, which kind of prime movers should be switched on in order to provide the highest ship's energy efficiency?"

Therefore, as already mentioned, the optimization procedure is one of operation that leads to determine the maximum ship's energy efficiency for each cruise's phase (or equivalently the minimum E_{fuel} burned), characterizing by specific electric (sum of propulsive and non-propulsive loads) and thermal loads. It is obvious that, maximizing/minimizing ship's energy efficiency/E_{fuel} burned for each cruise's phase results in maximizing the global efficiency, $\eta_{ship,global}$ reported in Eq. (4-5) or minimizing the $E_{fuel,global}$ burned reported in Eq. (4-6).
To answer to the above question, it is necessary to consider the cruise ship as an energy system consisted of those components, which have been described in Chapter 3.
Starting from input (electric and thermal loads reported in ¶2.2), the optimization procedure works on the ship's mathematical modelling giving as output the ship's energy efficiency.
Along with energy efficiency, pollutants emissions are calculated consequently. In the present work five kind of pollutants emissions are considered: NOx, SOx, CO, PM and HC. Among these, the first two kinds have been mostly considered because of the MARPOL regulations.
Determining pollutants' emissions just as a mere operation profile simulation's consequence, turns out to characterize the optimization problem as a single objective one although EA, used in the present work, is suitable enough to face up to multi-objective optimization problems. Multi-objective optimizations, focusing on both energetic and environmental aspects, could be implemented in further works.
In Figure 4-3, it has been figuratively reported how all the simulations carried out in his work could be schematized.

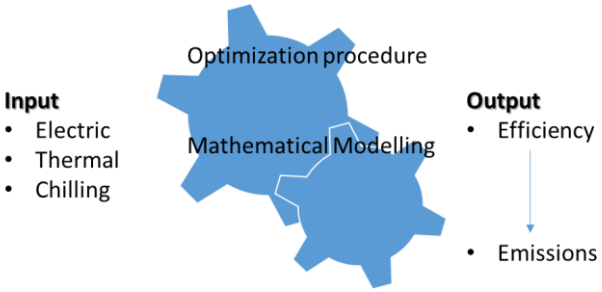

Figure 4-3 Scheme of the operation profile simulation

For each cruise' phase and season, operation profile simulation has been carried out with a code implemented in Micosoft Excel in which the Solver Add-In has been used to provide the best engines' combination ensuring the maximum efficiency, or the minimum $E_{fuel,global}$ burned.

4.2.1 Engines' Configurations

Reference cruise ship, which has been undergone to the operation profile simulations, has to be considered as an energy system where different options satisfying energy's load are possible.
Main possible option involves prime movers' configuration choice: employing particular kind of engines rather than another one turns out in considering other feasible opportunities aiming at covering the chilling load.
Besides that, equipping the reference cruise ship with ICEs means that exhaust gas after treatment devices ought to be inserted on board and therefore they must be considered as an integral part of the ship regarded as an energy system.
For what the prime movers' is concerned, the choice would be to have a cruise ship equipped by three kind of configurations, which differentiate from each other by the prime movers' typology used.
In the present work, configurations' classes based on ICEs, GTs as well as on the simultaneous presence of ICEs and GTs have been considered providing a sort of test matrix, which takes into account a wide spectrum of feasible solutions. Hereafter, the first two kind of configurations have been named "Standard configurations" while the third "Hybrid Configurations", for clarity's sake see Table 4-1.

Table 4-1 Nomenclature of the different possible engines' configurations

Engines' typology	Configurations' classes
ICE GT	Standard
ICE + GT	Hybrid

In the following, a brief description of the three major engines' typology configurations is provided.

ICEs class

For what concerns the ICEs class, it consists of two possible solutions: ICE and ICE_eco. The first one is the configuration actually employed on the reference cruise ship while the latter is an upgrade of the first one meaning that SCRs and Scrubber are also included on-board making the ship MARPOL compliant even if HFO is employed as fuel. As already assessed in Chapter 3, SCRs and Scrubbers need power to make auxiliaries working therefore an extra electric load has to be added to the original one.

GTs class

Switching kind of fuel (from HFO to MGO) offers the possibility to examine the GTs class.

It consists of two possible alternatives characterized by a different way of covering the chilling load. Indeed, because of GT's great amount of exhaust gas waste heat content, trigeneration system can be used in order to satisfy the chilling load rather than that actually used based on compression chillers devices. Given that, within GTs class there are two configurations named GT and Trigeneration (Trigen.). It comes clear that when analyzing this class, no kind of exhaust gas after treatment device ought to be conceived thanks to the fuel's major cleanliness. Furthermore, both thermal and electric loads have been revised. In detail, for both the configurations, thermal loads linked to Tanks heating and E.R. users have been dismissed because MGO does not need any kind of heating to be used, therefore the ship's total thermal loads correspond to the accommodation one. Besides that, Trigen. configuration needs a further modification of both thermal and electric loads. Indeed, electric load due to the compression chillers' use has been converted into thermal load as a direct consequence of having considered an absorption chiller to satisfy the ship's chilling load reported in Table 2-4. It follows that, the ship under exam has new Non-propulsive electric loads as well as new Accommodation thermal loads, which have to be calculated. The new cruise's ship loads are determined by Eq. (4-13) for Non-propulsive electric loads and Eq. (4-14) for Accommodation thermal loads:

$$Non\_propulsive_{Trigen.} = Non\_propulsive - El._{chilling} \quad [MW] \quad (4\text{-}13)$$

$$P_{TH,chilling} = \frac{El._{chilling}}{COP_{abs.}} \quad [MW] \quad (4\text{-}14)$$

where

- $Non\_propulsive_{Trigen.}$ are the new non-propulsive electric loads which refers to the Trigen. case
- $Non\_propulsive$ are non-propulsive electric loads reported in Table 2-3
- $El._{chilling}$ are chilling loads reported in Table 2-4
- $COP_{abs.}$ is the absorption chillers Coefficient of performance equal to 1.4 as reported in Table 3-9
- $P_{TH.,chilling}$ is the thermal load that has to be provided by the absorption chillers in order to satisfy the chilling loads.

Both Eq.(4-13) and Eq. (4-14) are clearly valid for each cruise's phase and season.
Using Eq. (4-13), it can be possible to calculate the $Non\_propulsive_{Trigen.}$ electric loads reported in Table 4-2 where, for sake of clarity, the $Non\text{-}propulsive$ electric loads of Table 2-3 are reported too, considering only the harbor and navigation cruise's phase.
From Table 4-2, it can be seen that in Trigen. configuration there is no distinction among the seasons. Indeed, using absorption chillers instead of compression chillers makes even the Non-propulsive electric loads, whose seasonal differences are precisely due to chilling loads.
Accommodation thermal loads reported in Table 2-6 are added by those determined with Eq. (4-14) as shown in Table 4-3, where, as already mentioned, data relatives to

the maneuvering phase have been omitted because of this phase scarce importance from the time consuming point of view.

Table 4-2 Non-propulsive and Non-propulsive$_{Trigen.}$ electric loads divided into cruise's phase season [MW].

		Non-propulsive		**Non-propulsive$_{Trigen.}$**	
		Harbor	Navigation	Harbor	Navigation
Season	W	7.5	9.3	7.15	7.8
	S	8.7	9.9		
	A	8	9.7		

Table 4-3 Reference and Trigen. case accommodation thermal loads divided into cruise's phase and season [kW].

		Navigation			**Harbor**		
		W	S	A	W	S	A
Reference accommodation thermal load (Table 2-6)	Pre-Re Heating	5272	1932	659	5272	1932	659
	Hot Water	3086	2374	2730	3086	2374	2730
	Galley User	817	817	817	817	817	817
	Swimming	81	811	446	81	811	446
	Loundry	1616	1616	1616	1616	1616	1616
	Chilling ($P_{TH,,chilling}$)	4681	6688	5684	950	4750	2850

Hybrid class

Meanwhile, adopting either ICEs or GTs as the only kind of prime movers is a quite clear choice, the reason why also hybrid solutions have been considered lies on the fact that they could combine the best aspects coming from the "one-kind" prime movers configuration. In particular, they could bring together different features respect to the prime movers' class:

ICEs' class → high efficiency

GTs' class → reduced weight and volume due to both smaller engines and the SCRs and scrubbers' absence, exhaust gas waste heat exploitation.

In particular, hybrid solutions have been divided/collected into three major sub-classes depending on the main prime movers employed on board:

1. *1.x* hybrid solutions are based on the simultaneous presence of three gas turbines and one internal combustion engine
2. *2.x* hybrid solutions are characterized by the employment of two gas turbines and two internal combustion engines
3. *3.x* hybrid solutions are marked by the existence of one gas turbine and three internal combustion engines.

Considering all the possible matching between the two available engines' size, the overall number of hybrid solutions considered in the present work is 13.

It is important to make readers acknowledged that hybrid solutions' Tanks heating and E.R. users thermal load reported in Table 2-5 have been revised and corrected. For sake of brevity, new total thermal loads are not reported here but it is worthwhile saying that they have been determined proportionally on the number of ICEs' employed on board.
Since all the hybrid solutions deal with ICE's presence, the same ICEs' number of exhaust gas after treatment devices have to be employed on board. Therefore, it is well worth noting that Hybrid configurations work in "eco" mode, represented by both the SCRs and scrubbers' presence on board.
Summing up these considerations, this kind of solutions are considered hybrid because of two aspects:

1. simultaneous presence of two kind of engines
2. GTs and ICEs class mixture of both thermal and electric loads.

Every considered prime movers' configuration respects the constraint imposed by the constructor on the total power installed on board for safety reasons eventually considering the adoption of an extra gas turbine as already done for GTs class, as reported in 3.1.2.
More in detail, engines' configuration for "Standard" and "Hybrid" configurations are reported in Table 4-4 and Table 4-5 respectively where the presence of an extra 5 MW GT is considered wherever it is necessary. In particular, this extra GT is installed on board in those engines' configurations, which have a discrepancy of the total power installed on board of more than 5% respect to the ICEs case.

Table 4-4 Standard configuration

		# Prime Movers	P [kW]	P TOT [kW]
GT	Type A	2	8342	43014
	Type B	2	10665	
	Extra GT	1	5000	
ICE (=ICE_eco)	W8L46C	2	8400	42000
	W12V46C	2	12600	

Table 4-5 Hybrid configurations

		1,1	1,2	1,3	1,4	2,1	2,2	2,3	2,4	2,5	3,1	3,2	3,3	3,4
GT	Type A	1	1	2	2	2	2	0	0	1	1	0	1	0
	Type B	2	2	1	1	0	0	2	2	1	0	1	0	1
ICE	W8L46C	1	0	1	0	2	0	2	0	1	1	1	2	2
	W12V46C	0	1	0	1	0	2	0	2	1	2	2	1	1
P tot		38072	42272	35749	39949	33484	41884	38130	46530	40007	41942	44265	37742	40065
Δ% P tot		-9%	1%	-15%	-5%	-20%	0%	-9%	11%	-5%	0%	5%	-10%	-5%
P tot+ Extra GT		43072		40749		38484		43130					42742	
Δ% P tot		3%		-3%		-8%		3%					2%	

For all these engines' configurations, operation profile simulations have been carried out with the aim of maximizing $\eta_{ship,global}$ defined in Eq. (4-5) providing that some constraints are fulfilled or minimizing the $E_{fuel,global}$ burned, as depicted in Eq. (4-6).
For sake of clarity, let readers consider the 1.1 configuration, which employs three gas turbines, one of those is Type A and two are Type B, and one small ICE, as it can be seen in Table 4-5. For every k-th cruise's phase (and for every season) the optimization statement is provided by Eq. (4-15), the first of those is the objective function and the others are constraints equations:

$$\begin{cases} \text{minimize } E_{fuel} \\ \\ subjected\ to \\ \\ 0 \leq t\ Type\ A \leq 1 \\ 0 \leq u\ Type\ B \leq 2 \\ 0 \leq v\ ICE \leq 1 \\ 0.5 \leq \%MCR \leq 1 \end{cases} \qquad (4\text{-}15)$$

where

- $t\ Type\ A$ is the number of Type A GT that works in the k-th cruise's phase
- $u\ Type\ B$ is the number of Type B GT that is on in the k-th cruise's phase
- $v\ ICE$ is the number of ICE that operates in the k-th cruise's phase

The term E_{fuel} is calculated by means of Eq. (4-16):

$$E_{fuel} = t \times E_{fuel,Type\ A} + u \times E_{fuel,Type\ B} + v \times E_{fuel,ICEs} + E_{fuel,OFBs} \quad [kJ] \qquad (4\text{-}16)$$

where

- $E_{fuel,Type\ A}$ is the amount of fuel burned in the Type A GT
- $E_{fuel,Type\ B}$ is the amount of fuel burned in the Type B GTs
- $E_{fuel,Type\ ICEs}$ is the amount of fuel burned in the W8L46C ICE
- $E_{fuel,OFBs}$ is the amount of fuel burned in OFBs

For each k-th cruise's phase, the EA has to decide not only which kind of prime movers switch on, but also how many of that: $t\ Type\ A$, $u\ Type\ B$ and $v\ ICE$ are, therefore, the decision variables.
The constraint of 0.5 imposed to the minimum allowable %MCR, has been set in order not to deal with low engines' loads that are not reached in the practice.
It should be pointed out that, the choice of minimizing the $E_{fuel,global}$ burned rather than $\eta_{ship,global}$ is justified in order to make comparison among all the engines' configurations the fairest possible. In particular, this choice is the rightest one to properly take into account all the beneficial effects in the Trigen. configuration.
Furthermore, amount of $E_{fuel,global}$ is given in terms of energy fuel content instead of tonnes of fuel to overcome the issue concerned the fact to handle fuels having different physical and chemical properties.

4.2.2 Emission modelling

Besides the proper optimization problem, whose goal is to minimize $E_{fuel,global}$, there is the environmental aspect to take into account too. As figuratively expressed in Figure 4-3, pollutants emissions' calculations are done once the optimization procedure has been completed.

Indeed, for what concerns the pollutants emissions, it has been chosen to follow the method suggested by Haglind [13], who reported a list of pollutants emissions factors in order to overcome the lack of pollutants emissions technical data provided directly by the constructor.

In particular, emission factors depend on the fuel's quality and the combustion's mode and they are expressed as $g_{pollutants}/kg_{fuel}$. Therefore, it comes clear now that ship's pollutants emissions is a consequence of how much fuel is burned in PMs and OFBs and so it represent a sub-output of the entire optimization procedure.

In more detail, pollutants emissions here considered can be divided into two groups:

1. PM, SO_x and HC
2. NO_x and CO.

This distinction is the result of each group's dependency on fuel's quality rather than combustion's mode: the first group is linked to the fuel's quality and the second one to the combustion's mode.

For what SO_x emission factor is concerned, it depends only on the fuel's sulphur content. Indeed, considering SO_x as SO_2, emission factor has been calculated as reported in Eq. (4-17) :

$$EF_{SO_x} = 2 \times \%S_{fuel} \qquad [g_{pollutants}/kg_{fuel}] \qquad (4\text{-}17)$$

From what it can be found in [7], the average percentage of sulphur content is 2.7% and 0.1% for HFO and MGO respectively. Consequently, emission factor calculated by means of Eq. (4-17) are 54 g_{SOx}/kg_{fuel} and 2g_{SOx}/kg_{fuel} for HFO and MGO.

In Table 4-6 emission factors for all the pollutants considered are reported depending on fuel quality (HFO and MGO) and combustion mode (OFB, GT and ICE).

Table 4-6 Pollutants emission factors [$g_{pollutants}/kg_{fuel}$] depending on the fuel's quality and combustion modes [13].

	ICEs_HFO	GTs_MGO	OFBs	
			HFO	MGO
CO	7.4	2.2 (=10 ppm)([31], [32])	0.14	0.14
PM	7.6	1.1	7.6	1.1
SOx	54	2	54	2
NOx	87	8 (=15ppm) ([31], [32])	28.6	28.6
HC	2.7	0.05	2.7	0.05

The dependency of pollutants emissions factors on fuel's quality rather than combustion's mode is particularly remarkable for OFBs's case. In Table 4-6, it can be seen indeed that, CO and NO_x emissions factors depend on the OFBs own combustion mode, which is a simply direct flame combustion, while others emissions factors change in conjunction with a fuel's switching.
Therefore, once having the total amount of Fuel burned, the general Eq. (4-18) is used for every type of pollutants:

$$PE_h = EF_h \times Fuel \quad [g] \qquad (4\text{-}18)$$

where
PE_h is the h-th pollutants emissions
EF_h is the h-th pollutants emission factors depending on fuel's quality and combustion mode as reported in Table 4-6
$Fuel$ is the total amount of fuel burned in ICEs, GTs and OFBs [kg].
In ICE_eco and Hybrid configurations, the abatement efficiency of SCR and scrubber are implemented in Eq. (4-18), which results in two new equations: Eq. (4-19) and Eq. (4-20) for what the ICEs's NO_x and SO_x emissions is concerned respectively:

$$PE_{NO_X} = EF_{ICE\_NO_X} \times Fuel_{ICE} \times \eta_{SCR} \quad [g] \qquad (4\text{-}19)$$

$$PE_{SO_X} = EF_{ICE\_SO_X} \times Fuel_{ICE} \times \eta_{scrubber} \quad [g] \qquad (4\text{-}20)$$

where

- EF_{ICE_NOx} is the NO_x emission factor specific for the ICE's combustion mode
- EF_{ICE_SOx} is the emission factor for HFO's use
- η_{SCR} is the SCR's abatement efficiency equal to 85%
- $\eta_{scrubber}$ is the scrubber's abatement efficiency equal to 97%.

4.3 Mathematical modelling of the Hull C.6194

To carry out the operation profile simulation's optimization is necessary to provide equations on which EA can operate.
As already mentioned, main goal in the present work is determine the minimum allowable $E_{fuel,global}$ satisfying all the ship's energy demands represented by electric, thermal and chilling loads, which are the problem's optimization input. Besides finding out $E_{fuel,global}$, the other provided result represents the pollutants emissions' assessments, whose values are linked to $E_{fuel,global}$. In conjunction with these results, for every engine's configuration, overall weight and volume occupied on board have been defined based on data reported in Chapter 3. Indeed, it is worthwhile reminding that saving weight and volume is a positive aspect enabling the possibility to enhance the pay-load or reducing the ship's DWT involving lower power demand. This fact would lead to re-design the ship, which is far beyond the present work's porpoise.
To achieve the targets, for every engines' configuration it has been followed the below logical sequence:

- $E_{fuel,global}$'s determination, hence the $\eta_{ship,global}$
- emissions pollutants evaluation
- connecting the found out results with weight and volume occupied by the devices included in the engine's configuration under exam.

The energy system's modelling equations are presented divided into the three engine's configurations above identified.

4.3.1 ICEs class model

First of all, it is necessary to calculate the global amount of fuel burned in both ICEs and OFBs, $E_{fuel,global\_ICEs}$ and $E_{fuel,global\_OFBs}$ respectively.

Fuel burned in ICEs is directly linked to %MCR as it has been already reported in Figure 3-4 from which it can be seen that the relation between %MCR and $SFOC_{ISO}^3$ can't be approximate with a linear relation.

Through an interpolation, it has been determined the behavior of ICEs' $SFOC_{ISO}^3$ respect the ICEs' %MCR, which is represented by Eq. (4-21), which is valid for both the engine's size:

$$SFOC_{ISO}{}^3 = A \times \%MCR^7 + B \times \%MCR^6 + C \times \%MCR^5 + D \times \%MCR^4 + E \times \%MCR^3 + F \times \%MCR^2 + G \times \%MCR + H \quad \text{[g/kWh]} \qquad (4\text{-}21)$$

where the %MCR's factors are reported in Appendix 4, Table A.4-1.

To take into account the fact that ISO conditions are not reached during the cruise's operation profile, it is necessary to determine SFOC in service ($SFOC_{is}$) with the Eq.(4-22) :

$$SFOC_{is} = \frac{SFOC_{ISO}}{H_i} * H_{i(ISO)} * (1 + DD.GG\ SFOC\ tolerance) \quad \text{[g/kWh]} \qquad (4\text{-}22)$$

where

- H_i is HFO's lower heating value (=9700 [kcal/kg])
- $H_{i(ISO)}$ is HFO's lower heating value in ISO conditions (=10200 [kcal/kg])
- $DD.GG.SFOC\ tolerance$ is a safety coefficient introduced by Fincantieri and is set equal to 5%.

From $SFOC_{is}$ it can be possible to find out the fuel used for every kind of engine ($Fuel_{ICE}$) by Eq. (4-23):

$$Fuel_{ICE} = NP \times MCR\% \times h \times n^{\circ} \times SFOC_{is} \quad \text{[ton]} \qquad (4\text{-}23)$$

where, along with the already introduced $SFOC_{is}$ and $\%MCR$

- NP is the switched on ICE's nominal power [kW]
- h is the considered cruise's phase duration [h]
- n^{o} is the switched on ICEs' number in the k-th cruise's phase [-]

For every cruise's phase, $E_{fuel,ICE}$ burned in ICEs can be determined by Eq. (4-24):

$$E_{fuel,ICE} = Fuel_{ICE} \times H_i \times 4{,}18 \times 1000 \quad \text{[kJ]} \quad (4\text{-}24)$$

Summing all the $E_{fuel,ICE}$, it can be possible to determine $E_{fuel,global}$.
This amount of fuel is necessary to satisfy firstly the ship's total electric loads.
Thermal loads consisting of Tanks heating, E.R. users, Accommodation loads are satisfied by exhaust gas' exploitation through EGB's use.
As reported by means of Eq.(4-12), thermal power content in the exhaust gas is proportional to both exhaust gas mass flow and temperature. From data reported in Table 3-7, it can be possible to build the graph reported in Figure 4-4 from which it can be possible to extrapolate the general Eq. (4-25), i.e. valid for every kind of ICE, between %MCR and thermal power recovered, P_{TH,WHR_ICE}.

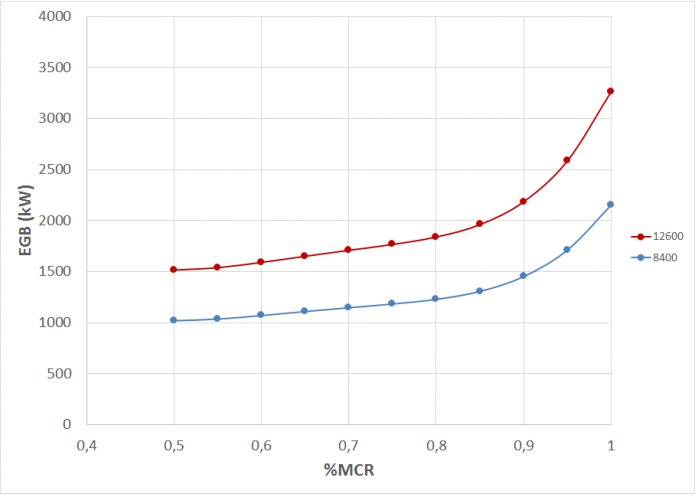

Figure 4-4 Thermal power recovered Vs. ICE's %MCR data obtained from [28].

$$P_{TH,WHR\_ICE} = (A \times \%MCR^5 + B \times \%MCR^4 + C \times \%MCR^3 + D \times \%MCR^2 + E \times \%MCR + F) \quad \text{[kW]} \quad (4\text{-}25)$$

where the coefficients are reported in Table A.4-2.
To determine the k-th cruise's phase total amount of the thermal power that can be recovered by EGBs, result of Eq. (4-25) has to be multiplied by the number of ICEs switched on in that specific cruise's phase.
If ship's total thermal loads are not satisfied by the exhaust gas waste heat recovery, OFBs have to be used in order to satisfy the remaining thermal loads as reported in Eq. (4-26) :

$$OFB_{TL} = Thermal\ Load - P_{TH,WHR\_ICE} \quad \text{[kW]} \quad (4\text{-}26)$$

where

- OFB_{TL} are thermal loads that have to be supplied by OFBs

- *Thermal load* are ship's thermal loads reported in Table 2-5
- P_{TH,WHR_ICE} are thermal loads covered by EGBs found out with Eq. (4-25).

Therefore, considering that OFBs have an efficiency of 90%, fuel burned in them for this porpoise is given by Eq. (4-27):

$$Fuel_{OFB} = \frac{OFB_{TL}}{\eta_{OFB} * H_i} * h * 3.6 \quad \text{[ton]} \qquad (4\text{-}27)$$

Using Eq. (4-24) it is possible to convert the amount of fuel burned in OFB from tonnes to energy content finding out, for every cruise's phase, $E_{fuel,OFB}$.

For what the fresh water production is concerned, engines' high temperature circuit is used and, if not sufficient, extra OFBs' work is required. Relation between thermal power recoverable and engines' load (%MCR) is shown in Figure 3-8 and it can be modelled with the following Eq. (4-28):

$$P_{HT\_FW_{ICE}} = A \times \%MCR^5 + B \times \%MCR^4 + C \times \%MCR^3 + D \times \%MCR^2 + E \times \%MCR + F \quad \text{[kW]} \qquad (4\text{-}28)$$

where the relative coefficient are reported in Table A.4-3.

Along with high temperature circuit, in order to provide the maximum waste heat recovery, further exhaust gas exploitation has been considered. Hence, the total amount of thermal power that is available for fresh water production is given by Eq. (4-29):

$$P_{FW,ICE} = P_{HT\_FW_{ICE}} + \dot{m}_g \times c_{p;g} \times \left(T_{g,OUT,EGB} - T_c\right) \quad \text{[kW]} \qquad (4\text{-}29)$$

where

$\dot{m}_g$ is the exhaust gas mass flow [kg/s]

$c_{p,g}$ is the thermal capacity at a constant pressure for the ICE exhaust gas flow [kJ/(kg*K)]

$T_{g,OUT,EGB}$ is the exhaust gas temperature once having been exploited firstly in the EGB [°C]

T_c is the minimum temperature required to exit the chimney equal to 110°C [43].

Exhaust gas temperature exiting EGB is determined by technical data reported in Table 3-7, and depicted in Figure 4-5, and they can be modelled by Eq. (4-30):

$$T_{g,OUT,EGB} = A \times \%MCR^4 + B \times \%MCR^3 + C \times \%MCR^2 + D \times \%MCR + E \quad \text{[°C]} \qquad (4\text{-}30)$$

where the coefficient are reported in Table A.4-4.

If this amount is not satisfying the fresh water thermal loads, further OFBs' use is necessary. For sake of brevity, it can be said that Eq.(4-26) and Eq.(4-27) can be applied also for this case.

Having the amount of $E_{fuel,ICE}$ and $E_{fuel,OFB}$ for every cruise's phase, it is possible to determine $E_{fuel,global}$ simply making a summation.

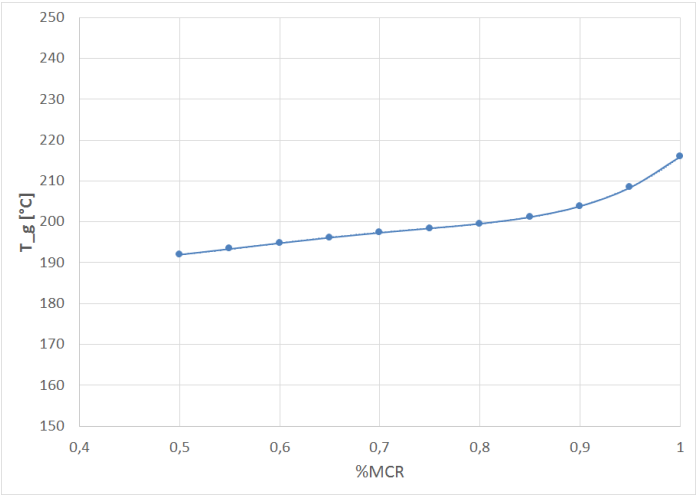

Figure 4-5 Relation between $T_{g,OUT,EGB}$ (T_g) and %MCR data obtained from [28].

The first result has been reached from which the global ship efficiency and pollutants emissions can be found using Eq. (4-18) and just in case of ICE_eco, Eq. (4-19) and Eq. (4-20) have to be used too.

The latter aspects to consider is the issue concerning weight and volume occupied on board by both the engines' configuration. Weight and volume are those linked to prime movers, EGB, exhaust gas after treatment devices as well as chilling compressors. Summarizing these data, which have been provided in Chapter 3, weight and volume for the different ICEs based configuration are reported in Table 4-7.

Table 4-7 Weight and volume for ICE and ICE_eco

	ICE	ICE_eco	
Weight	858	1001	[ton]
Volume	1060	1600	[m^3]

4.3.2 GTs class model

When handling gas turbines as prime movers, same kind of results has to be determined.

As already done for ICEs class, firstly the relation between $SFOC_{ISO}$ and %MCR ought to find out. Curve modelling GTs' fuel consumption at varying load have been already depicted in Chapter 3 and modelled with Eq. (4-31):

$$SFOC_{ISO} = A \times \%MCR^6 + B \times \%MCR^5 + C \times \%MCR^4 + D \times \%MCR^3 + E \times \%MCR^2 + F \times \%MCR + G \quad \text{[g/kWh]} \qquad (4\text{-}31)$$

where the coefficient are reported in Table A.4-5.
$SFOC_{ISO}$ becomes $SFOC_{IS}$ using the Eq. (4-22) provided that the lower heating value of MGO is considered equal to 10400 [kcal/kg].
Also for GTs class, Eq. (4-23) and Eq. (4-24) are used to determine $Fuel_{GTs}$ and $E_{fuel,GTs}$ respectively determining the fuel used to firstly satisfy the total ship's electric loads.
Up to now, any particular difference between the two class of "Standard" configuration has been not highlighted, letting unchanged the ship's model.
On the other hand, for what the thermal loads' coverage is concerned, a particular analysis ought to be done for this "Standard" configuration class. Indeed, the high amount of heat contented in the exhaust gas flow makes cogeneration, which is already implemented in the actual ship's engines configurations based on ICEs, even much fruitful and hence an *ad hoc* analysis must be done.
To calculate how much thermal load can be satisfied with exhaust gas exploitation, relation between waste heat recoverable and GT's %MCR have to be provided, as done for ICEs' class.
Since, exhaust gas's mass flow and temperature are very different if compared to those of ICEs, it is not possible to use the same kind of EGB already employed on board, i.e. Eq. (4-25) can not be used anymore. Therefore, the design of suitable GTs' EGB is necessary meaning that new EGBs have to be "created", one for each GTs' Type.
It follows that, for what GTs class is concerned, it has been done not only an operation optimization but also a design one with the aim of having those EGBs providing the best compromise between their weight and volume and ship's energy efficiency, or the percentage of cogeneration. In particular, this has been achieved connecting results provided by THERMOFLEX with operation profile simulations optimization. What the simulations carried out with THERMOFLEX are able to provide are the relations between GTs' %MCR and thermal power recoverable.
For what the weight and volume of new EGBs, they have been determined by those reported in table for ICEs making a proportion based on the thermal power exchanged between the two working fluids, i.e. the exhaust gas and water/steam flow. Eq. (4-32) and Eq.(4-33) have been used in order to provide weight and volume for the new EGBs:

$$V_{TOT} = V_{ECO} + V_{EVA} = P_{TH,ECO,GT} \times \left(\frac{V}{P_{TH}}\right)_{ECO,ICE} + P_{TH,EVA,GT} \times \left(\frac{V}{P_{TH}}\right)_{EVA,ICE} \quad [m^3] \quad (4\text{-}32)$$

$$W_{TOT} = W_{ECO} + W_{EVA} = V_{ECO} \times \left(\frac{W}{V}\right)_{ECO,ICE} + V_{EVA} \times \left(\frac{W}{V}\right)_{EVA,ICE} \quad [ton] \quad (4\text{-}33)$$

where

- V_{TOT} is the total volume occupied by EGB [m^3]
- V_{ECO} is the volume of the economizer [m^3]
- V_{EVA} is the volume of evaporator [m^3]

- $P_{TH,ECO,GT}$ is the thermal power exchanged in design mode in the GT's EGB economizer [kW]
- $P_{TH,EVA,GT}$ is the thermal power exchanged in design mode in the GT's EGB evaporator [kW]
- $P_{TH,ECO,ICE}$ is the thermal power exchanged in design mode in the ICE's EGB economizer [kW]
- $P_{TH,EVA,ICE}$ is the thermal power exchanged in design mode in the ICE's EGB evaporator [kW]
- W_{TOT} is the total EGB's weight [ton]
- W_{ECO} is the weight of economizer [ton]
- W_{EVA} is the weight of evaporator [ton].

To take into account a wide spread of EGBs' size, it has been chosen to consider 10 different EGBs which have different delta T pinch point[5]. Two extreme EGBs have been identified characterized by a delta T pinch point of 34°C and 304°C. These values are justified by the fact that 34°C is equal to that of ICEs and 304°C is the delta T pinch point if design ICEs steam flow is produced by GTs exhaust gas recovery. Within these two extreme EGB, other EGBs have been considered, as reported in Table 4-8.

Table 4-8 Delta T pinch point values @ design conditions for the 10 new different EGBs

# EGB	Delta T pinch point @ design conditions
1	34
2	64
3	94
4	124
5	154
6	184
7	214
8	244
9	274
10	304

Determination of EGBs's data in design mode has been done with THERMOFLEX meaning that parameters such as:

- water vapor mass flow
- water outlet of economizer temperature
- gas outlet of Economizer temperature
- economizer total heat transfer rate to water-side ($P_{TH,ECO}$)
- economizer global heat exchange coefficient (UA_{eco})

[5] It is important to remind that delta T pinch point is the most important design parameter dealing with heat exchangers. Indeed, the value of this parameter is linked with heat exchangers' size and consequently the thermal power that a particular heat exchanger could exchange in design mode.

- evaporator total heat transfer rate to water-side ($P_{TH,EVA}$)
- evaporator global heat exchange coefficient (UA_{eva})
- water outlet of economizer steam quality

have been provided for every Type of GT.
For further information on EGB's models and design parameters also implemented in THERMOFLEX, see Appendix 2.
In this way, determination of weight and volume by Eq. (4-32) and Eq. (4-33) is achieved.
Once design mode is provided, off design mode has been simulated too making vary GTs' %MCR with THERMOFLEX, finding out the behavior of the 10 EGBs with GTs' loads variations for each GT's size. As an example, Figure 4-6 shows the water vapor mass flow produced by the 10 EGBs connected to Type B GT at different %MCR whereas Figure 4-7 reports the behavior of the maximum thermal power that can be recovered by n°1 and n°10 EGB, connected to Type B GT.
Obviously, the same kind of results are achieved for the EGBs connected to the Type A GT.

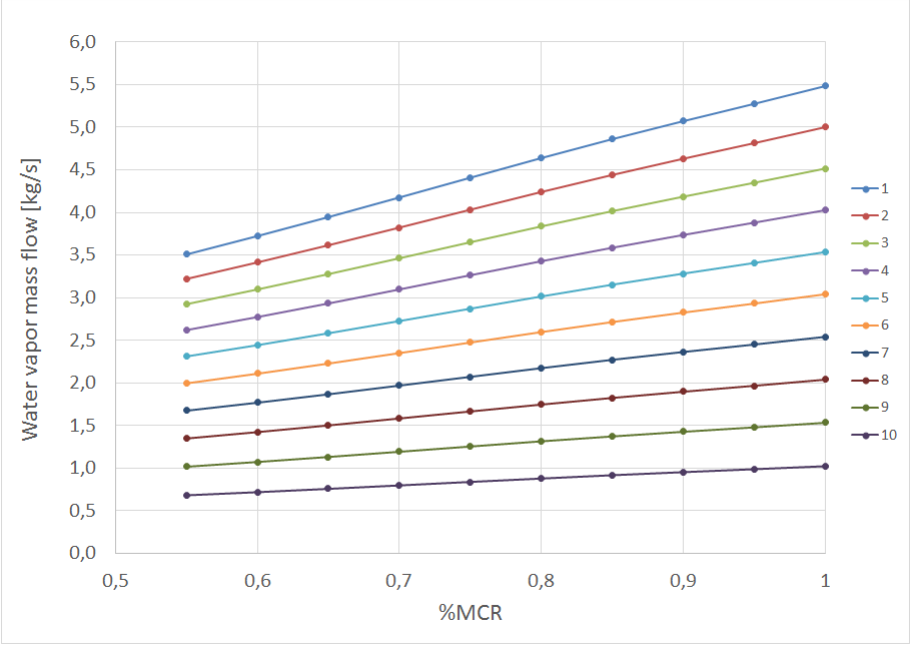

Figure 4-6 Water vapor mass flow produced at varying %MCR for every EGB considered and connected to Type B GT.

After this procedure, relation between thermal power recoverable and GT's loads has been implemented in the optimization procedure of the cruise ship's operation profile. For every kind of EGB, annual average global ship's efficiency has been calculated.

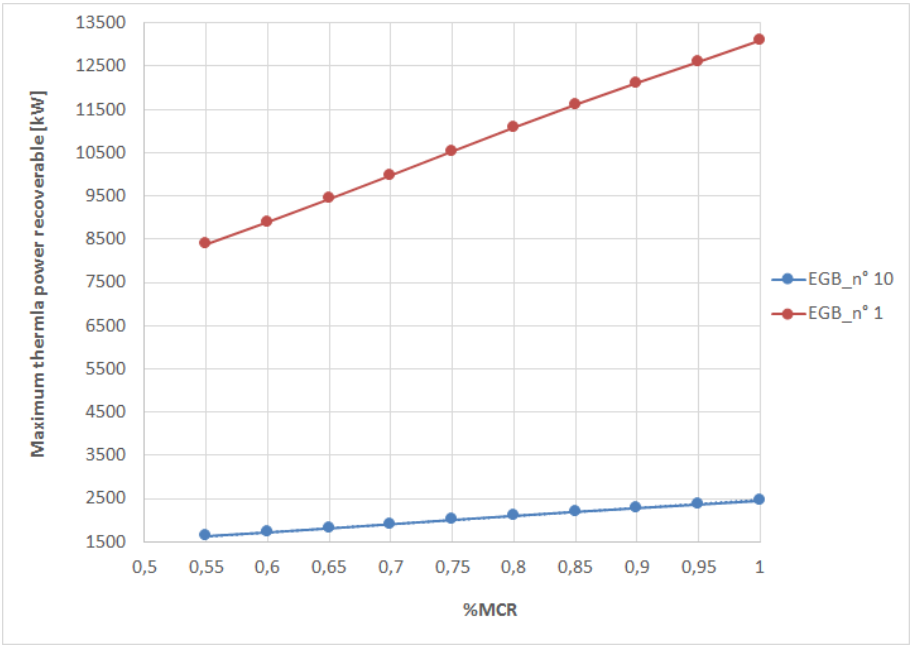

Figure 4-7 Relation between the maximum thermal power which can be recovered in EGB n°1 and EGB n° 10 connected to Type B GT.

In particular, the model sets that just the steam flow useful to cover ship's thermal loads is produced in the EGB.
This means that once thermal loads are satisfied, i.e. the useful steam production is reached, waste heat contented in exhaust gas flow is not exploited anymore.
As a consequence, exhaust gas could further be exploited to cover other thermal loads, i.e. that linked to the fresh water production.

Graph reported in Figure 4-8 suggests that the best EGB option is the number 4 since it allows to have a good enough ship's efficiency with a reasonable volume occupied.
From Figure 4-8, it can be noted that after a certain point, ship's efficiency does not increase anymore even if further water vapor could be produced, as depicted in Figure 4-6. This is due to the fact that, after a certain #EGB, which provides to satisfy thermal loads, increasing EGBs size to exploit all the waste heat content in the exhaust gas flow is not fruitful as it can be inferred by Figure 4-9. Indeed, the smallest EGB (n°1) provides the minor amount of energy recovered (EGB_{th}) but the highest exhaust gas temperature ($T_{g,OUT\ EGB}$) leaving the EGB. On the other hand, the biggest EGB (n°10) provides the major amount of energy recovered but the lowest exhaust gas temperature leaving EGB. Therefore, a compromise has to be reached and hence EGB n°4 has been selected.
With such a high exhaust gas temperature, as depicted in Figure 4-9, other exploitation is possible in order to cover other thermal loads. In particular, $T_{g,OUT\ EGB}$ can be found by Eq. (4-34) for Type A and for every cruise's phase.

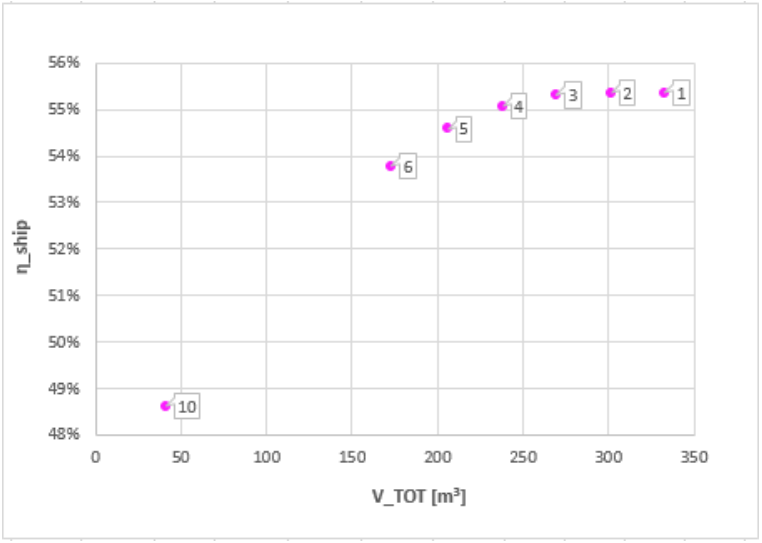

Figure 4-8 Annual average global ship efficiency for 6 of the 10 selected EGB Vs. the total volume occupied

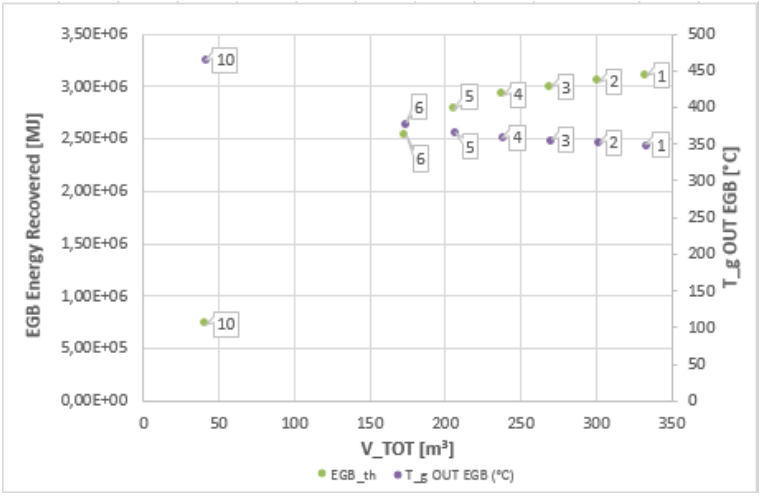

Figure 4-9 Annual average energy recovered by EGB's use, Temperature of exhaust gas Vs. total volume occupied for every #EGB

$$T_{g,OUT,EGB} = TOT_{Type\ A} - \left[TL \times \frac{TOT_{Type\ A} \times \dot{m}_{g,Type\ A}}{TOT_{Type\ A} \times \dot{m}_{g,Type\ A} + TOT_{Type\ B} \times \dot{m}_{g,Type\ B}}\right] \quad [°C] \qquad (4\text{-}34)$$

where

$TOT_{Type\,A}$ is the TOT of Type A GT
m_{gTypeA} is the exhaust gas mass flow of Type A GT
$TOT_{Type\,B}$ is the TOT of Type B GT
m_{gTypeB} is the exhaust gas mass flow of Type B GT
TL is the ship's thermal load reported in ¶ 4.2.1 in *GTs class*.
Eq. (4-34) is obviously valid also for Type B GT but it is not reported for brevity's sake.
Hence, for the best EGB (n°4), the maximum total thermal power that can be recovered is given by Eq. (4-35):

$$P_{TH,WHR\_GT} = A \times \%MCR + B \quad \text{[kW]} \qquad (4\text{-}35)$$

where the coefficients, which are different for Type A and Type B GT, are reported in Table A.4-6.
Once again, the procedure used for ICEs class to determine the amount of Fuel burned in prime movers and in OFBs, has been followed also for GTs class.
For what the fresh water production is concerned, it is necessary to determine the amount of thermal power that can be further exploited, which depends on $T_{g,OUT,EGB}$, i.e. the temperature of exhaust gas leaving EGB, and determined by Eq. (4-34).
Besides $T_{g,OUT,EGB}$,, for the selected EGB, a linear relation can be established between T_g and %MCR and it is reported in Eq. (4-36):

$$T_g = A \times \%MCR + B \quad \text{[°C]} \qquad (4\text{-}36)$$

where the coefficient are reported in Table A.4-7.
It is important to point out that T_g is reached just in case there is a complete exploitation of the heat content of the exhaust gas. In other words, T_g is the minimum temperature that the exhaust gas can reach once it has been completely exploited. If not, the exhaust gas leaving EGB has a higher temperature given by Eq. (4-34).
After having left its own EGB, all the exhaust gas mass flow are collected in another heat exchanger, which has the due to produce steam for the fresh water production.
The thermal power available for fresh water production is given by Eq. (4-37):

$$P_{TH,FW\_GT} = \left(\dot{m}_{g,Type\,A} + \dot{m}_{g,Type\,B}\right) \times c_{p,g} \times (T - T_c) \quad \text{[kW]} \qquad (4\text{-}37)$$

where
$m_{g,Type\,A}$ is the Type A exhaust gas mass flow [kg/s]
$m_{g,Type\,B}$ is the Type B exhaust gas mass flow [kg/s]
$c_{p,g}$ is the thermal capacity [kJ/(kg*K)]
T is the weighted average temperature of the gas stream based on exhaust gas mass flow exiting EGB [°C] and given by Eq. (4-38):

$$T = \frac{TOT_{Type\,A} \times \dot{m}_{g,Type\,A} + TOT_{Type\,B} \times \dot{m}_{g,Type\,B}}{\dot{m}_{g,Type\,A} + \dot{m}_{g,Type\,B}} \quad \text{[°C]} \qquad (4\text{-}38)$$

T_c is the minimum allowable at chimney's outlet (equal to 110 °[C]).

Once again, the procedure followed for ICEs' class can be repeated also for this GT's configuration in order to provide the total amount of fuel burned in GTs and OFBs.
On the other hand, if Trigen. configuration is taken into account, the maximum steam flow production is requested for each of the 10 different EGB since water vapor is used in absorption chillers. Figure 4-10 shows that the best EGB is different since what was no sense in GTs configuration, thus the maximum exploitation of waste heat content in the exhaust gas flow, is now necessary. But, it has to be said that exploiting too much exhaust gas flow means lower too much the exhaust gas temperature and hence OFBs have to been used affecting negatively to the ship's efficiency.

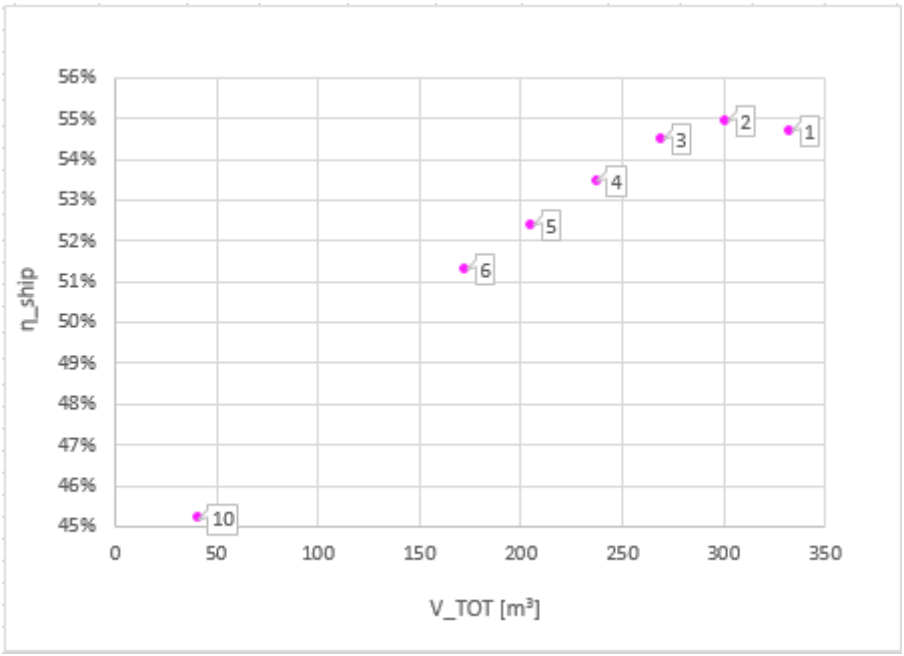

Figure 4-10 Annual average global ship efficiency for 6 of the 10 selected EGB Vs. the total volume occupied for Trigen. configuration.

For sake of brevity, it can be said that the same equations provided for GT and ICEs configuration can be applied tout court also for the Trigen. one.
It can be concluded that in GT case EGB n°4 is selected both for Type A and Type B GT on the other hand, for what the Trigen. case is concerned, EGB n°2 has been chosen as the best one for both the employed size's GTs.
In Table 4-9 the overall weights and volumes relative to GT and Trigen. configurations are reported highlighting those weights and volumes, which are linked to the different selected EGBs for both the configurations.
For sake of clarity, EGBs' weights' values are found out by means of Eq. (4-33).

Table 4-9 Overall GT and Trigen. weights and volumes underlying the values relative to the selected EGBs, namely n°4 for GT case and n°2 for Trigen.

	GT	Trigen.	
Weight	625	501	[ton]
EGBs	182	231	
Volume	935	1137	[m^3]
EGBs	371	470	

4.3.3 Hybrid solutions configurations

Being hybrid solutions, ship's energy system modelling equations can be inferred from those reported for GT and ICE class.

As done for the standard configurations, in Table 4-10 it has been reported the overall weights and volumes for all the hybrid engines configurations.

Table 4-10 Overall weights and volumes for all the hybrid engines configurations.

	1,1	1,2	1,3	1,4	2,1	2,2	2,3	2,4	2,5	3,1	3,2	3,3	3,4	
Weight	709	783	679	752	711	877	771	937	815	939	969	865	877	[ton]
Volume	1071	1134	1039	1102	1137	1339	1202	1404	1233	1470	1502	1407	1363	[m^3]

Chapter 5

RESULTS

In this paragraph, results obtained by the optimization procedure, described in Chapter 4, are presented.
Given the thesis objectives outlined in Chapter 1, results are given in terms of:

- energy efficiency
- amount of pollutants emissions
- weight and volume occupied

relative for all the engines' configurations analyzed and selected, whose descriptions readers should refer to Chapter 4.
Firstly, it has been presented results concerning the operation profile simulation carried out when a "one-kind" engine and basic waste heat recovery solutions are used. This means that the first depicted results are those relative to ICE, ICE_eco and GT in order to give a general overview of what can be bettered/worsened by GT and ICE_eco configurations with respect to the actual ICE.
Following that, results obtained for all the engines' configurations, including the hybrid one, are shown and compared.
For sake of brevity, seasonal variation of ship's efficiency, major pollutants emissions (NO_x and SO_x) and fuel energy consumption are highlighted just for "one-kind" engine configurations.

5.1 "One-kind" engine configurations

5.1.1 Global ship efficiency

Figure 5-1 reports a comparison of cruise averaged values of the global ship's energetic efficiency computed for the three cases and for different seasons.
The highest efficiency is always attained by ICE case. ICE_eco is negatively affected by the supplementary energy demand of the auxiliaries of SCR and scrubber systems that cause a ship efficiency drop of about 1%. Both ICE and ICE_eco cases are only marginally affected by the seasonal changes.

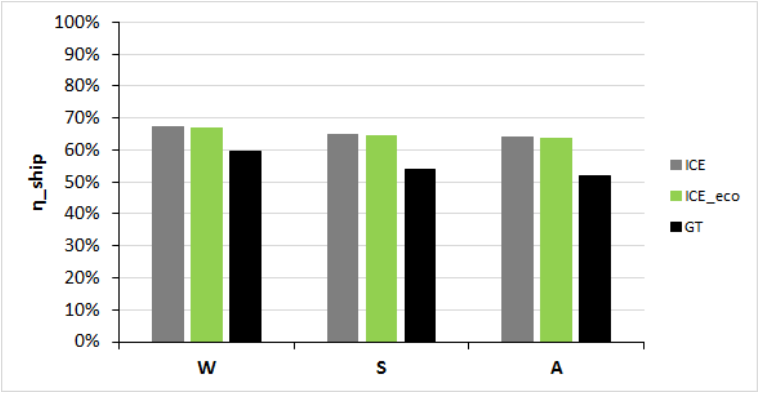

Figure 5-1 Global ship's efficiency for every season and "one-kind" engines' configuration.

On the contrary, GT configuration is rather more sensitive to climate variability resulting to strong variations of the efficiency gap with respect to ICE case, ranging from –6% for winter up to –13% for autumn.
Even if not reported for brevity, it can be seen that thanks to the cogeneration of the thermal loads, the initial gap between the electric efficiency of ICE and GT as PMs can be effectively reduced or even erased as happens for winter-harbor condition. Nevertheless the available heat for GT case often exceeds the thermal ship demand, hence causing a remarkable energy waste that, at the end, results in the observed gap about $\eta_{ship,global}$. The same observation allows also to explain the strong dependence of GT efficiency from seasonal changes, being the thermal loads strictly linked to the climate conditions. Readers are invited to refer to what is reported in Appendix 5 in order to deepen these concepts.

5.1.2 Emissions analysis

Figure 5-2 provides the overall NOx emissions produced during the cruise for the analyzed configurations and separating the three seasonal conditions as well. Data have been computed relying on specific factors provided by the producers, in particular 12 g NOx/kWh for ICEs [29] and 15ppmv of NOx at 15%O_2 for GTs [31], [32].
A comparison with MARPOL requirements is provided by reporting the threshold values resulting by both Tier II and Tier III limits (dashed lines). In particular, the threshold specific factors for ICEs are directly computed on the basis of the actual engine's speed (514 rpm), conversely for GTs a lack in the regulations has been highlighted. Indeed, IMO documentation regards only the use of ICEs, therefore, in order to compute a reference limit for the GTs, a conservative choice has been made by considering the lowest values reported in the regulations (i.e. the ones for ICEs above 2000 rpm, see. Figure 1-4). The results obtained for ICE case show that the traditional configuration is by far above the limits imposed by Tier III (about +360%) and exceeds also the ones of Tier II even if for a rather small amount. If the latter issue could be easily overcome thanks to the improvements of the combustion systems adopted on modern ICEs, at present, Tier III limits can be reached only by the adoption of SCR systems as done in the ICE_eco case. Conversely, and as expected, GTs NO_x emissions are remarkably

reduced, even without SCR devices, and turned out to be comparable to the strict thresholds limits here considered. Moreover, nowadays even lower NO_x emissions factors (about 9 ppmv [55]) can be easily attained thanks to novel Dry Low NO_x combustion systems, as reported in Figure 5-3.
In order to make a fair comparison, even if not specifically considered by MARPOL, in the present study also the NO_x emissions coming from OFB have been taken into account. By doing so, the negative gap of ICE case widens considerably, and also for ICE_eco case the limits are exceeded; on the contrary, as it will be clearer hereafter, GT configuration is not affected being the use of OFB rather marginal.

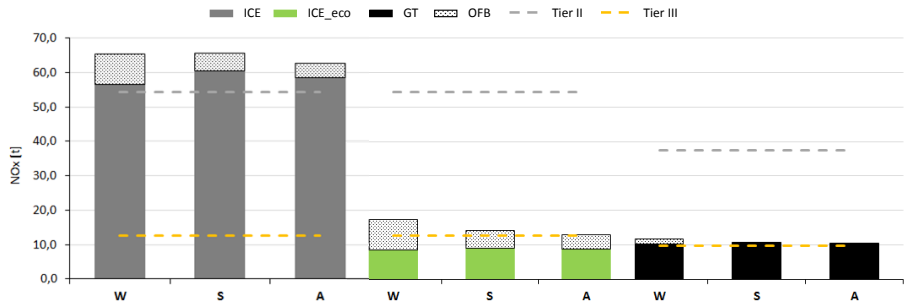

Figure 5-2 NOx emissions for every season and "one-kind" engines' configuration compared with Tier II and Tier III emissions.

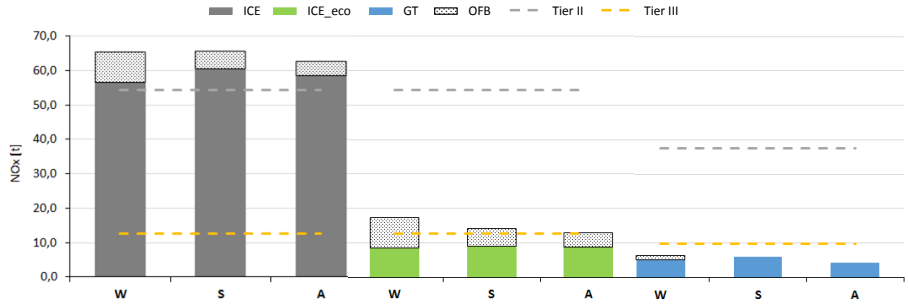

Figure 5-3 NOx emissions for every season and "one-kind" engines' configuration compared with Tier II and Tier III emissions when Dry-Low NOx gas turbines are employed.

The results about SOx emissions are reported in Figure 5-4. Dashed lines indicate MARPOL limits computed on the basis of the different thresholds imposed on the fuel sulphur content (see Table 1-2). The data show that in order to travel through SECA seas, ICE configuration ought to reduce SO_x emissions by at least a 63% average. Said reduction is by far attained by the ICE_eco solution where the scrubber abatement efficiency allows to respect even the stricter future limitations. Thanks to the use of MGO, SO_x emission in the GT case are comparable to the ones of ICE_eco, but they are a little higher than the "SO_x 0.1" threshold level (i.e. the SO_x emissions resulting from ICE burning fuel with 0.1% sulphur content, such as MGO). This issue is a direct consequence of the higher fuel consumption of GTs with respect to ICEs. Finally,

regarding SOx, if the contribution of the OFB is added to the PMs, the difference between GT and ICE_eco cases widens considerably, with the latter exceeding also SOx 0.5 limit.
It has been considered only total (OFB's+PMs's) pollutants emissions occurring in the intermediate season, i.e. autumn, which can be considered the most likely because of the assumed temperatures (see Table 2-1).

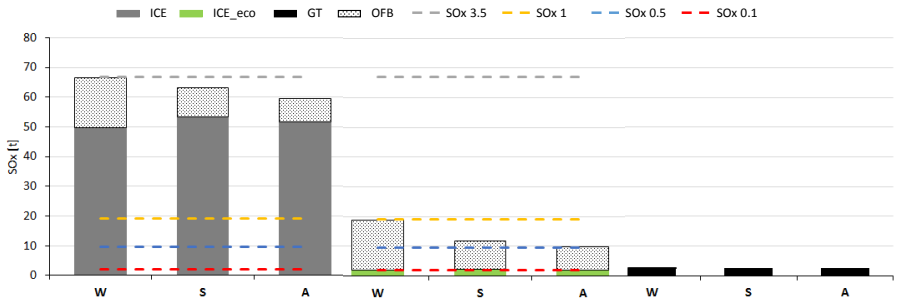

Figure 5-4 SOx emissions for every season and "one-kind" engines' configuration compared with different Sulphur content fuel.

Figure 5-5 shows the comparison between pollutants emissions between ICE, ICE_eco and GT.

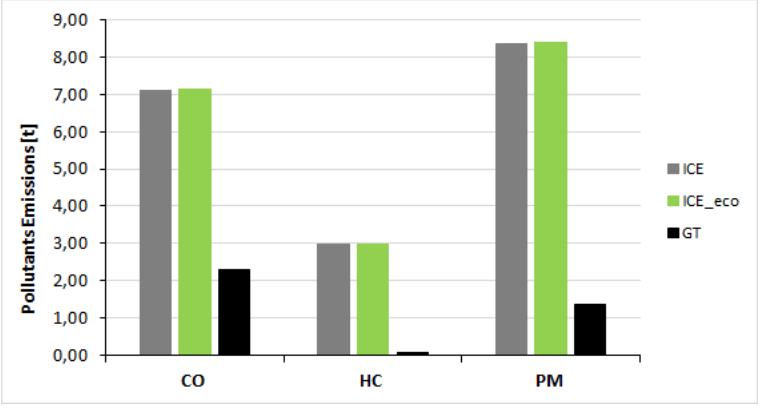

Figure 5-5 Reference cruise ship overall autumn's CO,HC and PM emissions

Abatement devices are effectiveless against CO, HC and PM emissions, therefore ICE and ICE_eco are equal regarding these pollutants. In particular the latter has a little more (+0.44% CO; +2.80% HC and PM) pollutants emissions than the former because of the bigger fuel consumption.
Thanks to a different kind of combustion, GTs are the cleanest one from this point of view. GTs have -97% CO and -83% of HC and PM than ICEs.

5.1.3 Weight and volume

The last comparison consists in quantifying the gap existing between all the configurations in terms of room and weight versus the fuel consumption. Given the different LHV of MGO and HFO, the fuel consumption is provided in terms of fuel energy (FE) instead of tons on fuel and it has been computed considering the fuel burned by both PMs and OFBs[6]. The data about weight and room consider the contribution of PMs, EGBs, Chilling compressors and pollutant abatement devices (when necessary), and derive by the technical specifications of the different systems (see Chapter 3 and Chapter 4).

In order to ease the analysis, the data reported in Figure 5-6 (a) and (b) have been normalized with respect to the values of ICE case.

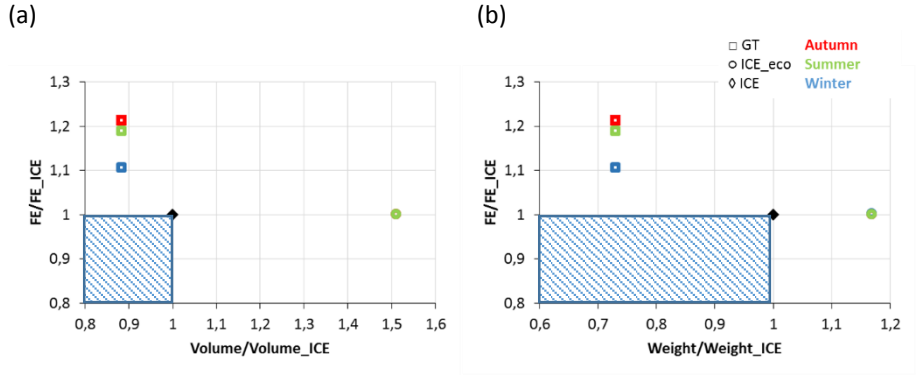

Figure 5-6 ICE's Normalized FE Vs. Volume (a) and (b) Weight.

The expected room and weight savings consequent to the use of GT is rather clear, with a reduction of respectively 11% and 27% of volume and weight with respect to the current ICE case. These percentages correspond to free 125m^3 and to lighten the reference cruise ship of 232 ton.

For what the ICE_eco is concerned, the use of abatement device involves to increase of 50% the volume occupied on board (+440m^3) and to increase the ship's weight of 17% respect the ICEs (+144 ton).

The comparison between GT case and ICE class is even more striking if the ICE_eco case is considered. In particular the use of pollutant abatement devices of ICE_eco solution increase the ratio with respect to GT case up to more than 150% both the volume and the weight: in these two configurations, the difference of volume occupied on board and the weight is equal to 666 m^3 and 376 ton respectively.

From the evaluation of these first graphs, it could be said that employing GTs as prime movers leads both environmental and weight and volume benefits but has a penalty in terms of global ship efficiency. In particular, it would like to have engines' configurations that are inside the blue-dashed box of Figure 5-6 and are capable to reduce the environmental impact typical of ICE.

[6] It is important to notice that FE is just an acronyms for $E_{fuel,global}$ defined by Eq. (4-24).

5.2 Hybrid engines configuration

In this paragraph, results obtained by the operation profile simulation of Hybrid engines' configuration are shown.
The Table 5-1 reports all the considered hybrid engines' configurations highlighting just the number and kind of those engines, which a specific hybrid configuration consists of. For sake of clarity, annual average's fuel energy consumption and pollutants emissions are here considered, as already mentioned.

Table 5-1 Hybrid configurations

		1,1	1,2	1,3	1,4	2,1	2,2	2,3	2,4	2,5	3,1	3,2	3,3	3,4
GT	Type A	1	1	2	2	2	2	0	0	1	1	0	1	0
	Type B	2	2	1	1	0	0	2	2	1	0	1	0	1
ICE	W8L46C	1	0	1	0	2	0	2	0	1	1	1	2	2
	W12V46C	0	1	0	1	0	2	0	2	1	2	2	1	1

Moreover, it is important to remind that every hybrid engines' configuration is equipped with a number of SCRs and scrubbers equal to the ICEs employed on board.
Because of the importance of environmental issue and fuel energy consumptions, the operation profile simulation's results reporting ICE's normalized fuel energy consumption Vs. ICE's normalized NO_x and SO_x are firstly shown in Figure 5-7 and Figure 5-8 respectively.

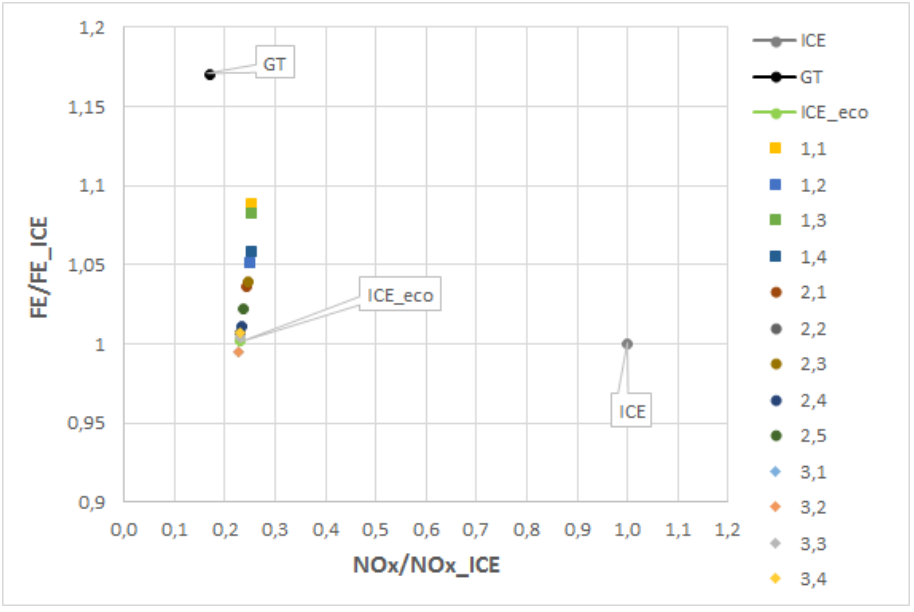

Figure 5-7 ICE's Normalized FE Vs. NOx emissions

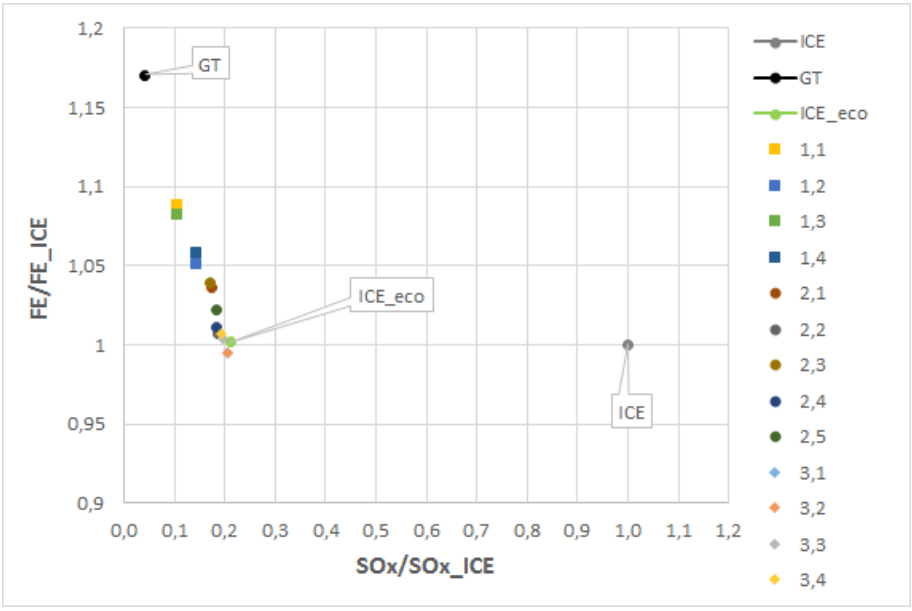

Figure 5-8 ICE's Normalized FE Vs. SOx emissions

It can be seen that all the hybrid engine's configurations are characterized by a strong reduction of both NO_x and SO_x emissions being located into a very limited range of variation.

For what the NO_x emissions is concerned, it can be said that adopting hybrid engine's' configurations instead of ICE, an average of 75% reduction of NOx emissions is achieved. In particular, the best is the 3,2 solution and the worst the 1,4, which are characterized by a reduction of 77% (-50 ton) and 75% (-48,3 ton) respectively if compared to ICE case. Other hybrid solutions show intermediate NO_x emissions reduction compared to the ICE's one.

Considering SOx emissions, hybrid configuration are capable of an even stronger reduction, reaching a decrease of 85% as average. In particular, 1,x engines' configurations are the best while the 3,x the worst. This fact is obviously linked to the kind of fuel adopted: in 1,x engines' configurations MGO is the mostly used fuel but the least in 3,x engines' configurations. Among 1,x configurations, it can be noted that 1,1 and 1,3 are the best being characterized by a reduction of 89% (-56,3 ton) for both of them respect to those of ICE. For what the 3,x configurations is concerned, it can be said that an 80% (-50 ton) reduction is achieved regardless the kind of 3,x configuration is considered.

The 2,x engines' configurations work in a similar fashion to 3,x engines' configurations for both NOx and SOx emissions. Indeed, they mark an average of 77% (-48,7 ton) and 82% (-51 ton) reduction of NOx and SOx emissions respectively. In conclusion, it can be said that adopting hybrid solutions fulfills the request to find out particular engines' configurations capable of reducing NOx and SOx emissions respect to ICE case.

Analyzing what the graphs reported in both the Figure 5-7 and in Figure 5-8, if hybrid engines' configurations are compared to ICE_eco, the following statements can be assessed:

- hybrid engines configurations behave similarly to ICE_eco when NOx emissions are considered;
- hybrid engines configurations show a better behavior than that observed in ICE_eco when SOx are under exam.

When CO, HC and PM emissions are taken into account, Figure 5-9 has to be analyzed. Hybrid configurations have the possibility to cut down the amount of CO, HC and PM emissions respect to ICE case even if the reductions' magnitude is not as high as those observed for NOx and SOx. Moreover, the same trade-off can be noted regardless the kind of pollutants under exam.

From Figure 5-9, it can be noted that the best options are the 1,x engines' configurations. In particular, 1,1 and 1,3 report the highest reduction for all the three kind of pollutants, namely:

- 57% (- 4 ton) for CO emissions
- 64% (- 2 ton) for HC emissions
- 55% (- 4,9 ton) for PM emissions

respect to ICE case.

The lowest reductions are linked to 3,x configurations, which result to behave like ICEs. In more detail, 3,2 is the worst one resulting in a reduction of:

- 0% for CO emissions
- 17% (-0,6 ton) for HC emissions
- 15% (- 1,4 ton) for PM emissions

respect to ICEs.

Contrary to what happens for NOx and SOx emissions, 2,x engines' configurations have an intermediate performance between 1,x and 3,x ones, achieving a reduction's range of:

- 77-91% (-0,6 → 1,6 ton) for CO emissions
- 64-75% (-0,8 → 1,2 ton) for HC emissions
- 69-79% (-1,9 → 2,8 ton) for PM emissions

if compared to ICE.

On the other hand, satisfying the environmental goal involves a penalty in terms of fuel energy consumptions for the majority of hybrid engines' configuration taken into account. Indeed, analyzing this aspect, all the 1,x and 2,x hybrid configurations show an increase of fuel energy consumptions respect to both ICE and ICE_eco case but a decrease respect to GT case, which can be awarded as the cleanest engines' configuration but the most fuel energy consuming.

Furthermore, the range, in which data regarding all the hybrid configurations' fuel energy consumptions are located, is very narrow. Indeed, the maximum variation is that relative to 1,1 configuration, which involves a fuel energy consumption's increase of just 9% respect to ICE case and a decrease of 7% respect to GT case.

The 3,x hybrid solutions are the only that can be achieved the same ICE's fuel energy consumption.

(a)

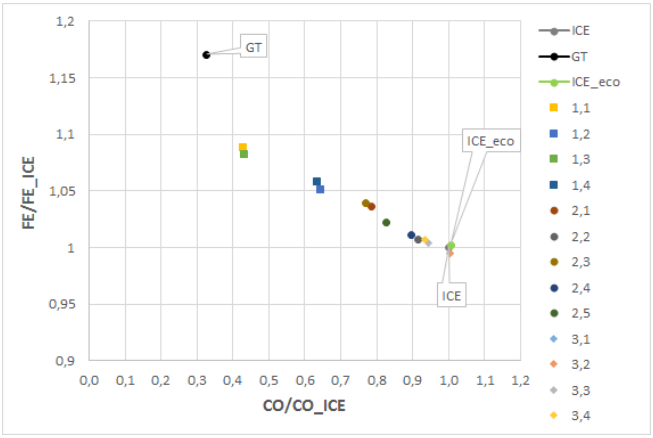

(b)

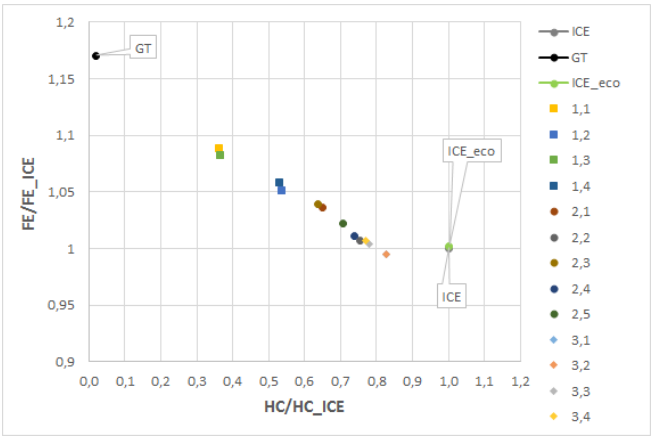

(c)

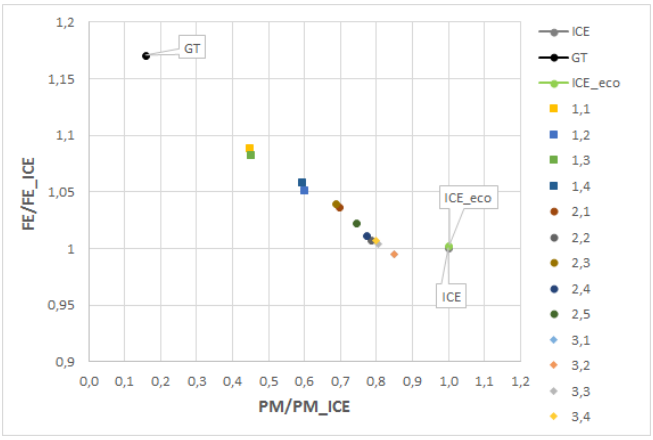

Figure 5-9 ICE's Normalized FE Vs. CO (a), HC (b) and PM (c) emissions.

From Figure 5-7-Figure 5-9, it can be concluded that 1.x and 3.x engines' configurations are more grouped than the 2.x engines' configurations. In other words, not so a deep discrepancy is observed within the same kind of engines' configuration in terms of fuel energy consumption. Indeed, considering 1.x engines' configurations, it can be noted that the range in which data are located is very narrow being less than 1% from the worst to the best one. For what the 3.x engines' configuration is concerned, it can be observed an even smaller discrepancy (less than 0.1 %) to that observed for 1.x engines' configuration. Data relative to 2.x engines' configurations seem not to show any kind of particular behavior being located in the middle of the two reversed engine's configurations.

Focusing the attention on 1.x engines' configuration, it can be seen that there is a sort of coupling among the four configurations: (1,1 & 1,3) Vs. (1,2 & 1,4)
Analyzing all the kind of engines employed in these two coupled configurations, see Table 4-5, this particular behavior is likely to be linked to the kind of ICE employed. Indeed, 1,1 and 1,3 use the smallest ICE while 1,2 and 1,4 the biggest one.
Furthermore, among these configurations, it can be noted that:

- 1,1 is the worst
- 1,2 is the best

Since the optimization procedure has the role to decide which kind of engine has to be switched on with the aim at minimizing the fuel energy consumption, this results has to be inevitably associated to the optimization's problem decision variables, i.e. number and kind of engines that work in a single cruise's phase.
Therefore, it has been thought to extrapolate the graph reported in Figure 5-10 showing the percentage of working hours in which a specific kind of engine is switched on.

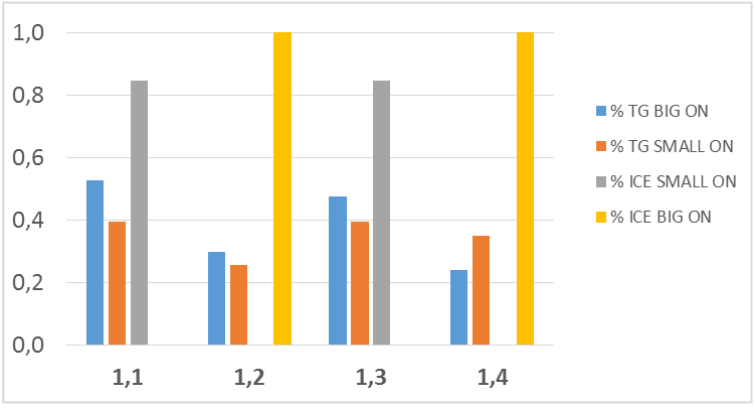

Figure 5-10 Percentage of PMs' working hours for every 1,x engines' configuration and the whole cruise.

To be even clearer, when a specific kind of engine reports 100% of working hours, it means that that engine is always switched on during the whole cruise. On the contrary, when a specific kind of engine reports 0% of working hours, it means that that engine is never switched on during the whole cruise.

From Figure 5-10, it can be noted that the best 1,x engines' configuration, namely the 1,2, is characterized by the lowest amount of GTs' working hours (26% and 30% for Type A and Type B respectively) and the highest amount of ICE's working hours: ICE is always switched on. The other configuration, which shows the same kind of behavior, is the 1,4, in which Type A and Type B works for 35% and 24% of the whole cruise. The very little discrepancy (almost equal to 0,6%) between these two configurations in term of fuel energy consumption (Figure 5-7-Figure 5-9) can be explained by the fact that they differentiate by the number of GT's typology, see Table 4-5. This fact suggests that, adopting more Type B than Type A (1,2 configuration) is more suitable than using more Type A than Type B (1,4 configuration) for the reference cruise's ship. In other words, replacing one Type A GT with the bigger ICE leads to a lower fuel energy consumption.
Within the other couple of engine configuration (1,1 and 1,3), it can be noted a different result. Indeed, replacing one Type A GT with the smaller ICE leads to an higher fuel energy consumption.
Same kind of analysis can be carried out for 3.x engines' configuration. This time, the coupling can be observed between (3,1 & 3,2) and between (3,3 & 3,4)
This behavior is linked to the kind of ICE employed:
3,1 and 3,2 → 1 small ICE + 2 big ICE
3,3 and 3,4 → 2 small ICE + 1 big ICE
It can be noted that:

- 3,1 and 3,2 are the best
- 3,4 is the worst

As for 1,x configurations, it can be explained by the percentage of GT's working hours during the whole cruise, as reported in Figure 5-11.

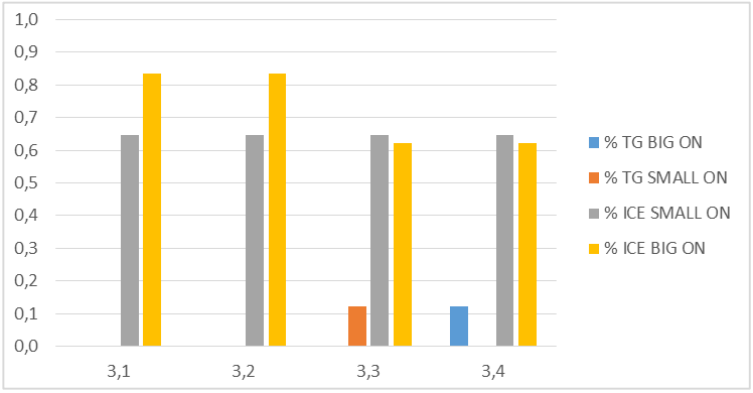

Figure 5-11 Percentage of PMs' working hours for every 3,x engines' configuration and the whole cruise.

The configurations 3,1 and 3,2 are in practice the same from the energy efficiency point of view. Furthermore, they are better than ICE because they have just 3 ICEs and consequence a minor thermal load connected to HFO handling.
Since 3,3 and 3,4 have the same ICEs CFG, the difference in term of fuel energy consumption is due to the kind of GT employed.

It comes out that the smaller one is more suitable.
As a consequence, it comes out also the fact that the 2,x configurations have a mixed up behavior between what it can be noted in the 1,x and 3,x engines' configurations.
Summarizing what can be inferred from graphs reported from Figure 5-7 to Figure 5-11, the following statements can be assessed:

- for GT case, replacing one Type A GT with the biggest ICE, leads to better the fuel energy consumption's performance but to worsen the environmental impact
- for ICE case, replacing one smallest engine with a GT, no-matter which size, leads to maintain the fuel energy consumption registered for ICE and, at the same time, decreasing the environmental impact.

Besides pollutants emissions' evaluation, the aspect linked to the analysis of volume and weight has been considered too, see Figure 5-12 and Figure 5-13 respectively.
As done before, the data reported in Figure 5-12 and Figure 5-13 have been normalized with respect to the values of ICE case.

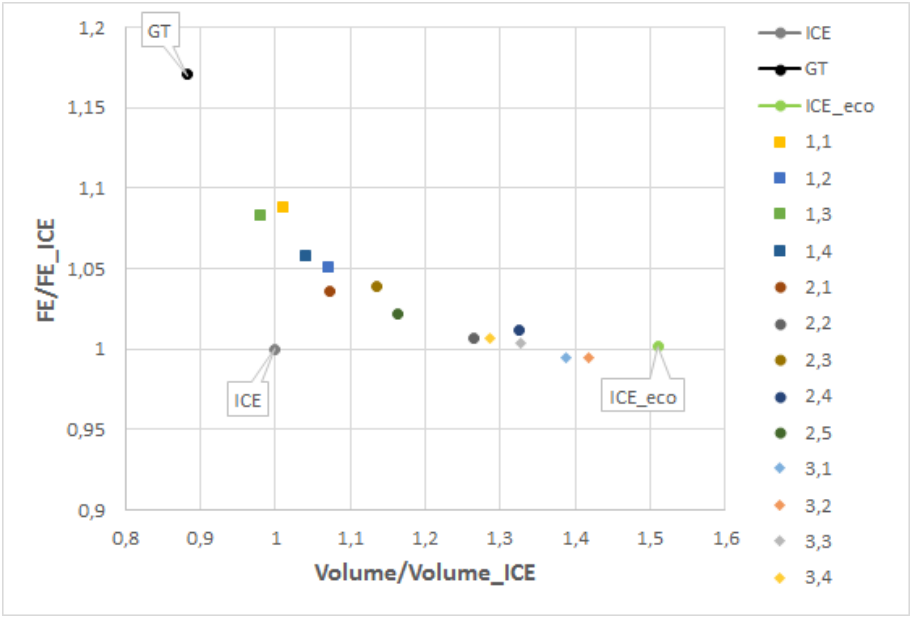

Figure 5-12 ICE's Normalized FE Vs. Volume for every engine's configuration

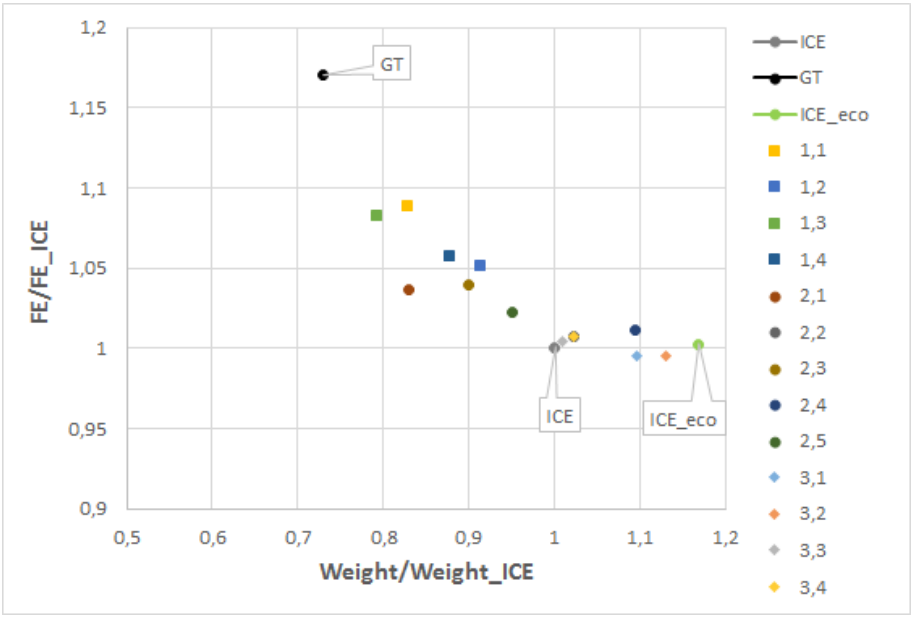

Figure 5-13 ICE's Normalized FE Vs. Weight for every engine's configuration

Analyzing Figure 5-12 and Figure 5-13, it can be said that a volume reduction is achieved for only one hybrid engines' configuration whereas for what the weight reduction is concerned, more options can be taken into account.

In particular, the best volume reduction option belongs to the 1,x engines' configuration and it is the 1,3. Despite of being the best one, this hybrid configuration is able to reduce the volume occupied in ICE case of just 2%, which correspond to free 21 m^3. Moreover, 1,1 brings with it a volume increase of 11% respect to GT case. All the other hybrid solutions show negative performance respect to ICE but, at the same time, they are characterized by a lower volume occupied respect to ICE_eco. Considering the 3,2, which is the worst one from this point of view, it can reduce the volume occupied on board of 6% (-98 m^3) respect to ICE_eco.

For what the weight reduction is concerned, all the 1,x engines' configurations result to be better than ICE case, on the other hand, 3,x engines' configurations involve higher weight than ICE. Among 2,x engines' configuration, the first three (2,1, 2,2 and 2,3) are better than ICE, contrary to what can be noted for 2,4 and 2,5.

In more detail, 1,1 and 1,3, which can be considered the best options among the 1,x engines' configuration, decrease the weight of 17% (- 149 ton) and 21% (-179 ton) respectively when compared to ICE. A similar reduction is achieved by the 2,1 one.

Among the 3,x engines' configuration, the worst is the 3,2, which marks a weight's increase of 13% (+ 112 ton) respect to ICE but a reduction of 3% (- 72 ton) respect to ICE_eco. In conclusion, what has been considered to be the best option from the fuel energy consumption point of view, is the worst in terms of weight and volume reduction respect to ICE.

Summarizing all the results concerned the environmental, energetic and weight and volumes aspects, it can be considered the *radar* graph reported in Figure 5-14. This kind of graph aims at underlying how much better/worse GT, ICE_eco and all the hybrid engines' configurations behave respect to ICE case. From Figure 5-14, it can be observed that the configurations, whose values are for the most located inside the deep red octagon (representing the ICE case) and hence can be considered the best solutions, are:

- GT
- all the 1,x hybrid engines' configurations
- 2,1
- 2,3

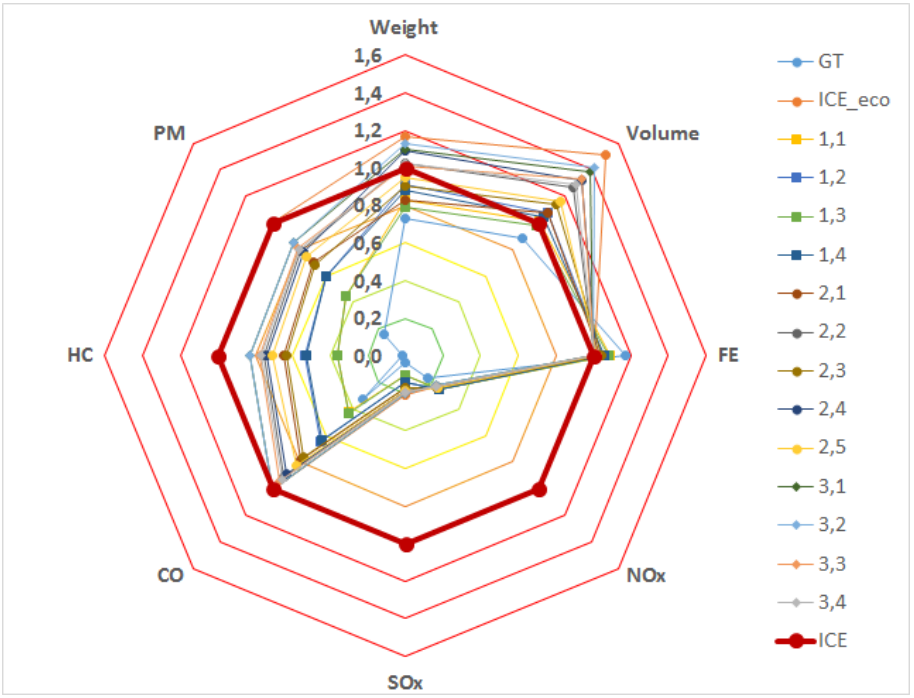

Figure 5-14 ICE's normalized Weight, Volume, FE, NOx, SOx, CO, HC and PM radar graph for GT, ICE_eco and all the hybrid engines' configurations.

On the other hand, the ICE_eco's polygon is that, which reports the minor number of vertex inside the deep red octagon.

5.3 Trigeneration

If, innovative solutions to recover all the possible waste heat contained in the GT's exhaust gas are taken into account, operation profile simulation results for the Trigen. case have to be considered.

Furthermore, since 1,x engines' configurations are mainly based on GTs' use (i.e. there is the possibility to further exploit the waste heat contained in the GT's exhaust gas), the adoption of trigeneration systems has been considered also for these hybrid engines' configurations. Therefore, a new hybrid engines' configuration has been determined, namely the 1,x Trigen.
Given that, this paragraph has been divided accordingly.

5.3.1 "One-kind" engines configuration

Firstly, comparisons of ICE's normalized fuel energy consumption Vs. NOx and SOx emissions are depicted in Figure 5-15 and Figure 5-16 respectively.
From Figure 5-15 and Figure 5-16 it can be immediately noted that Trigen. case has the same behavior of GT case when pollutants emissions are taken into account. Therefore, conclusions drawn for GT case, could be apply also to the Trigen. one. The latter achieves an NOx's reduction of 83% (- 53,5 ton) and an SOx's one of 96% (-60,7 ton) respect to ICE. Furthermore, Trigen. case provides better results than all the hybrid engines' configurations for both the NOx and SOx emissions.
Besides NOx and SOx, ICE's normalized emissions of CO, HC and PM are shown in Figure 5-17.
Quite predictable, Trigen. case's CO, HC and PM emissions show the same trade-off already outlined for NOx and SOx emissions.

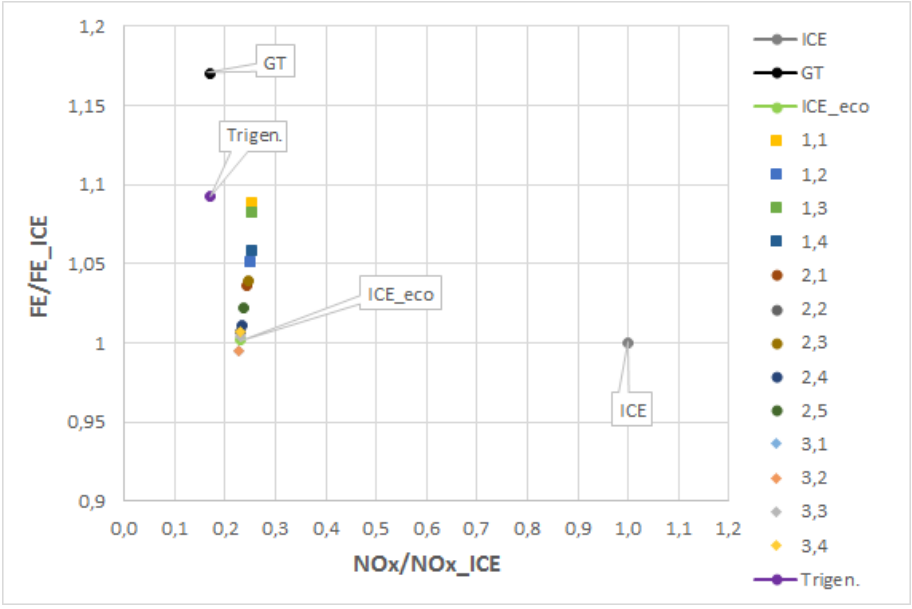

Figure 5-15 ICE's Normalized FE Vs. NOx emissions including Trigen. case.

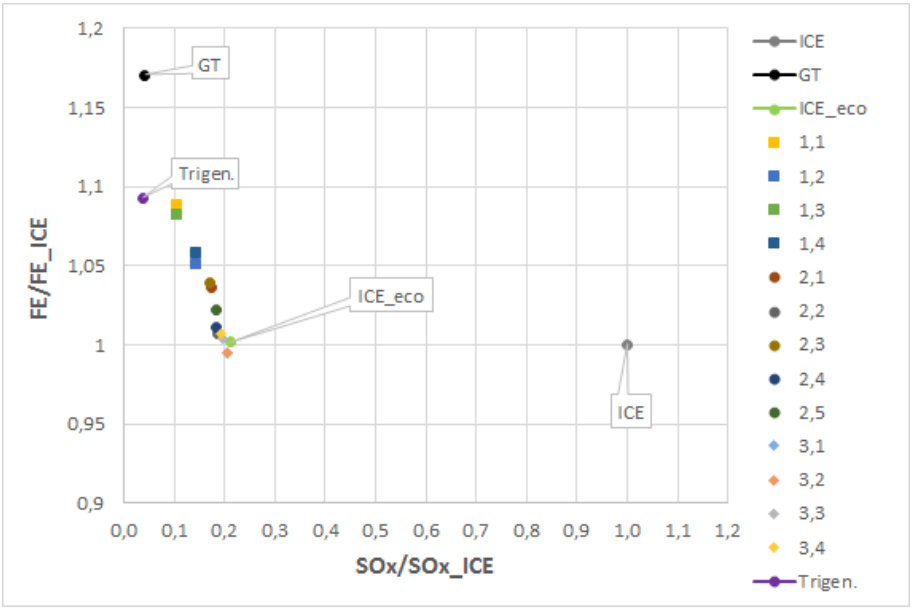

Figure 5-16 ICE's Normalized FE Vs. SOx emissions including Trigen. case.

Indeed, it can be observed the same results reached in GT case. In particular, Trigen. case leads a reduction of:

- 70% (- 5 ton) for CO emissions
- 98% (- 3 ton) for HC emissions
- 85% (- 7,5 ton) for PM emissions

respect to ICE one.

Along with the environmental benefits, Trigen. case is able to limit the GT's fuel energy consumption. Indeed, as average, it can be observed that Trigen. case marks its fuel energy consumption below the 10% threshold respect to ICE, meaning that a reduction of 7% (- 66[7] ton) is achieved if compared to GT case.

The different fuel energy consumption's behavior is mainly linked to these aspects:

- the different way which the reference cruise ship's thermal loads are satisfied
- the amount of waste heat, still contained in the exhaust gas, released in the environment
- the different non-propulsive electric loads caused by the lack of compressors chillers and the introduction of the absorption one.

The results of the two first aspects are depicted in Figure 5-18, where an annual average of the cruise ship's thermal loads coverage percentages are reported for the whole cruise.

[7] It is worth noting that, comparison in terms of fuel ton can be fairly done since these two engines' configurations use the same kind of fuel.

(a)

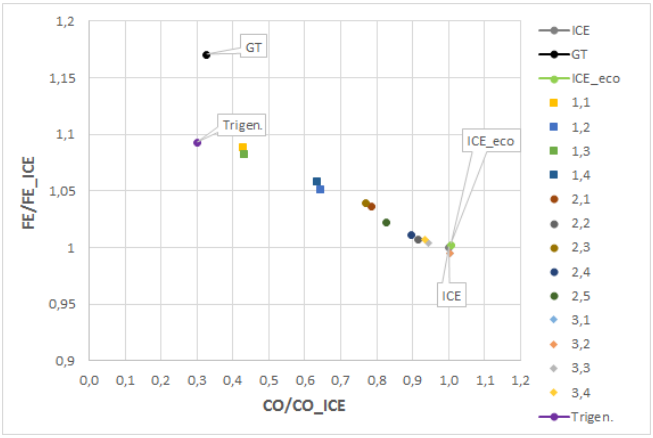

(b)

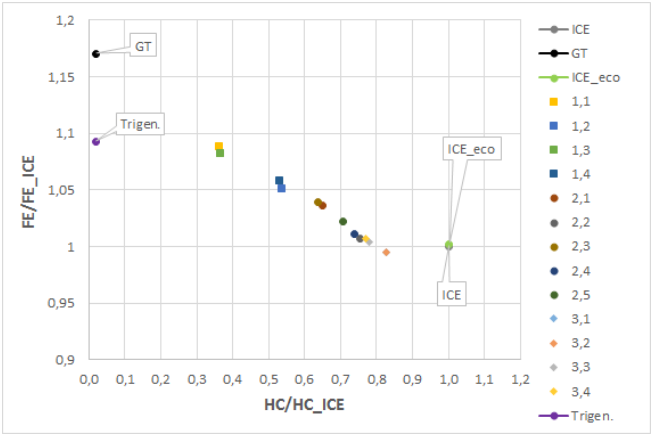

(c)

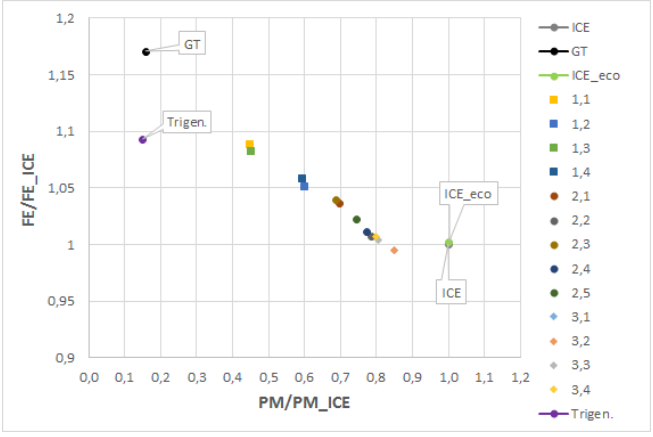

Figure 5-17 ICE's Normalized FE Vs. CO (a), HC (b) and PM (c) emissions including Trigen. case.

Figure 5-18 shows the percentage amount of thermal loads covered by both EGBs and OFBs as well as the amount of waste heat, which is not exploited anymore and, consequently released into the environment.

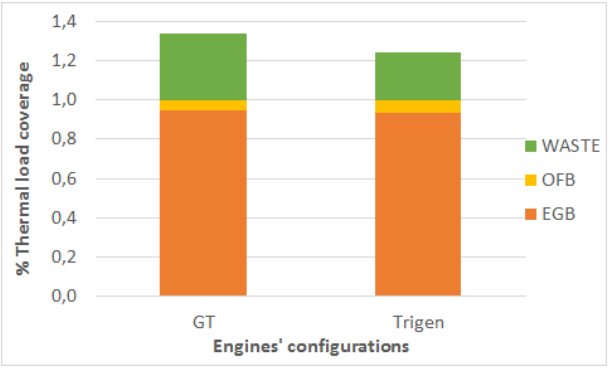

Figure 5-18 Annual average reference cruise ship's thermal loads coverage in GT and Trigen. case for the whole cruise.

From Figure 5-18 it can be noted that the thermal loads are covered almost similarly indeed there is just a 2% difference between the two engines' configurations from the EGBs' use point of view. This means that, even if Trigen. case has more thermal loads to be satisfied, amount of waste heat contained in the GTs' exhaust gas is so great that a remarkable increase of the OFBs' use is not registered. On the other hand, having more thermal loads leads to have less waste (-10%) as well as a different gas temperature exiting the chimney (287°C Vs. 129 °C for GT and Trigen. respectively).

For what the last aspect mentioned above is concerned, the lack of chiller compressors and the introduction of absorption one, involve minor non-propulsive electric loads to be satisfied.
This leads the optimization procedure to choose different kind of engines to switch on aiming to provide the most suitable engines' combinations for the new waste heat recovery system employed on board. For sake of clarity, Table 5-2 reports the autumn engines' combination for every cruise's phase. As done before, it has taken into account the intermediate season because it is considered the most highly probable.
The different engines' combinations result in a Trigen.'s lower fuel consumption than that observed for GT's case. In particular, Trigen. case is able to consume 1170 ton of MGO instead of 1247 ton of MGO registered for GT, namely a reduction of 6%.
As done before, the last comparison regards the weight and volume whose data are reported in Figure 5-19 and in Figure 5-20 respectively.
Trigen. case is the best option for the weight reduction, i.e. it can be achieved one half of ICE weight. On the other hand, Trigen. case is worse than ICE when volume analysis is considered. This fact is the result that absorption chillers are lighter and, at the same time, bulkier than compression chillers, which are adopted in all the other engines' configurations.

Table 5-2 Autumn engines' combinations for every cruise's phase for GT and Trigen. case.

		GT		Trigen.	
		Type A	Type B	Type A	Type B
Harbor		1	0	0	1
Maneuvering		0	2	1	1
Navigation					
Barcelona	Sète	2	1	2	1
Sete	Marseille	0	2	1	1
Marseille	Villefranche	1	0	0	1
Villefranche	Portofino	0	2	1	1
Portofino	Livorno	2	0	2	0
Livorno	Olbia	0	2	1	1
Olbia	Civitavecchia	1	1	0	1
Civitavecchia	Amalfi	0	2	1	1
Amalfi	Sorrento	1	0	0	1
Sorrento	Corfu	0	2	1	1
Corfu	Dubrovnik	2	1	0	1
Dubrovnik	Venezia	0	2	1	1

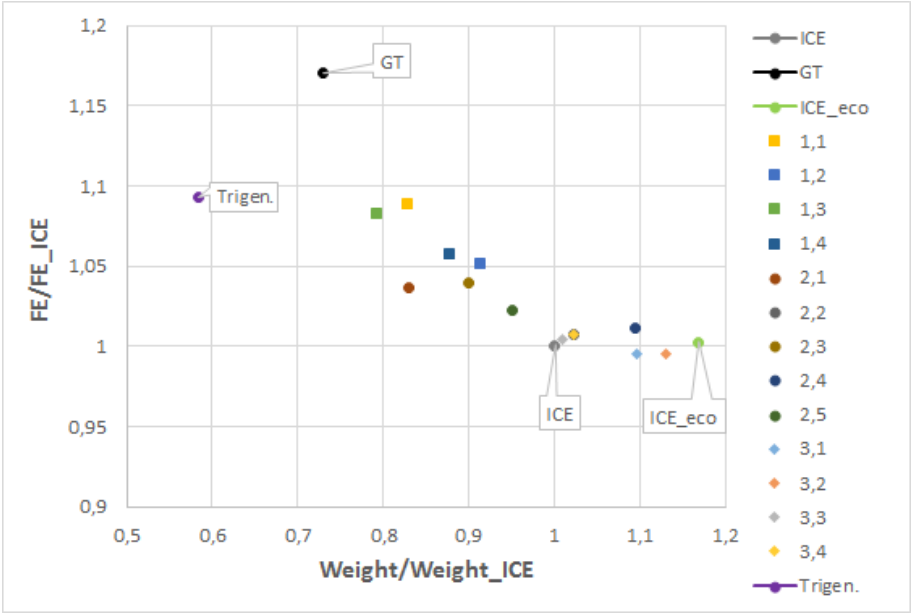

Figure 5-19 ICE's Normalized FE Vs. Weight for every engine's configuration, Trigen. case included.

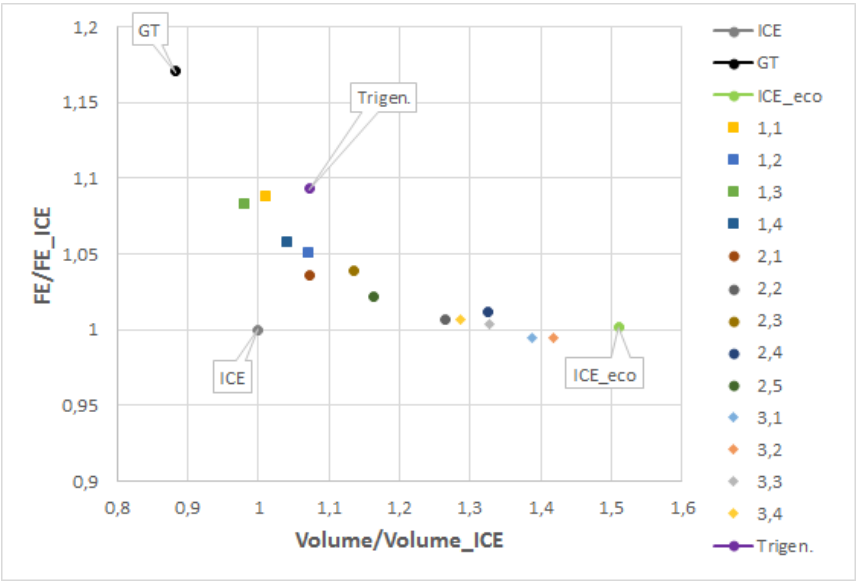

Figure 5-20 ICE's Normalized FE Vs. Volume for every engine's configuration, Trigen. case included.

5.3.2 Hybrid engines configuration

Results concerning the ICE's normalized fuel energy consumption Vs. volume and weight for ICE's class, GT's class and the new hybrid class (1,x Trigen.) are reported in Figure 5-21 and Figure 5-22 respectively.

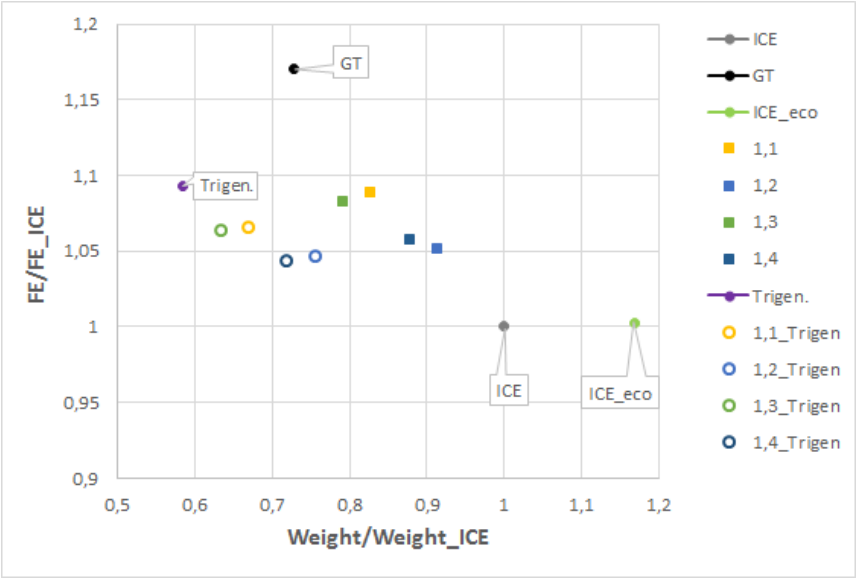

Figure 5-21 ICE's Normalized FE Vs. Weight for ICE's class, GT's class and 1,x Trigen..

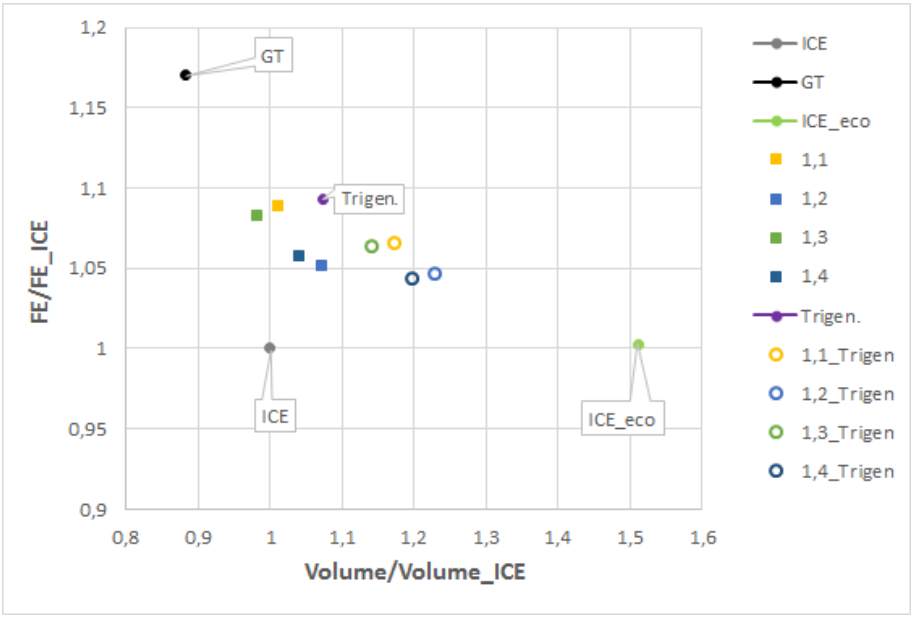

Figure 5-22 ICE's Normalized FE Vs. Volume for ICE's class, GT's class and 1,x Trigen..

It can be seen that there is just a slightly reduction in terms of fuel energy consumption when 1,x and 1,x Trigen. solutions are compared to ICE.
In more detail, the difference which has been noted before between the two coupled 1,x configurations (1,1 & 1,3) Vs. (1,2 & 1,4) is reduced. From the energy point of view, trigeneration makes almost equal all the 1,x configurations which are in a very narrow range. This result can be explained by the graph reported in Figure 5-23 where the annual average % of cogeneration is reported for all the 1,x and 1,x Trigen. configurations.
From Figure 5-23, it can be noted that the introduction of absorption chillers leads to:

- a strong increase for 1,1 and 1,3 passing from 80% to 93% for both of them
- a slightly increase for 1,2 passing from 68% to 75%
- a little decrease for 1,4 passing from 72% to 67%

of % cogeneration.
It can be concluded that the strongest is the difference reported between 1,x and 1,x Trigen. in terms of % cogeneration, the highest are the benefits brought by the absorption chiller's introduction. Indeed, the 1,x engines' configurations, which mostly take advantage of the trigeneration system, are the 1,1 and 1,3.
Analyzing weight and volume, 1,x Trigen. configurations:

- have benefits for what the weight's reduction is concerned
- have drawbacks for what the volume's reduction is concerned

from the absorption chillers' adoption if compared to ICE.
For what the pollutants emissions is concerned, Figure 5-24 reports the results of NOx (a) and those for SOx (b) for ICE's class, GT's class and 1,x Trigen. class.

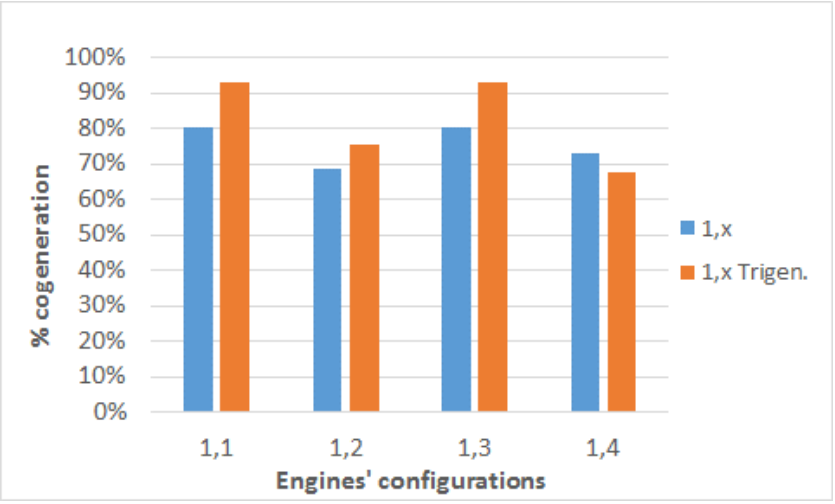

Figure 5-23 Annual average % cogeneration for all the 1,x and 1,x Trigen. configurations.

From Figure 5-24, it can be noted that there is not a considerable variation of both NOx and SOx emissions between 1,x and 1,x Trigen. when compared to ICE. Despite of behaving similarly when compared to ICE, 1,x and 1,x Trigen. show these differences:

- (1,1 Trigen. & 1,3 Trigen.) emit less NOx than the respective couple (1,1 & 1,3), an average of 10% reduction is registered
- (1,1 Trigen. & 1,3 Trigen.) emit more SOx than the respective couple (1,1 & 1,3), an average of 6% increase is registered
- 1,2 Trigen. emit more than 1,2 both for what NOx and SOx emissions is concerned, of 9% and 43% respectively
- 1,4 Trigen. emit less NOx (-18%) but more SOx (+40%) than 1,4

Because of the different behavior, it can not be possible to assess that 1,x Trigen. are best than the others.

For sake of brevity, results linked of CO, PM and HC are not showed because the trade-off is like those observed for NOx and SOx.

Having analyzed all the aspects, it can be concluded that adopting absorption chillers instead of compression one represents a good option just for GT class indeed, 1,x engine's configurations are less positively affected by the absorption chillers' introduction.

Indeed, summarizing all the results above, it can be possible to consider the new *radar* graph of Figure 5-25, which is a basically the same of that reported in Figure 5-14 but considering just the: ICE class, GTs class, 1,x and 1,x Trigen. hybrid engines configurations.

Figure 5-25 suggests that the configurations, whose values are for the most located inside the deep red octagon (representing the ICE case) and hence can be considered the best solutions, are:

- Trigen. (that is equal to GT + absorption chillers)
- 1,3 Trigen.

along with GT and all the 1,x hybrid engines configurations, as already outlined in Figure 5-14.

(a)

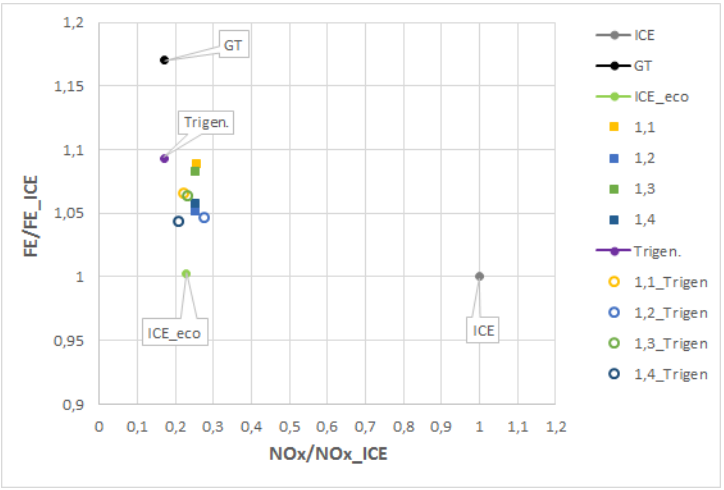

(b)

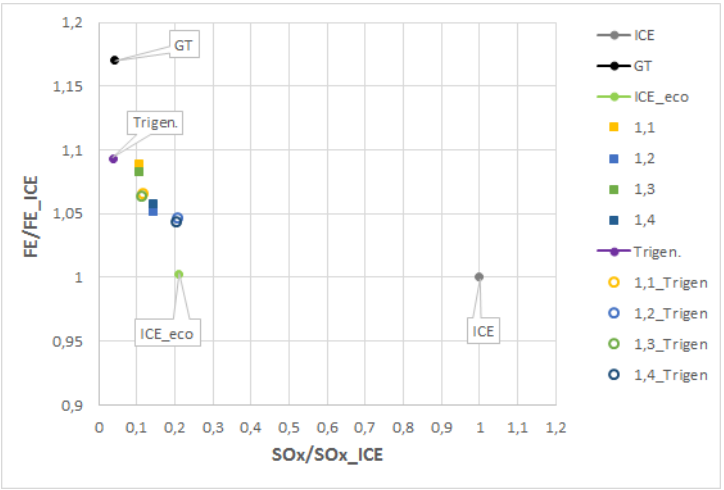

Figure 5-24 ICE's Normalized FE Vs. NOx (a) and SOx (b) for ICE's class, GT's class and 1,x Trigen..

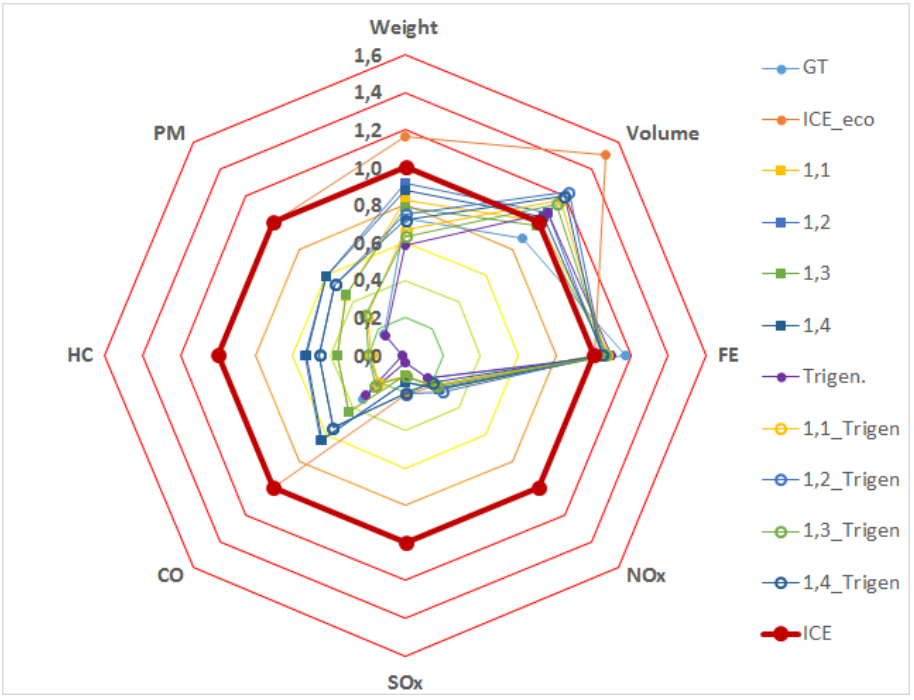

Figure 5-25 ICE's normalized radar graph for GT, ICE_eco, Trigen., 1,x and 1,x Trigen. Vs. pollutants emission, fuel energy consumption, weight and volume

5.4 Power management

A further analysis has been carried out in order to achieve better environmental performances for the 3,x hybrid engines' configurations. It has been chosen to consider just the 3,x hybrid configurations because they show the best performance in terms of fuel energy consumptions but they ought to pollute less in order to be the best options when considering all the three aspects: environmental, energy and weight and volume. Indeed, it could be considered to use always the GT when the ship is in harbor, where the environmental issue is more important.

Firstly, harbor's NOx and SOx emissions are depicted in Figure 5-26 (a) and (b) respectively for ICE's class, GT and the 3,x configurations.

It can be seen that when in harbor, ship emits much more in 3,x configurations respect to GT case by an average percentage of

- 30% for NOx
- 400% for SOx

Therefore, it could be interesting to observe to what happens if GTs are switched on in harbor, meaning that a sort of power management is done. It follows that a further hybrid engines' configurations has been considered, namely the 3,x Pow., which are equal to the 3,x from the engines' configurations point of view. In practice, the optimization procedure's results could be ignored by the management engineer with

the aim to prefer the environmental aspects to the energetic ones, at least for what the harbor phase is concerned.

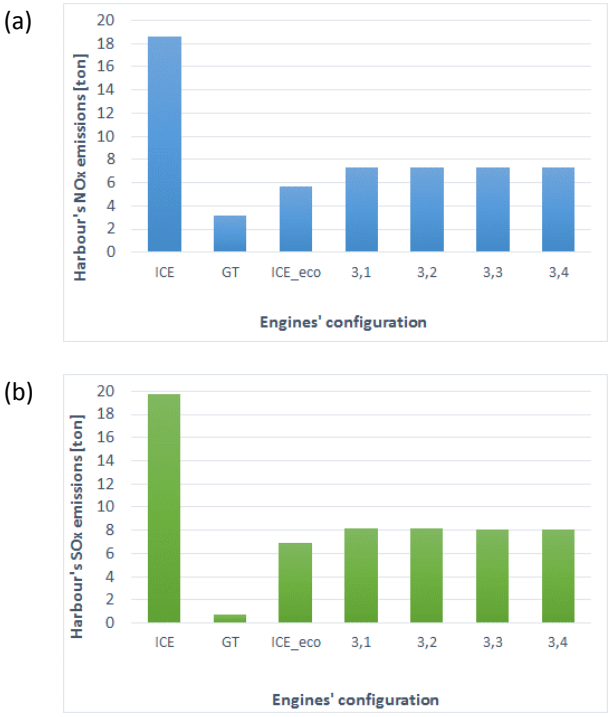

Figure 5-26 Annual average NOx (a) and SOx (b) harbor's emissions for some engines' configurations.

Results are reported in Figure 5-27 for NOx (a) and SOx (b) where 3,x Pow. are the engines' configurations in which it has been carried out the power management.
In Figure 5-27 it can be observed that the use of GT in harbor brings with it a remarkable reduction in terms of both NOx and SOx emissions. In particular, passing from 3,x to 3,x Pow. an average reduction of:

- 10% for NOx (at least a reduction of 6% is marked, see 3,3 and 3,x Pow.)
- 27% for SOx (at least a reduction of 16% is registered, see the comparison between 3,3 and 3,3 Pow.)

is achieved.
Although environmental benefits are surely achieved, it is necessary analyzed what happens from the fuel energy consumption point of view: it is necessary to see how much 3,x Pow. configurations pay in terms of fuel energy consumption. Annual average 3,x and 3,x Pow. fuel energy consumptions for the whole cruise are reported in Figure 5-28.
Switching on GT when ship is in harbor cause just a little increase of the total fuel energy consumption:

- 1,25% in 3,1
- 1,49% in 3,2

- 1,29% in 3,3
- 1,56% in 3,4

Considering the environmental and the energy aspects, it can be concluded that 3,2 Pow. is the best one among all the 3,x engines' configurations, as it can be inferred from the radar graph reported in Figure 5-29.

(a)

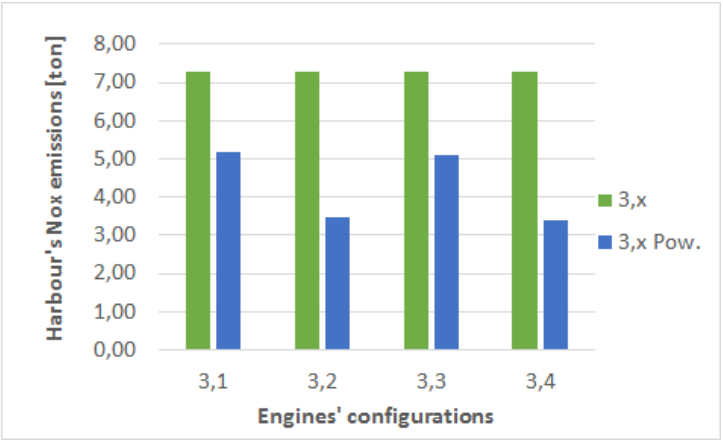

(b)

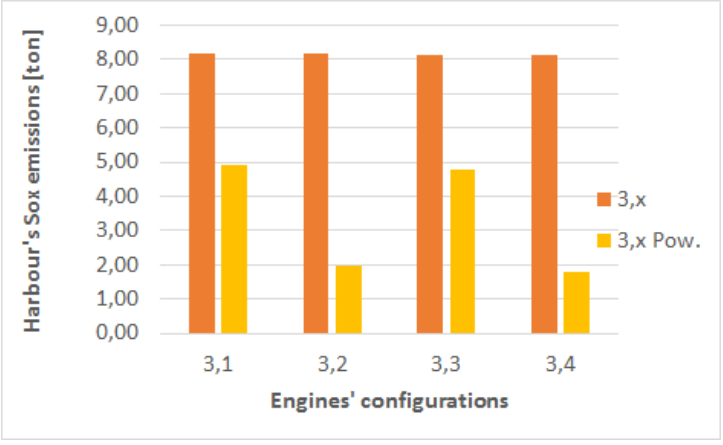

Figure 5-27 Annual average NOx (a) and SOx (b) harbor's emissions for 3,x and 3,x Pow.

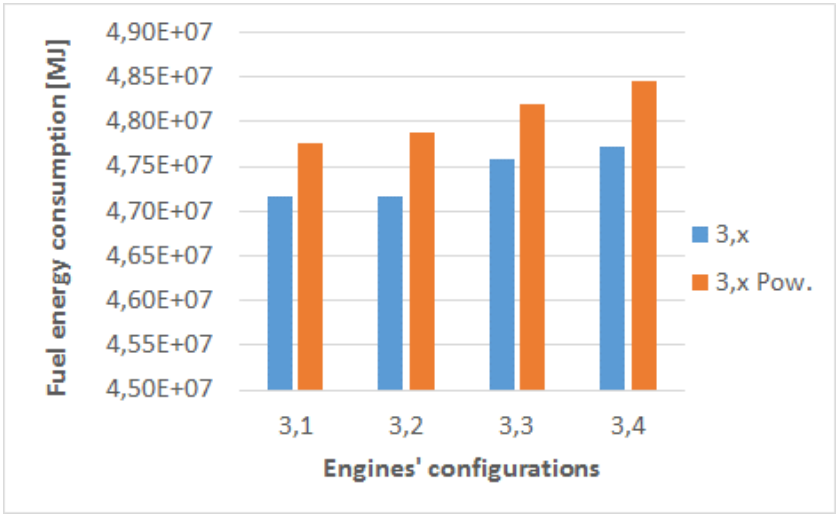

Figure 5-28 Annual average fuel energy consumption for 3,x and 3,x Pow. for the whole cruise.

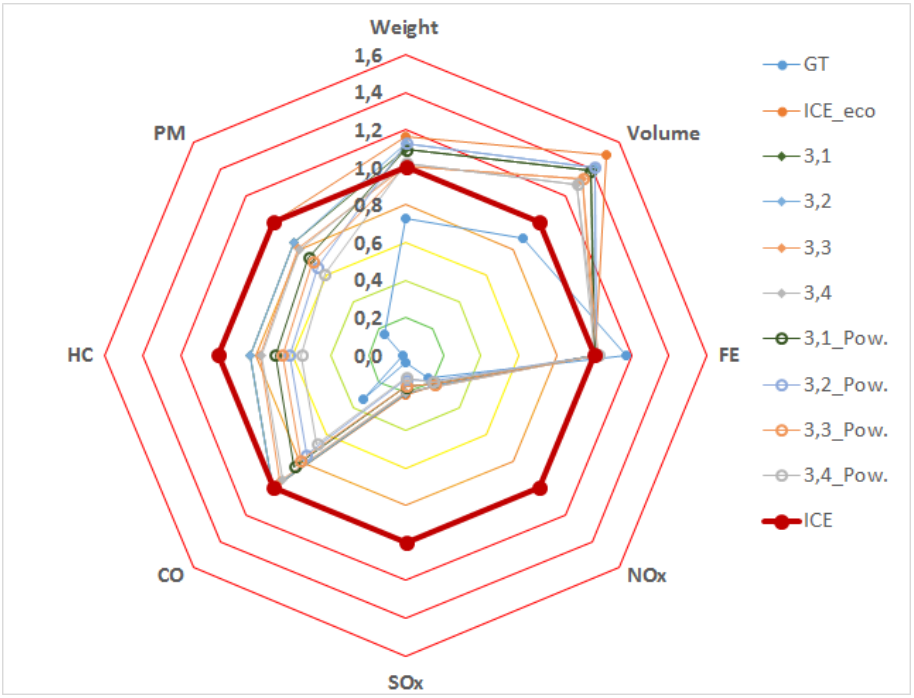

Figure 5-29 ICE's normalized radar graph for the GT, ICE_eco, 3,x and 3,x Pow. Vs. pollutants emission, fuel energy consumption, weight and volume

5.5 Costs analysis

The author is aware that ship-owners ought to have the possibility to take their decisions including also costs analysis beside the energetic, environmental and weight and volume analysis, which have been carried out in the present work. From this point of view, the thesis is not entirely fulfilling the ship-owners' request. The reason of this lack is due to the fact that to make a very good, strong, coherent, complete costs analysis, it should have been considered all these aspects:

- Operational and maintenance costs (OPEX)
- Capital costs (CAPEX)
- Economic advantages linked to the weight and volume analysis.

Moreover, from the author's point of view, it would be interesting to analyze also the economic advantages resulted from the environmental pollution decrease, which is linked to the specific kind of engines configuration selected.

OPEX is not so easy to calculate since it consists of many different addends and it can't be referred just on the fuel's consumption cost, which could be found on www.bunkerworld.com [56], from where it can be also noted that the fuel cost is not unique but it varies from harbor to harbor. Moreover, it has to be considered the operational and maintenance costs of exhaust gas after-treatment devices (i.e. urea's usage, SCR's catalysts replacement, scrubber's chemical additives), trigeneration systems as well as those linked to EGBs and OFBs. Therefore, determining OPEX is not banal as it could be expected. Besides that, even much more problems arise in the moment, which both the second and third item are considered.

Capital costs' (CAPEX) gathering is an extremely difficult duty since all the components, which are presented in Chapter 3, have to be taken into account. Therefore, not only the prime movers' costs but also those related to the WHR systems, exhaust gas after treatment devices and absorption chillers have to be considered. The though prompt availability of these data and consequently the necessity to collect the useful information consulting directly the firms, have made useless the author's attempts, which could have bettered the costs analysis.

It has to point out that both OPEX and CAPEX are dependent on the kind of contract the ship-owners make with the suppliers. Therefore, it is quite difficult to carry out an economic analysis without the direct ship-owners' intervention.

The last items, i.e. that linked to the economic advantages linked to the weight and volume analysis, is even more difficult. All the analyzed engines' configurations, ICE_eco excluded, bring with them both weight and volume savings if compared to ICE, in other words, the gas turbines' employment on board results in freeing volume on board as well as lighten the ship. The way to convert these savings into an economic advantage is not trivial and univocal requiring absolutely the ship-owners' intervention. Indeed, many scenarios are feasible:

- the volume's reduction frees room which could be occupied by other cabins increasing the pay load. This would change the accommodation thermal loads making the gas turbines' great capacity to cogenerate even more interesting

and useful, reducing the overall ship's energetic efficiency gap existing between gas turbines' configurations and ICE

- weight's reduction leads to lighten the ship's DWT and consequently to decrease the propulsion loads maintaining the current pay load. The change of the propulsion loads results in choosing different prime movers, smaller and more efficient. Choosing smaller prime movers would have consequences on ship's volume.
- at last, it could think to design a new ship lighter and smaller with completely different electric loads and the thermal ones too.

It can be seen that deciding wat to do is not banal and it requires a collaboration with the ship's designers and ship-owners too.

Therefore, to make the present work more completed, a collaboration between researchers and companies should have been created.

Chapter 6

CONCLUSIONS AND FURTHER WORKS

The present work aimed at quantifying the differences in terms of weight, volume, and fuel consumption of different designs of a cruise ship that, in order to be compliant with new IMO regulations about pollutant emissions, considers either to install DeSOx and DeNOx abatement systems on the original configuration of HFO fueled ICEs or replacing the current PMs with MGO fueled GTs.

6.1 Conclusions

All the quantitative results achieved using the optimization procedure described in Chapter 4 and exhaustively reported and commented within the Chapter 5, could be summarized in an easy and fashion way by means of Table 6-1.

Table 6-1 highlights all the aspects, on which the decisions made by ship-owners and maritime sector's engineers should have been based.

It is important to say that the ICE case, which is the actual engine's configuration employed on the Hull C.6194, has been taken as reference for weight, room and fuel energy consumption. Their values are reported in bold characters and grey-framed in Table 6-1. Meanwhile, the pollutants emissions of the ICE_eco case are considered as reference points and their values are also in bold characters but light-green framed in Table 6-1. This choice has been made because, comparing ICE's emissions to those of the other engines' configurations could result in misleading judgments due to their different order of magnitude.

Therefore, other engines' configurations are evaluated in respect to the ICE case for weight, volume and fuel energy; but at the same time they are compared to the ICE_eco case for pollutants emissions.

Table 6-1 Qualitative comparison of all the engines' configurations analyzed respect to ICE's case by means of Weight, Volume, annual average fuel energy consumption and to ICE_eco's case by means of pollutants emissions.

	Weight [ton]	Volume [m^3]	Fuel Energy [MJ]	Pollutants emissions NOx [ton]	SOx [ton]	CO [ton]	HC [ton]	PM [ton]
ICE	**858**	**1060**	**4,74E+07**	*64,56*	*63,07*	*7,09*	*3,15*	*8,88*
ICE_eco				**14,81**	**13,46**	**7,13**	**3,16**	**8,90**
GT								
1,1								
1,2								
1,3								
1,4								
2,1								
2,2								
2,3								
2,4								
2,5								
3,1								
3,2								
3,3								
3,4								
Trigen.								
1,1_Trigen								
1,2_Trigen								
1,3_Trigen								
1,4_Trigen								
3,1_Pow.								
3,2_Pow.								
3,3_Pow.								
3,4_Pow.								

As can be imagined, the symbols in Table 6-1 are displayed to look like a multitude of "traffic-lights".
The variation ranges are different with respect to weight, volume, fuel energy and pollutants emissions as reported in Table 6-2.
It is clear that changing the variation ranges could bring up different results. On the other hand, thanks to the selected variation range distribution's choice, the qualitative judgments can be considered fair enough.
From Table 6-2, it can be inferred that there are different best options according to which point of view the decision makers look from.

Hybrid configurations are to be considered as valid alternatives both to the current ICE and to other configurations based on only one prime mover.

Table 6-2 "Traffic-light" indicators

	Normalized ICE's variations ranges				Normalized ICE_eco's variations ranges		
	Weight	Volume	Fuel Energy		NOx	SOx	Others
	<0,9	<0,8	<0,99		<0,85	<0,25	<0,25
	0,9-1	0,8-1	0,99-1		0,85-0,9	0,25-0,5	0,25-0,5
	1-1,1	1-1,2	1-1,03		0,9-0,95	0,5-0,75	0,5-0,75
	1,1-1,2	1,2-1,4	1,03-1,06		0,95-1	0,75-1	0,75-1
	>1,2	>1,4	>1,06		>1	>1	>1

Indeed those configurations perform well in only some of the categories brought to the analysis, where Hybrid configurations display good results in mostly all of them.

In more detail, the following statements can be finally assessed:

the engine's configurations which can be considered the most affordable are: 1,4, 2,1, 2,5, 1,4_Trigen. and 3,4 Pow. engines' configurations

because:

- 1,4, 2,1, 2,5 allow weight reduction, a non excessive volumes expansion and they also limit fuel consumption with respect to the ICE's configuration. Moreover, emissions are better than the ICE_eco's expect for NOx in the 1,4 where they go up by 10% even though still within MARPOL limits.

- 1,4_Trigen. This is a twin configuration of the "1,4 standard" which allows better resulds in emissions

- 3,4 Pow. allows to obtain lower emissions compared to its "twins" keeping in check increases in weight and volume.

This means that, for the reference cruise ship, the choice to employ GTs as prime movers either in "one-kind", or in innovative (hybrid) engines' configurations, as well as to improve the ship's waste heat recovery capability through trigeneration systems, turns out to be of interest.

Hybrid configurations meet with Multi-Objective demands. More to the point, for the economic analysis, those highlighted, which have little increase in consumption could have very interesting implications, especially bearing in mind that they reduce both weight and volume. Not to talk about emissions: they are better even than the ICE_eco's.

Even if the study has been conducted on a specific cruise ship's operation profile, the followed methodology is general: meaning that the optimization procedure is aimed to

be a reliable and flexible tool that can be applied, with appropriate adjustments, to other case studies.

6.2 Further research

Thanks to the methodology's universality, the analysis carried out in the present thesis can be adopted to evaluate other solutions employable on board.
For example, since GT's employment leads to some improvements, it could be interesting to study the adoption of combine cycles on board as well as the use of Organic Rankine Cycle to enhance the ship's waste heat recovery capability.
Furthermore, being the environmental issue extremely considerable in harbor, *cold ironing*[8] *systems*, could be regarded as an option too.
One last suggestion to continue the research work, it would be to spread the ship's selection choice, i.e. including bulk carriers, cargo, tank carrier, container ship and so on.

[8] This systems provides electric power to the ship allowing to switch off the engines.

REFERENCES

[1] International Energy Agency, “CO2 Emissions from fuel combustion. Beyond 2020 Online Database,” 2012.

[2] K. Buhaug, Ø., Corbett, J.J., Endresen, Ø., Eyring, V., Faber, J., Hanayama, S., Lee, D.S., Lee, D., Lindstad, H., Markowska, A.Z., Mjelde, A., Nelissen, D., Nilsen, J., Pålsson, C., Winebrake, J.J., Wu, W., Yoshida, “Second IMO GHG Study.” International Maritime Organization, London, UK, 2009.

[3] International Maritime Organization, “International Shipping Facts and Figures – Information Resources on Trade, Safety, Security, Environ-ment,” 2012.

[4] A. Maragkogianni and S. Papaefthimiou, “Evaluating the social cost of cruise ships air emissions in major ports of Greece,” *Transp. Res. Part D Transp. Environ.*, vol. 36, pp. 10–17, 2015.

[5] CLIA, “The Cruise Industry: Contribution of Cruise Tourism to the Economies of Europe.” Cruise Lines International Association, 2014.

[6] IPCC, “Climate Change 2014: Synthesis Report. Contribution of Working Groups I, II and III to the Fifth Assessment Report of the Intergovernmental Panel on Climate Change,” Geneve, Switzerland, 2014.

[7] G. Endresen, Ø., Sørgård, E., Sundet, J.K., Dalsøren, S.B., Isaksen, I.S.A., Berglen, T.F., Gravir, “Emission from international sea transportation and environmental impact,” *J. Geophys. Res.*, vol. 108, 2003.

[8] J. Helfre, P. Andre, C. Boot, J. Helfre, P. Andre, and C. Boot, “Emission Reduction in the Shipping Industry : Regulations , Exposure and Solutions Emission Reduction in the Shipping Industry : Regulations , Exposure and Solutions,”

2013.

[9] “www.imo.org.” .

[10] International Maritime Organization, “MARPOL 73/78. Annex VI.” 1997.

[11] International Maritime Organization, “RESOLUTION MEPC.176(58).” 2008.

[12] R. McArthur, “Gas-fuelled mechanical propulsion solutions offer major emissions reductions,” *Twentyfour7*, vol. 1, 2011.

[13] F. Haglind, “A review on the use of gas and steam turbine combined cycles as prime movers for large ships. Part III: Fuels and emissions,” *Energy Convers. Manag.*, vol. 49, no. 12, pp. 3476–3482, 2008.

[14] IPCC, “Climate Change 2007: The Physical Science Basis. Contribution of Working Group I to the Fourth Assessment,” Geneve, Switzerland, 2007.

[15] A. Järvi, “Methane slip reduction in Wärtsilä lean burn gas engines,” in *26th CIMAC World Congress on Combustion Engines*, 2010.

[16] J. Herdzik, “LNG AS A MARINE FUEL – POSSIBILITIES AND PROBLEMS,” *Powertrain Transp.*, vol. 18, no. 2, 2011.

[17] Santa Barbara County Air Pollution Control District, “Air Pollution from Marine Shipping - Marine Shipping Retrofit Project (MSRP),” 2012.

[18] Maersk Group’s, “Sustainability Report 2013,” 2013.

[19] Lloyd’s Register, “LNG-fuelled deep sea shipping,” 2012.

[20] Lloyd’s Register, “Owners denied state aid for SOx compliance.” 2013.

[21] A. A. Azzara, D. Rutherford, and H. Wang, “Feasibility of IMO Annex VI Tier III implementation using Selective Catalytic Reduction,” 2014.

[22] “http://www.mvdc.it/en.” .

[23] B. N. Sannemann, “Pioneering gas turbine-electric system in cruise ships: a performance update,” *Marit. Technol.*, vol. 41, 2004.

[24] F. Haglind, “A review on the use of gas and steam turbine combined cycles as prime movers for large ships. Part II: Previous work and implications,” *Energy Convers. Manag.*, vol. 49, no. 12, pp. 3468–3475, 2008.

[25] G. M. Tostevin and J. C. Nealy, “Computer synthesis for the design of marine power plants,” *J. Mar. Res.*, vol. B, no. 5, 2003.

[26] A. Kougioufas, “Marine energy system optimization with reliability and availability considerations,” National Technical University of Athens, 2005.

[27] Fincantieri S.p.A., “Electric Loads.” 2012.

[28] Fincantieri S.p.A., “Thermal Loads.” 2012.

[29] Wärtsilä, “Project Guide.” Vaasa, 2007.

[30] Wärtsilä, “Wärtsilä46 Technology Review.” Vaasa, 2008.

[31] Siemens, “SGT-300 Technical Data.” pp. 0–3, 2012.

[32] Siemens, “SGT-400 Technical Data,” vol. 31, no. 0. 2013.

[33] “No Title.” [Online]. Available: www.thermoflow.com.

[34] Thermax, “Technical Data SD 80A TCU.” .

[35] R. M. Heck and R. J. Farrauto, *Catalytic Air Pollution Control – Commercial Technology*. New York, USA: Van Nostrand Reinhold, 1995.

[36] M. Koebel, G. Madia, and M. Elsener, “Selective catalytic reduction of NO and NO2 at low temperatures,” *Catal. Today*, vol. 73, 2002.

[37] G. Lepperhoff and J. Schommers, “Verhalten von SCR-Katalysatoren im dieselmotorischen Abgas,” *MTZ Mot. Zeitschrift*, vol. 49, 1988.

[38] F. Baldi, S. Bengtsson, and K. Andersson, “The influence of propulsion system design on the carbon footprint of different marine fuels,” *Low Carbon Shipp. Conf.*, pp. 1–12, 2013.

[39] S. Brynolf, M. Magnusson, E. Fridell, and K. Andersson, “Compliance possibilities for the future ECA regulations through the use of abatement technologies or change of fuels,” *Transp. Res. Part D Transp. Environ.*, vol. 28, no. 2013, pp. 6–18, 2014.

[40] S. Brynolf, M. Magnusson, E. Fridell, and K. Andersson, “Compliance possibilities for the future ECA regulations through the use of abatement technologies or change of fuels,” *Transp. Res. Part D Transp. Environ.*, vol. 28, pp. 6–18, May 2013.

[41] European Commission, *Euro VI emission standards*. 2009.

[42] Wärtsilä, “WÄRTSILÄ ENVIRONMENTAL PRODUCT GUIDE.” Vaasa, 2015.

[43] Fincantieri S.p.A., “Private communications.” 2014.

[44] CE Delft, “The market for Scrubbers,” 2015.

[45] IMO, “MEPC_681.” 2009.

[46] G. Caiazzo, G. Langella, F. Miccio, and F. Scala, “An Experimental Investigation on Seawater SO2 Scrubbing for Marine Application,” *Environ. Prog. Sustain. Energy*, vol. 32, no. 4, 2013.

[47] U.S.A. Environmental Protection Agency, “Exhaust Gas Scrubber Washwater

Effluent," Washington (USA), 2011.

[48] C. A. Frangopoulos, M. R. von SPAKOVSKY, and E. Sciubba, "A Brief Review of Methods for the Design and Synthesis Optimization of Energy Systems," *Int.J. Appl. Thermodyn.*, vol. 5, no. 4, pp. 151–160, 2002.

[49] G. G. Dimopoulos, A. V. Kougioufas, and C. a. Frangopoulos, "Synthesis, design and operation optimization of a marine energy system," *Energy*, vol. 33, no. 2, pp. 180–188, Feb. 2008.

[50] J. H. Holland, *Adaption in Natural and Artificial Systems*. The University of Michigan Press, 1975.

[51] D. MANOLAS, C. FRANGOPOULOS, T. GIALAMAS, and D. TSAHALIS, "OPERATION OPTIMIZATION OF AN INDUSTRIAL SYSTEM BY A GENETIC ALGORITHM," *Energy Convers. Manag.*, vol. 38, no. 15, pp. 1625–1636, 1997.

[52] K. Nieminen, S. Ruuth, and I. Maros, "Genetic algorithm for finding a good first integer solution for MILP," London, UK, 2003.

[53] A. Sinha, "Progressively Interactive Evolutionary Multiobjective Optimization," Aalto University, 2011.

[54] M. Wall, *GAlib: A C++ Library of Genetic Algorithm Components*. Massachussets Institute of Technology, 1996.

[55] G. Lozza, *Turbine a gas e cicli combinati*. Bologna (IT): Progetto Leonardo, 2007.

[56] "No Title." [Online]. Available: www.bunkerworld.com.

[57] G. a. Livanos, G. Theotokatos, and D.-N. Pagonis, "Techno-economic investigation of alternative propulsion plants for Ferries and RoRo ships," *Energy Convers. Manag.*, vol. 79, pp. 640–651, Mar. 2014.

Appendix 1

Optimization Problem Script

In the following it is reported a brief description of Excel Solver (starting from now, it will be recalled simply "Solver") and its use to solve the optimization problem analysed in Chapter 4.

A1.1 Optimization Solver tool

Solver is an Excel tool that is invoked trough the Data tab. To install it, it must use the Add-in capability under the File-Excel Options menu.
Two fundamental steps must be followed:

1. identifying the cells that are the variables for the problem and all the equations need to be entered in different cells
2. solver is invoked, which results in in the display of the Solver Parameters dialog box, where the problem is defined. The cells containing the variables for the problem, the objective function and the constraints are identified. Various Options for the Solver are also invoked.

A generic Solver's dialog box is depicted in Figure A1-1 where:

- Target Cell is the cell containing the objective function
- Equal to represents the kind of problem, which could be a maximization (Max) or a minimization (Min) one. The last possibility is to set a specific value (Value of) to which the target cell has to be equal
- By Changing Cells are the cells containing the decisional variables
- Subject to the Constraints are the relations that have to be respected for the optimization problem. In this list, it can also be imposed "integer" as well as "binary" constraint.

Since the optimization problem has to be repeated for every cruise's phase, it has been resorted to using a VBA code in order to make the optimization procedure fast and automatic.

For this purpose, various Solver's functions have been used. The most important are described in the following and they are: SolverOk, SolverAdd, SolverOptions and SolverSolve.

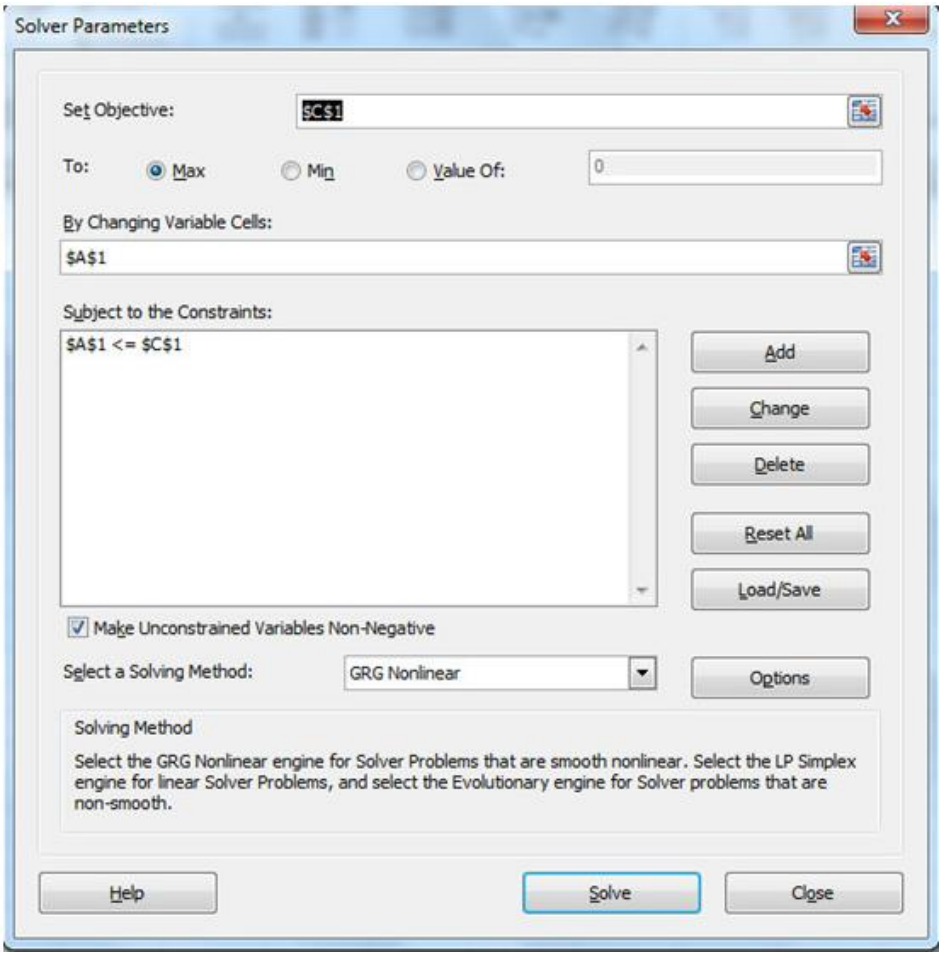

Figure A1-1 Generic Solver's dialog box.

SolverOk

Function script: SolverOk (SetCell, MaxMinVal, ValueOf, ByChange, Engine)

Description:

- SetCell optional Variant. It refers to a single cell on the active worksheet. It corresponds to the Set Target Cell box in the Solver Parameters dialog box.
- MaxMinVal Optional Variant. It corresponds to the Max, Min, and Value options in the Solver Parameters dialog box, see Figure A1-1. Users have to specify a value equal to 1, 2 or 3 accordingly to what is reported in Table A.1-1.

Table A.1-1 Values corresponding to the optimization problem typology.

MaxMinVal	Specifies
1	Maximize
2	Minimize
3	Match a specific value

- ValueOf Optional Variant. If MaxMinVal is 3, users must specify the value to which the target cell is matched.
- ByChange Optional Variant. It represents the cell or range of cells that will be changed so that users will obtain the desired result in the target cell. It corresponds to the By Changing Cells box in the Solver Parameters dialog box, see Figure A1-1.
- Engine Optional Variant. It describes the Solving method that will be used to solve the problem. Users can select among Simplex LP method, GRG Nonlinear method, or Evolutionary method by inserting value equal to 1, 2 or 3 respectively. It corresponds to the Select a Solving Method dropdown list in the Solver Parameters dialog box, see Figure A1-1.

SolverAdd

Function script: SolverAdd (CellRef, Relation, FormulaText)

Description:

- CellRef requires Variant. It represents a cell or a range of cells that forms the left side of a constraint.
- Relation requires Integer. It is the arithmetic relationship between the left and right sides of the constraint. Users have to select a value among 1, 2 and 3 in order to impose respectively a minority, an equality or a majority relations between the left and the right side of the constraints equations. Besides that, users can also impose the CellRef to be an integer, a binary value or to be different and integers by typing 4, 5, or 6. All the possibilities are reported in Table A.1-2. If users select 4, 5 or 6 CellRef must refer to decision variable cells, and FormulaText should not be specified.
- FormulaText optional Variant. It is the right side of the constraint.

SolverOptions

Function: SolverOptions (MaxTime, Iterations, Precision, AssumeLinear, StepThru, Estimates, Derivatives, SearchOption, IntTolerance, Scaling, Convergence, AssumeNonNeg, PopulationSize, RandomSeed, MultiStart, RequireBounds, MutationRate, MaxSubproblems, MaxIntegerSols, SolveWithout, MaxTimeNoImp)

Description of the main important function's parameters:

Table A.1-2 Relations and arithmetic relationships between the right and left side of the constraints' equations.

Relation	Arithmetic relationship
1	<=
2	=
3	>=
4	Cells referenced by CellRef must have final values that are integers.
5	Cells referenced by CellRef must have final values of either 0 (zero) or 1.
6	Cells referenced by CellRef must have final values that are all different and integers.

- MaxTime Optional Variant. It is the maximum amount of time (in seconds) Solver will spend solving the problem. The value must be a positive integer.
- Iterations Optional Variant. It is the maximum number of iterations Solver will use in solving the problem. The value must be a positive integer.
- Precision Optional Variant. It is the number between 0 (zero) and 1 that specifies the degree of precision with which constraints (including integer constraints) must be satisfied. The default precision is 0.000001. A smaller number of decimal places (for example, 0.0001) indicates a lower degree of precision. In general, the higher the degree of precision you specify (the smaller the number), the more time Solver will take to reach solutions.
- IntTolerance Optional Variant. It corresponds to a decimal number between 0 (zero) and 100 that specifies the Integer Optimality percentage tolerance. This argument applies only if integer constraints have been defined; it specifies that Solver can stop if it has found a feasible integer solution whose objective is within this percentage of the best known bound on the objective of the true integer optimal solution. A larger percentage tolerance would tend to speed up the solution process.
- Convergence Optional Variant. A number between 0 (zero) and 1 that specifies the convergence tolerance for the GRG Nonlinear Solving and Evolutionary Solving methods. For the Evolutionary method, when 99% or more of the members of the population have "fitness" values whose relative, that is percentage, difference is less than this tolerance, Solver stops. In both cases, Solver displays the message "Solver converged to the current solution. All constraints are satisfied."
- PopulationSize Optional Variant. It equals True to have Solver assume a lower limit of 0 (zero) for all decision variable cells that do not have explicit lower limits in the Constraint list box (the cells must contain nonnegative values). False to have Solver use only the limits specified in the Constraint list box.
- RandomSeed Optional Variant. It is a positive integer specifies a fixed seed for the random number generator used by the Evolutionary Solving method and the multistart method for global optimization. This means that Solver will

find the same solution each time it is run on a model that has not changed. A zero value specifies that Solver should use a different seed for the random number generator each time it runs, which may yield different solutions each time it is run on a model that has not changed.

- MutationRate Optional Variant. It is a number between 0 (zero) and 1 that specifies the rate at which the Evolutionary Solving method will make "mutations" to existing population members. A higher Mutation rate tends to increase the diversity of the population, and may yield better solutions.
- MaxTimeNoImp Optional Variant. When the Evolutionary Solving method is used, the maximum amount of time (in seconds) Solver will continue solving without finding significantly improved solutions to add to the population. The value must be a positive integer.

SolverSolve
Function: SolverSolve(UserFinish, ShowRef)
Description:

- UserFinish Optional Variant. If it equals True, it returns the results without displaying the Solver Results dialog box. False or omitted to return the results and display the Solver Results dialog box.
- ShowRef Optional Variant. You can pass the name of a macro (as a string) as the ShowRef argument. This macro is then called, in lieu of displaying the Show Trial Solution dialog box, whenever Solver pauses for any of the reasons listed below.The ShowRef macro must have the signature Function name (Reason As Integer).

A.1-2 Optimization application

Having said that, it has been reported the VBA script for the case reported in Chapter 4.
For sake of clarity, it is well worth reporting that:

- Columns S, T and U corresponds the number of engines that can be employed on board.
- Column Y represents the %MCR that has to be included within the range imposed by the cells Q1 and Q2

```
Dim j As Integer

 j = Row

For j = 26 To 75

    SolverReset
```

```
    SolverOk SetCell:="$BZ$" & j, MaxMinVal:=1, ByChange:="$S$" & j & ":$U$" & j,
Engine:=3
    SolverOptions Precision:=0.001, MaxTimeNoImp:=5, PopulationSize:=80,
MutationRate:=0.75
    SolverAdd CellRef:="$S$" & j, Relation:=1, FormulaText:="2"
    SolverAdd CellRef:="$T$" & j, Relation:=1, FormulaText:="1"
    SolverAdd CellRef:="$U$" & j, Relation:=1, FormulaText:="1"
    SolverAdd CellRef:="$S$" & j, Relation:=3, FormulaText:="0"
    SolverAdd CellRef:="$T$" & j, Relation:=3, FormulaText:="0"
    SolverAdd CellRef:="$U$" & j, Relation:=3, FormulaText:="0"
    SolverAdd CellRef:="$S$" & j, Relation:=4, FormulaText:="Integer"
    SolverAdd CellRef:="$T$" & j, Relation:=4, FormulaText:="Integer"
    SolverAdd CellRef:="$U$" & j, Relation:=4, FormulaText:="Integer"
    SolverAdd CellRef:="$Y$" & j, Relation:=1, FormulaText:="$Q$2"
    SolverAdd CellRef:="$Y$" & j, Relation:=3, FormulaText:="$Q$1"
    SolverOk SetCell:="$BZ$" & j, MaxMinVal:=1, ByChange:="$S$" & j & ":$U$" & j,
Engine:=3
    SolverSolve UserFinish:=True
    SolverFinish KeepFinal:=1

Next j

End Sub
```

Appendix 2

EGB model

A general Heat Recovery Steam Generator, and hence the EGB employed on board, generates steam utilizing the energy in the exhaust from the gas turbine.
The present Appendix has the scope to highlight some of the basics about gas turbine EGBs.
It is important to remind that, EGBs used on board consist of just economizer and evaporator in order to provide saturated steam.
Steam's production as well as both the gas and steam temperature profiles are strictly linked to two variables: pinch and subcooling point. The first is the difference between the gas temperature leaving the evaporator and the temperature of saturated steam, the latter is the difference between the temperature of saturated steam and the temperature of the water entering the evaporator, see Figure A2-1.

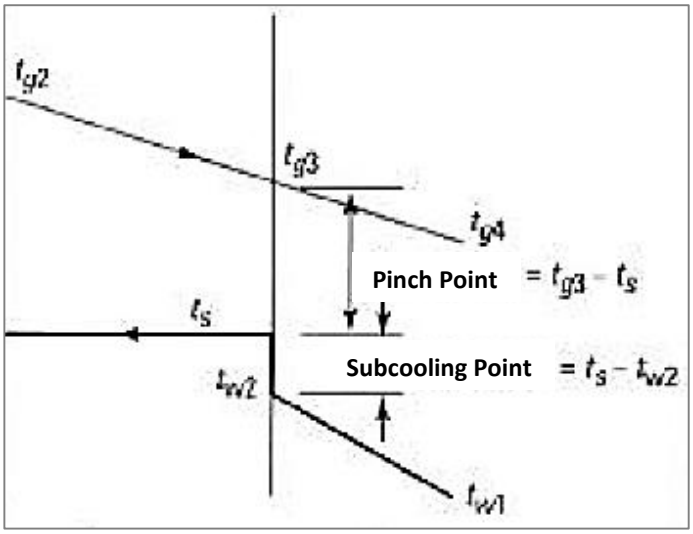

Figure A2-1 EGB's temperature profiles

Evaporator and economizer size are also affected by the selection of these two variables. Based on the sizes of evaporators that can be built and shipped economically, the pinch and approach points for unfired EGBs are usually in the range of 15°C to 30°C. Pinch and approach points are selected for a particular case or exhaust gas condition called the "design case."
Contrary to the typical steam generator, the steam production in an EGB depends on the conditions (i.e. flow rate, temperature..) of the exhaust gas leaving the gas turbine and entering the EGB. Furthermore, these parameters vary with ambient conditions, elevation, gas turbine load, and fuel fired. Hence, the design case could be 20°C ambient condition at 100% load of the gas turbine, or any other accepted gas inlet parameters.
Using exhaust gas parameters at this condition, the design temperature profile, which forms the basis for sizing the EGB, is determined. The EGB is then designed, or sized, once the pinch and subcooling points are selected - that is, the surface areas are determined indirectly.
Once selected, the pinch and approach points will vary if gas flow and exhaust gas temperature vary. These cases are called "off-design" cases. It can be said that there is only one design case, but several off-design cases.
The EGB simulation has been carried out, with THERMOFLEX's help, in order to mimic its design and off-design performances.

Design temperature profile calculations

The starting point for determining gas and steam temperature profiles and steam generation is the assumption of pinch and subcooling points, as discussed above. The known values are (respect to Figure A2-1):

- Gas flow rate (W_g)
- Gas temperature at EGB inlet (t_g1)
- Feed water temperature (t_w1)
- Steam pressure (P_s).

The saturation temperature (t_s) at the evaporator is determined from the steam pressure.

Once the pinch point is selected (as reported in Table 4-8), the temperature of the gas leaving the evaporator (t_g3) is known and the subcooling point gives the temperature of the water leaving the economizer (t_w2), since the saturation temperature is known.
Considering the evaporator's energy balance (Figure A2-1), the thermal power exchanged between steam and exhaust gas flow is given by Eq. (A2 - 1):

$$P_{TH,EVA} = W_g \times c_{p,g} \times (t_g1 - t_g3) = W_{sD}\left[(h_s - h_w2) + (h_f - h_w2)\right] \quad \text{[kW]} \qquad (A2 - 1)$$

Since t_g1 and t_g3 are known, $P_{TH,EVA}$ can be computed and the design steam flow (W_{sD}) can be determined.
The economizer energy balance gives the Eq. (A2 - 2) from which the gas temperature leaving the economizer (t_g4) can be obtained:

$$P_{TH,ECO} = W_{sD} \times (h_w 2 - h_w 1) = W_g \times c_{p,g}(t_g 3 - t_g 4) \quad \text{[kW]} \quad (A2 - 2)$$

Thus, the complete gas/steam profiles and steam generation rate for the design case can be determined by assuming the pinch and subcooling points.
In addition, once the pinch and subcooling points are selected, the log-mean temperature differences (ΔT_{lm}) at the various surfaces (A) are fixed because of the Eq. (A2 - 3):

$$A = \frac{P_{TH}}{U \times \Delta T_{lm}} \quad [m^2] \quad (A2 - 3)$$

Economizer and evaporator surface areas are fixed once U is computed. (To calculate U one should have such mechanical data as tube size, fin density, tube pitch, etc.). But if U is not known, UA is, which indirectly fixes the surface areas.
In order to know how the EGB behaves at different gas conditions, off-design calculations have to be performed using the "surface areas", which have been indirectly established.

Evaluating off-design performance

Besides design performances, simulations predict EGB performance at any other gas inlet conditions or steam parameters.
In simple terms, the factor UA is obtained using the equation $P_{TH}/\Delta T_{lm}$ for each surface in the design case. Then in the off-design case, the values of UA are corrected for the effects of gas flow, temperature, and composition. Then, the energy transferred across each surface is obtained through an iterative process after first assuming a steam flow rate to begin.
The total energy transferred across each surface is computed, and the actual steam generation rate (W_s) is obtained. This information is then used to correct the assumed steam flow.

All the passages described above have been implemented with THERMOFLEX's usage.

Appendix 3

Hybrid configuration's thermal loads

Since hybrid configurations are based on the simultaneous presence of both ICE and GT, all those thermal loads, which are directly linked to the number and kind of engines, have to be revisited. Said thermal loads are:

- Tanks heating
- E.R. users

It is well worth reminding that, because of the MGO's physical properties, GTs engines configuration does not need any kind of fuel's tanks heating and also the thermal loads connected to E.R. users are zero value, as reported and highlighted in Table A.3-1.

Table A.3-1 GTs engines configurations thermal loads

		Navigation			Harbour		
		Winter	Summer	Autumn	Winter	Summer	Autumn
Tanks	3606	0	0	0	0	0	0
ER	13579	0	0	0	0	0	0
Accomod	22018	16360	11361	9432	16360	11361	9432
Total	39203	16360	11361	9432	16360	11361	9432
Pre-Re Heating	8462	7933	2908	992	7933	2908	992
Hot Water	7144	4644	3572	4108	4644	3572	4108
Galley User	1757	1230	1230	1230	1230	1230	1230
Swimming	1220	122	1220	671	122	1220	671
Loundry	3435	2432	2432	2432	2432	2432	2432

It follows that, the hybrid engines configuration's tanks heating and E.R. users thermal loads have been determined deriving from those relative to ICEs engines configurations, which are reported and framed in Table A.3-2.

Table A.3-2 ICEs engines configurations thermal loads

		Navigation			Harbour		
		Winter	Summer	Autumn	Winter	Summer	Autumn
Tanks	3606	1260	490	863	1103	490	755
ER	13579	1660	1602	1660	1374	1288	1374
Accomod	22018	16360	11361	9432	16360	11361	9432
Total	39203	19279	13453	11955	18836	13139	11561
Pre-Re Heating	8462	7933	2908	992	7933	2908	992
Hot Water	7144	4644	3572	4108	4644	3572	4108
Galley User	1757	1230	1230	1230	1230	1230	1230
Swimming	1220	122	1220	671	122	1220	671
Loundry	3435	2432	2432	2432	2432	2432	2432

Therefore, the hybrid engines configurations' thermal loads are calculated by scaling the ICEs ones accordingly to the number of ICEs. Eq. (A3 - 1)has been used for this purpose:

$$Thermal\ load_{i,HC} = \frac{Thermal\ load_{i,ICE}}{n°_{ICE}} \times n°_{ICE,HC} \quad [kW] \qquad (A3 - 1)$$

where

- $Thermal\ load_{i,HC}$ are either the tanks heating or the E.R. users thermal loads in the hybrid engines configurations [kW]
- $Thermal\ load_{i,ICE}$ are either the tanks heating or the E.R. users thermal loads in the ICEs engines configurations [kW]
- $n°_{ICE}$ is the standard number of engines employed in the reference cruise ship
- $n°_{ICE,HC}$ is the number of internal combustion engines employed in a specific hybrid engines configurations.

It is important to say that the thermal loads values' depend also on the ICEs' size. This results in both different and repetitive thermal loads within the same hybrid engines configuration typology, i.e. the 1,x, the 2,x and the 3,x. For sake of clarity, it has been reported all hybrid engines configurations (Table 4-5) in Table A.3-3 below.

Table A.3-3 Hybrid engines configurations

		1,1	1,2	1,3	1,4	2,1	2,2	2,3	2,4	2,5	3,1	3,2	3,3	3,4
GT	Type A	1	1	2	2	2	2	0	0	1	1	0	1	0
	Type B	2	2	1	1	0	0	2	2	1	0	1	0	1
ICE	W8L46C	1	0	1	0	2	0	2	0	1	1	1	2	2
	W12V46C	0	1	0	1	0	2	0	2	1	2	2	1	1

The new thermal loads, determined with Eq. (A3 - 1), are reported in the following Tables.

Table A.3-4 Thermal loads of the 1,1 and 1,3 hybrid engines configurations.

		Navigation			Harbour		
		Winter	Summer	Autumn	Winter	Summer	Autumn
Tanks	858,25	284	103	194	253	103	172
ER	3364,75	385	370	385	313	292	313
Accomod	22018	16360	11361	9432	16360	11361	9432
Total	26241	17029	11834	10011	16926	11756	9918
Pre-Re Heating	8462	7933	2908	992	7933	2908	992
Hot Water	7144	4644	3572	4108	4644	3572	4108
Galley User	1757	1230	1230	1230	1230	1230	1230
Swimming	1220	122	1220	671	122	1220	671
Loundry	3435	2432	2432	2432	2432	2432	2432

Table A.3-5 Thermal loads of the 1,2 and 1,4 hybrid engines configurations.

		Navigation			Harbour		
		Winter	Summer	Autumn	Winter	Summer	Autumn
Tanks	944,75	345	142	236	299	142	204
ER	3424,75	445	430	445	373	352	373
Accomod	22018	16360	11361	9432	16360	11361	9432
Total	26388	17150	11933	10113	17032	11855	10009
Pre-Re Heating	8462	7933	2908	992	7933	2908	992
Hot Water	7144	4644	3572	4108	4644	3572	4108
Galley User	1757	1230	1230	1230	1230	1230	1230
Swimming	1220	122	1220	671	122	1220	671
Loundry	3435	2432	2432	2432	2432	2432	2432

Table A.3-6 Thermal loads of the 2,1 and 2,3 hybrid engines configurations.

		Navigation			Harbour		
		Winter	Summer	Autumn	Winter	Summer	Autumn
Tanks	1716,5	569	206	388	505	206	345
ER	6729,5	770	741	770	627	584	627
Accomod	22018	16360	11361	9432	16360	11361	9432
Total	30464	17698	12308	10590	17492	12151	10404
Pre-Re Heating	8462	7933	2908	992	7933	2908	992
Hot Water	7144	4644	3572	4108	4644	3572	4108
Galley User	1757	1230	1230	1230	1230	1230	1230
Swimming	1220	122	1220	671	122	1220	671
Loundry	3435	2432	2432	2432	2432	2432	2432

Table A.3-7 Thermal loads of the 2,2 and 2,4 hybrid engines configurations.

		Navigation			Harbour		
		Winter	Summer	Autumn	Winter	Summer	Autumn
Tanks	1889,5	691	284	472	597	284	408
ER	6849,5	890	861	890	747	704	747
Accomod	22018	16360	11361	9432	16360	11361	9432
Total	30757	17940	12506	10793	17704	12349	10586
Pre-Re Heating	8462	7933	2908	992	7933	2908	992
Hot Water	7144	4644	3572	4108	4644	3572	4108
Galley User	1757	1230	1230	1230	1230	1230	1230
Swimming	1220	122	1220	671	122	1220	671
Loundry	3435	2432	2432	2432	2432	2432	2432

Table A.3-8 Thermal loads of the 2,5 hybrid engines configurations.

		Navigation			Harbour		
		Winter	Summer	Autumn	Winter	Summer	Autumn
Tanks	1889,5	691	284	472	597	284	408
ER	6849,5	890	861	890	747	704	747
Accomod	22018	16360	11361	9432	16360	11361	9432
Total	30757	17940	12506	10793	17704	12349	10586
Pre-Re Heating	8462	7933	2908	992	7933	2908	992
Hot Water	7144	4644	3572	4108	4644	3572	4108
Galley User	1757	1230	1230	1230	1230	1230	1230
Swimming	1220	122	1220	671	122	1220	671
Loundry	3435	2432	2432	2432	2432	2432	2432

Table A.3-9 Thermal loads of the 3,1 and 3,2 hybrid engines configurations.

		Navigation			Harbour		
		Winter	Summer	Autumn	Winter	Summer	Autumn
Tanks	2747,75	975	387	666	850	387	580
ER	10214,25	1275	1231	1275	1060	996	1060
Accomod	22018	16360	11361	9432	16360	11361	9432
Total	34980	18610	12980	11372	18270	12744	11072
Pre-Re Heating	8462	7933	2908	992	7933	2908	992
Hot Water	7144	4644	3572	4108	4644	3572	4108
Galley User	1757	1230	1230	1230	1230	1230	1230
Swimming	1220	122	1220	671	122	1220	671
Loundry	3435	2432	2432	2432	2432	2432	2432

Table A.3-10 Thermal loads of the 3,3 and 3,4 hybrid engines configurations.

		Navigation			Harbour		
		Winter	Summer	Autumn	Winter	Summer	Autumn
Tanks	2661,25	914	348	624	804	348	549
ER	10154,25	1215	1171	1215	1000	936	1000
Accomod	22018	16360	11361	9432	16360	11361	9432
Total	34834	18489	12880	11271	18164	12645	10981
Pre-Re Heating	8462	7933	2908	992	7933	2908	992
Hot Water	7144	4644	3572	4108	4644	3572	4108
Galley User	1757	1230	1230	1230	1230	1230	1230
Swimming	1220	122	1220	671	122	1220	671
Loundry	3435	2432	2432	2432	2432	2432	2432

Appendix 4

Coefficients

In the following tables are reported the non-linear coefficient mentioned in Chapter 4.

Table A.4-1 ICEs %MCR SFOCiso factors

A	-1,47E-11
B	2,53E-09
C	3,68E-07
D	-1,28E-04
E	1,29E-02
F	-5,99E-01
G	1,21E+01
H	1,22E+02

Table A.4-2 EGB's coefficient for both the ICEs' size

	W8L46C	W12V46C
A	38039	65949
B	-68307	-133276
C	12584	61119
D	43543	36906
E	-30693	-36704
F	6987,5	9270,2

Table A.4-3 High temperature circuit coefficient

	W8L46C	W12V46C
A	-2,52E+03	-6,22E+03
B	7,19E+03	4,84E+04
C	-6,90E+03	-98410
D	4,76E+03	79078
E	-1,57E+02	-19459
F	6,76E+02	1,67E+03

Table A.4-4 $T_{g,OUT,EGB}$ *coefficient*

A	1213,1
B	-3198,1
C	3114,5
D	-1302
E	388,3

Table A.4-5 GTs SFOCiso coefficient

	Type A	Type B
A	-4358	-3357,5
B	18107	13804
C	-30296	-22710
D	25770	18755
E	-11379	-7788,6
F	2199,7	1230,8
G	164,64	273,62

Table A.4-6 EGB coefficient for the best EGB configuration

	Type A	Type B
A	5254,9	7547
B	1219,6	2121

Table A.4-7 T gas coefficient for the best EGB configuration

	Type A	Type B

A	66,913	60,093
B	202,4	199,98

Appendix 5

Global ship efficiency

In the following, the energy analysis' results, already commented and reported in ¶ 5.1.1, are analyzed deeply.
Firstly, for sake of clarity, Figure 5-1 is recalled below, as Figure A5-1.

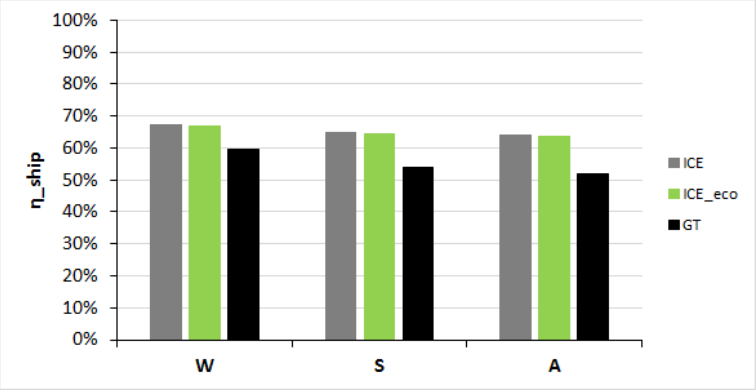

Figure A5-1 Global ship's efficiency for every season and "one-kind" engines' configuration.

The lower GT's configuration ship efficiency can be explained if a detailed analysis is carried out. Firstly, for each season, it has been determined the ship's efficiency for harbor and navigation phase, as reported in Figure A5-2. The phase of maneuvering has not been taken into account because it has a very little impact on this analysis.
It can be noted that, the global ship efficiency gap between GT and ICEs configurations showed in Figure A5-1, is erased when the only harbor phase is taken into account, indeed all the three one kind engines' configurations have almost the same ship's efficiency (>70%), see Figure A5-2 (a). On the other hand, GT configuration is 10 points percentage less efficient than ICEs configurations if the navigation phase is considered, as shown in Figure A5-2 (b).
This result could be explained if a further energy analysis is carried out.

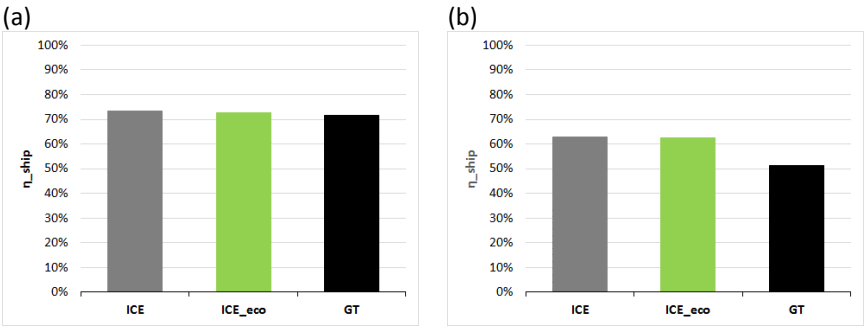

Figure A5-2 Harbor (a) and navigation (b) ship's efficiency for every season and "one-kind" engines' configuration.

Said analysis consists in subdividing the ship annual average efficiency, for each cruise phase (harbor (a) and navigation (b)), into propulsion efficiency and cogenerable fraction of thermal load. The first is shown with the blue bar and the latter with the orange one in the Figure A5-3. Results are shown for every season.
Thanks to this kind of analysis, whose results are reported in Figure A5-3, it can be understood the reason why GT configuration has the same energy efficiency in harbor but not during the navigation phase. Indeed, in all the season analyzed, GT configuration can reach the same ship's energy efficiency thanks to the GTs' high capability of cogeneration that allows reducing the gap existing in terms of propulsion efficiency when the ship is in harbor. This situation does not happen on navigation, where the cogenerable part of the thermal load is not enough to reduce the propulsion efficiency gap, which remains more or less invariant. It's clear that making an optimal thermal load cogeneration is a key factor in determining the different ship efficiency.
Results of a more detailed analysis regarding how thermal loads are covered, are shown in Figure A5-4. These graphs show how the thermal load is covered, if through cogeneration (orange bar) or employing OFB (yellow bar). In addition, also the waste heat flux (green bar), namely that part of exhaust gas flows thermal content which is in surplus, is displayed.

To maximize ship efficiency it is essential to cover the most part of thermal load by using the exhaust gas flows thermal content instead of the OFB, and at the same time, without making a huge amount of waste heat. This condition is favorable to GT on harbor, where the limited surplus and the high possibility to cogenerate, allow the reduction of the existing gap in propulsion efficiency. Things are different on navigation, where the heat flux's surplus frustrates the benefits obtained by the cogeneration of the whole thermal load. This is particularly true during the coldest season.
Having carried out such an analysis, the different average ship efficiency values, see Figure A5-1, as well as the different behavior occurring in harbor and in navigation, see Figure A5-2, are therefore justified.

WINTER

(a)

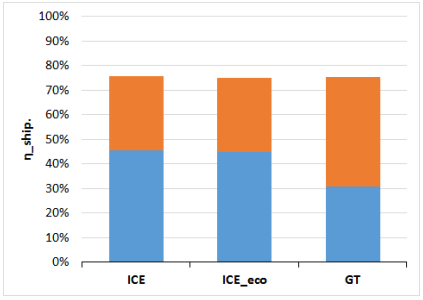

(b)

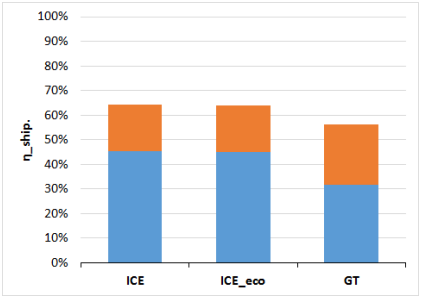

SUMMER

(a)

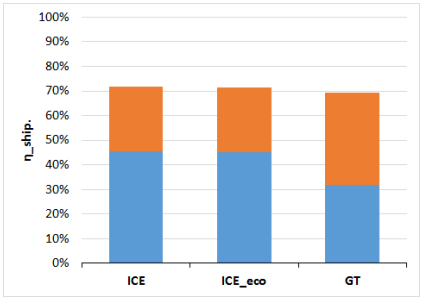

(b)

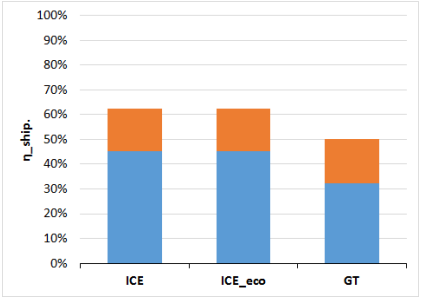

AUTUMN

(a)

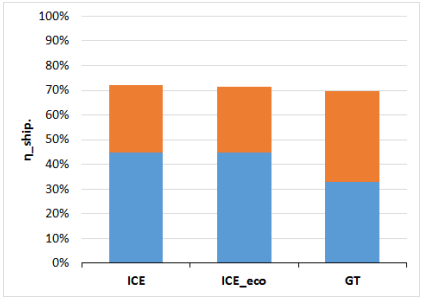

(b)

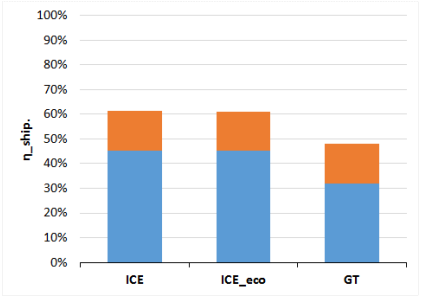

Figure A5-3 Ship's propulsion efficiency (blue bar) and cogenerable part (orange bar) for harbor (a) and navigation (b) for every season.

WINTER

(a)

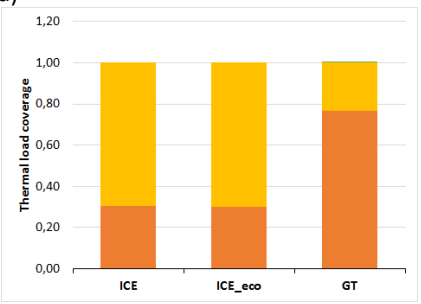

(b)

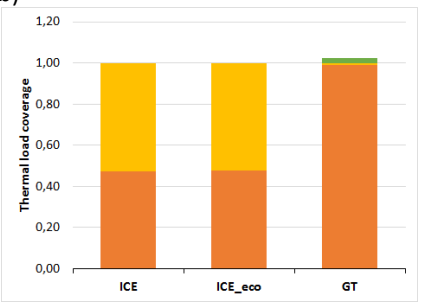

SUMMER

(a)

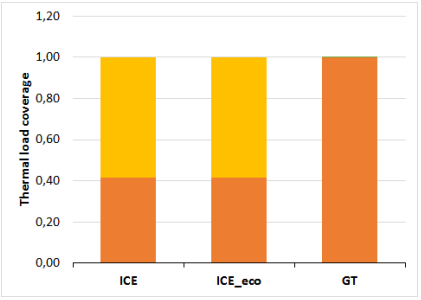

(b)

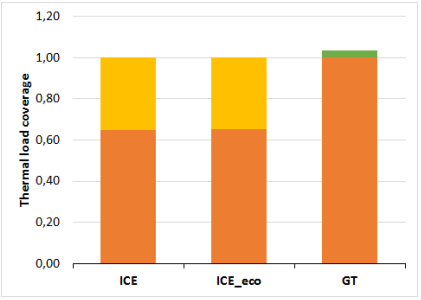

AUTUMN

(a)

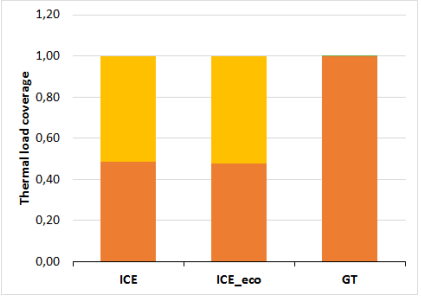

(b)

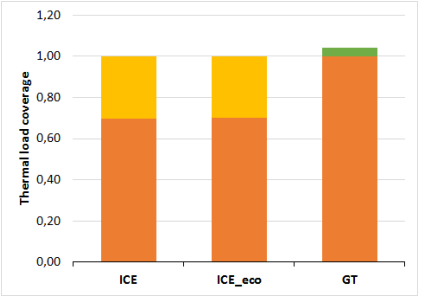

Figure A5-4 Ship's thermal load coverage: cogeneration (orange bar), OFB (yellow bar) and waste heat (green bar) for harbor (a) and navigation (b) for every season.